Identifying Roles of *dlx* Paralogs in Zebrafish Development

Emily Yu

Thesis submitted to the University of Ottawa
in partial Fulfillment of the requirements for the
Doctorate In Philosophy degree in Biology

Department of Biology
Faculty of Science
University of Ottawa

Abstract

The *Dlx* homeobox genes are conserved among vertebrates and encode homeodomain transcription factors involved in development of multiple tissues. These genes are organized as bigene clusters that are partially regulated by conserved cis-regulatory elements. These regulatory elements contain binding sequences for Dlx proteins suggesting they are sites of cross-regulation. The *Dlx* genes are important in the differentiation and migration of GABAergic neurons in the mouse brain. Additionally, *Dlx* are also important in the development of craniofacial tissues by providing patterning information to neural crest cells. However, deletion of single and compound *Dlx* mutants in the mouse lead to early lethality, precluding detailed analysis on the role of individual *Dlx* during development. In zebrafish, these genes are also involved in the development of craniofacial tissues and are co-expressed in brain areas containing GABAergic neurons. Therefore, the role of four paralogs *dlx1a*, *dlx2a*, *dlx5a*, and *dlx6a* in the nervous system and craniofacial development were investigated in this project. Two additional mutants, *inter56* where the enhancers of *dlx5a/dlx6a* are deleted, and *dlx5i6* where the entire *dlx5a/dlx6a* locus is deleted were created for further analysis. These mutants were generated by CRISPR-Cas9 genome editing and all homozygotes were found to be viable and fertile as adults. They were also capable of normal feeding indicating no abnormalities in jaw function. Whole mount *in situ* hybridization for *dlx* genes in *dlx* mutants demonstrated *dlx* can cross-regulate in zebrafish. Relationships observed in the mouse were identified in zebrafish however some differences were also elucidated, such as the presence of *dlx5a* expression in *dlx2a* mutants until 3dpf. During craniofacial development, loss of *dlx* genes affected the size of ventral cartilage structures. In particular, the Meckel's cartilage (MC) of $dlx5a^{-/-}$ and $dlx5i6^{-/-}$ larvae had consistent morphological defects. The expression

of chondrogenic markers and proliferation was also altered in *dlx5a*$^{-/-}$ and *dlx5i6*$^{-/-}$ mutants at 2-3dpf. Importantly, the size and shape of the MC may be due to abnormal expression of the non-canonical Wnt *wnt5b* during morphogenesis. These mutants exhibited more random distribution of microtubule organizing center in MC chondrocytes indicative of abnormal non-canonical Wnt signaling. To address consequences of *dlx* loss in the nervous system of zebrafish, the distribution and number of calretinin (CR) neurons, a type of GABAergic neuron were investigated. There was a trend towards fewer CR+ neurons in the optic tectum of *dlx5a*$^{-/-}$ and *dlx5i6*$^{-/-}$ mutant adults suggesting possible defects in integrating visual, auditory and vestibular information. These mutants also have abnormal swimming behaviour at around 2 months old characterized by frequent turning and spinning during a swim bout without changes in inactivity duration or total distance travelled. The number of neuromasts, a type of sensory organ that provides positional information, was reduced in *dlx5a* mutants and have reduced regeneration. The maintenance and regeneration of neuromasts depend on Schwann cells, a type of neural crest derivative. Defects in craniofacial development and neuromast biology suggest *dlx5a* may have a general role in neural crest cell biology beyond craniofacial development.

Acknowledgements

This project took me to some unexpected places and the journey would not have been possible without firstly, my supervisor Dr. Marc Ekker. Thank you so much for the opportunity to be in your lab, for your guidance, support, and patience in the past years. I am also grateful for all your encouragement, both experimentally and for all the opportunities to present my work at conferences. I was mostly decided on pursuing a career in academia and research prior to starting this PhD. but your influence cemented me on that path.

I also want to thank my advisory committee, Marie-Andrée Akimenko, Tuan Bui and Iain McKinnell for their time and valuable suggestions, criticisms, and support. If not for your advice to focus, I am sure I would still be performing all the experiments I initially wanted to do in my proposal!

To the Ekker and Akimenko lab members past and present, I am grateful for such a friendly and fun atmosphere. You all certainly made moving to a new city easier. I am especially thankful to Michael Kalyn (misery loves company), Hellen Weinschutz Mendes (*dlx* buddies!), Khang Hua (who encouraged me to join the lab at the 2017 Zebrafish Disease Models conference) and Rawan Merhi (it was a shame we were on opposite sides of the lab and often in at opposite times!)—without all your help, support, encouragement and friendship, I am not sure this work would have been completed. To end my first year in the lab with a conference shared with you all was one of the highlights of this journey.

I would also like to thank Vishal Saxena, our fish "guru" and horror movie aficionado. Thank you for your support, encouragement, advice, and stories. I also want to thank Sofia Perin-although we overlapped only briefly, I am grateful for you showing me around the lab and of

course, all the work you previously put into this *dlx* project. Thank you also to Gary Hatch, who knew where everything was. I enjoyed our quiet early mornings together in the lab. My gratitude also to all the technical staff at University of Ottawa, especially Jacky Liang and Andrew Ochalski, for all the imaging expertise.

I am deeply thankful for my family who supported me in such a long journey in education- your patience astounds. I also want to thank my friends for all the encouragement and levity when things were hardest.

Finally, I want to thank my partner. This degree would not have been possible without you. You are my rock during the hard times and the first one to celebrate when I had successes. You believed in me more than I ever did in myself. This achievement is yours as well.

Statement of Contributions

The experiments presented in this thesis were executed by myself. However, some contributions should be noted. All mutants except dlx*2a*$^{-/-}$*; dlx5a*$^{-/-}$ lines were created by Sofia Perin, a former laboratory technician. She carried out the design of sgRNAs, identification of primary injected zebrafish containing germline mutations, breeding of lines to the F1 generation for *dlx1a, dlx2a* and *dlx5i6* lines, breeding of mutants past the F2 generation for *dlx5a, dlx6a* and *inter56* lines including identification and sequence confirmation of homozygous fish. Vishal Saxena also contributed to making the mutants used in this work. The following students all carried out experiments under my supervision. Dana Elsaid, a former UROP student performed some of the histology stains used in the analysis in Section 3.2.1 and 3.2.2. Hadeel Al Hadi was a former UROP and NSERC summer student who contributed to the results presented in Sections 3.3.2- 3.3.4. Jinane El Hage was another UROP student who performed some of the experiments in Section 3.3.1. Finally, Emily Lam was a fourth-year honors student who performed all larval analysis mentioned in Section 3.3.1 and made the figure found in Appendix A.

Table of Contents

List of Figures

List of Tables

List of Abbreviations

Ascl1 – Achaete-scute homolog 1

ASD – autism spectrum disorder

BMP – bone morphogenic proteins

bp – base pairs

BrdU – bromodeoxyuridine

Cas9 – CRISPR-associated

CB – calbindin

cDNA – complementary DNA

CGE – caudal ganglionic eminence

CH – ceratohyal cartilage

CNCC – cranial neural crest cells

CNS – central nervous system

Col11a2 – collagen 11 a 2

CR – Calretinin

CRE – cis-regulatory elements

CRISPR – clustered regularly interspaced short palindromic repeat

D. tele – dorsal telencephalon

DASPEI - 2-(-(Dimethylamino)styryl)-N-ethylpyridinium iodide

Dll – Distal-Less

Dlx - *Drosophila* distal less homeobox

dpf – days post fertilization

Edn-1 – Endothelin-1

EMT – epithelial- to – mesenchyme transition

Eph – ephrin

ES – embryonic stem (cell line)

Evf2 – embryonic ventral forebrain 2

FGF – fetal growth factor

Foxd3 – forkhead box d3

frzb – frizzled related protein

frzd7a – frizzled receptor 7a

GABA- γ-amino butyric acid

GAD – glutamic acid decarboxylase

GAD65 (GAD1) – GAD isoform 65 (GAD isoform 1)

GAD67 (GAD2) – GAD isoform 67 (GAD isoform 2)

gDNA – genomic DNA

GE – ganglionic eminence

HD – Homeodomain

Hox – Homeobox gene

hpf – hours post fertilization

Kat6a – lysine acetyltransferase 6a

LGE – lateral ganglionic eminence

MC – Meckel's cartilage

Mef2c – myocyte enhancer factor 2c

MGE – medial ganglionic eminence

Mmp2 – metalloprotease 2

MTOC – microtubule organizing center

NCC – neural crest cells

NM – neuromast

Nrp2 – Neuropilin 2

OB – olfactory bulb

P – Prosomere 1, 2

PA – pharyngeal arch

Pak3 – p21 activated kinase 2

PCP – planar cell polarity

PFA – paraformaldehyde

PGZ – periventricular gray zone of the optic tectum

PLL – posterior lateral line

PNS – peripheral nervous system

PPA – preplacodal area

PQ – palatoquadrate cartilage

PV – parvalbumin

r – rhombomere

RT- qPCR – reverse transcribed quantitative PCR

Sema3 – Semaphorin 3

sgRNA – single stranded guide RNA

Shh – Sonic Hedgehog

SOM – somatostatin

Sox9, 10 – SRY-Box 9, 10

SVZ – subventricular zone

TeO – optic tectum

TGF-β – transforming growth factor beta

URE – upstream regulatory element

UTR – untranslated region

V. tele – ventral telencephalon

VIP – vasopressin

VZ – ventricular zone

WBS – Williams-Beuren syndrome

WISH – whole mount *in situ* hybridization

Wnt – Wingless/integrated

Chapter 1

Introduction

1.1 Overview of homeobox genes

Homeobox genes encode transcription factors that are found in all animals, plants and fungi (Bürglin & Affolter, 2015). They are involved in a variety of functions including axis patterning, stem cell maintenance and metabolic responses (Dolzblasz et al., 2016; Pick & Heffer, 2012; Tao et al., 2016; T. Wu et al., 2011). These proteins play an essential role in development since mutation in homeobox genes often lead to homeotic transformations wherein one part of the body is transformed to resemble a different part (Emerald and Roy, 1997). The homeobox is a shared sequence element of 180 bp that encodes a homeodomain (HD) of about 60aa long (McGinnis et al., 1984; Scott & Weiner, 1984). The basic structure of the HD is globular with 3 alpha helices in a helix-turn-helix motif (Bürglin & Affolter, 2015; Laughon & Scott, 1984). Other structures are also possible due to influences from additional flanking domains and cofactors. This domain can recognize and bind to a tetranucleotide ATTA core-motif downstream of a GG dinucleotide (Kissinger et al., 1990). Most of the HD-DNA interaction is through contact at the major groove however the strength of binding is influenced by the N-terminal arm at the minor groove (Rohs et al., 2009). Due to the short length and AT-rich nature of the binding sequence, it has been suggested that specificity of HD transcription factor target genes may be attributed to additional factors such as other flanking domains, other DNA binding domains, interaction with other transcription factors and even chromatin landscape(Andzelm et al., 2015; Choe et al., 2014; Hojo et al., 2016; Mann et al., 2009).

About 15-30% of all transcription factors found in most vertebrates contain a HD (de Mendoza et al., 2013; Holland, 2013). HD transcription factors can be broken into different classes based on sequence similarity of protein motifs and presence of similar flanking domains.

One of the largest classes of HD transcription factors is the antennapedia class, to which *Dlx* genes belong(Bürglin & Affolter, 2015).

1.2 Overview of *Dlx* genes

The *Dlx* family of homeobox genes are related to the *Drosophila* distal-less (*Dll)* gene, so named due to the loss of distal limbs in *Dll* mutants resulting in embryonic lethality (Cohen & Jurgens, 1989). Less severe *Dll* alleles were found to result in fusion of leg segments or tarsi, loss of tarsal segments, and loss of antennae (Cohen et al., 1989; Si Dong et al., 2000; Sunkel & Whittle, 1987). Analysis of clones generated from *Drosophila* distal leg cells found *Dll* null cells delaminate from the distal imaginal disc epithelium and migrate towards the presumptive proximal cells, demonstrating *Dll* plays a crucial role in specifying the proximal-distal axis during development(J. Wu & Cohen, 1999).

Vertebrates have at least six *Dlx* genes thought to be due to a tandem gene duplication event early in chordate evolution followed by genome duplication events (di Gregorio et al., 1995; Stock et al., 1996). The six *Dlx* paralogs in vertebrates are organized in convergently transcribed, linked pairs (Zerucha & Ekker, 2000) (Fig. 1.1). Sequence similarity of motifs within the homeodomain and the carboxyl terminus can also separate the six genes into two groups. The first group is composed of *Dlx2*, *Dlx3* and *Dlx5* and the second of *Dlx1*, *Dlx4* and *Dlx6*. The first group contains an additional conserved motif in the N terminus. Each pair is made of one *Dlx* from each group: *Dlx1/Dlx2, Dlx3/Dlx4 and Dlx5/Dlx6.* Zebrafish possess two additional *dlx* genes that are unpaired and thought to have arisen through at least one additional genome duplication event (Robinson-Rechavi et al., 2001). Each *dlx* gene is made of three exons and two introns with the homeobox split between exons 2 and 3 (Ellies et al., 1997; J. K. Liu et

al., 1997). In the intergenic region of each *Dlx* gene pair are regulatory elements that are able to modulate the expression of neighbouring *Dlx* genes (Ghanem et al., 2003, 2007; M. Yu et al., 2011; Zerucha et al., 2000). Additionally, the *Dlx1/Dlx2* cluster also possess two 5' regulatory elements closest to *Dlx1* that are active where *Dlx1/Dlx2* expression occurs (Ghanem et al., 2007).

In addition to the DNA-binding HD, DLX proteins possess a consensus sequence of tryptophan-aspartic acid-tryptophan-tyrosine at the C-terminal end of the HD (Panganiban & Rubenstein, 2002). Based on the propensity of other HD transcription factors to interact at tryptophan residues in conserved motifs, it is possible that this is a site where DLX proteins may interact with other transcription factors to increase specificity of target activation (Knoepfler et al., 1999; Neuteboom et al., 1995; Passner et al., 1999). DLX proteins are also proline-rich upstream and downstream of the HD suggesting oligomerization and importance in transcriptional activation. This was demonstrated to be the case in the case of the proline rich N-terminus of *Dlx5* and the C terminus of DLX3 (Masuda et al., 2001; Mermod et al., 1989; Xiao et al., 2000)

Of the six *Dlx* genes shared among vertebrates, only four (*Dlx1/dlx1a*, *Dlx2/dlx2a*, *Dlx5/dlx5a*, *Dlx6/dlx6a*) will be described in this thesis and will be the only *Dlx* genes considered for the rest of this chapter.

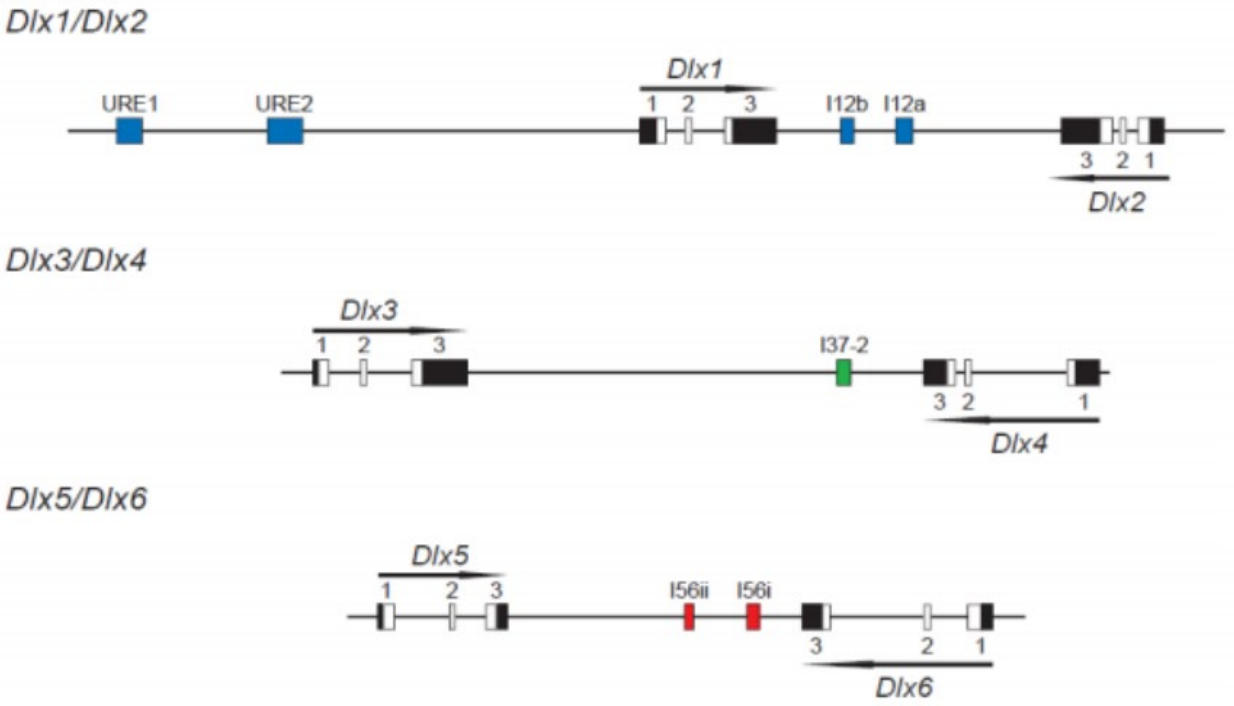

Figure 1.1. Schematic representation of genomic organization of the mouse *Dlx* genes.

White boxes represent coding regions. Intergenic cis-regulatory elements are depicted in coloured boxes (blue for Dlx1/Dlx2, green for Dlx3/Dlx4 and red for Dlx5/Dlx6). Schematic taken from Darbandi, 2014.

1.3 Regulation of *Dlx* gene expression

1.3.1 Cis-acting regulatory elements (CRE) of *Dlx* expression

As mentioned previously, within each *Dlx* gene pair locus are conserved CRE that are able to modulate the expression of the neighbouring *Dlx* genes (Fig.1). Within the *Dlx1/Dlx2* locus are four CRE that appear to be active in different tissues and contexts. The first CRE is Upstream Regulatory Element 1 (URE1), a 600bp sequence located upstream of *Dlx1*. This CRE is able to activate expression of reporter transgene in the retina but not the forebrain, limbs, or craniofacial elements in the developing mouse (Ghanem et al., 2007). URE2 is a ~900 bp sequence that is active in the forebrain, specifically the subpallial telencephalon, Prethalamus and hypothalamus. This enhancer can also activate reporter expression in the hyoid arch, somites, and limbs. Importantly, reporter expression recapitulates expression regions of *Dlx1/Dlx2* demonstrating this enhancer is active in the same areas *Dlx1/Dlx2* are expressed. The two other CREs found within the *Dlx1/Dlx2* locus are found within the intergenic regions between the two genes. I12b was found to induce reporter activity in the mouse forebrain starting at E10.0 and in migrating cells at E11.5 (Ghanem et al., 2003; Poitras et al., 2007). I12a is also in the intergenic region and is between I12b and *Dlx2*. This enhancer was shown to drive reporter expression in some mesenchyme cells of the first and second pharyngeal arches in both mouse and zebrafish (Ghanem et al., 2003; Park et al., 2004).

Within the *Dlx5/Dlx6* locus are two CREs found in the intergenic region. Reporter expression under the activity of I56i was observed in the ventral thalamus and basal telencephalon in both zebrafish and mice (M. Yu et al., 2011; Zerucha et al., 2000).

Additionally, the mouse version of this CRE was also active in the branchial arches, olfactory placode and developing limb bud. The second CRE in this locus, I56ii, can drive reporter expression in the telencephalon, specifically in distinct regions of the ganglionic eminences and in select striatal neurons (described in 1.4.2.4)(Ghanem et al., 2008). It may also be able to modulate the activity of I56i to label additional cells in the zebrafish telencephalon, diencephalon, and midbrain tectum (M. Yu et al., 2011). Finally, an enhancer upstream of *Dlx6* was identified that is specific for pharyngeal arch reporter expression (Verzi et al., 2007).

1.3.2 Trans-acting regulators of *Dlx* expression

A common feature of all the CRE listed above is that they all possess binding sequences for DLX, suggesting that *Dlx* genes can cross-regulate expression using these enhancer regions. For example, *Dlx1*, *Dlx2* and *Dlx5* are able to bind directly to I56i (Poitras et al., 2010). Furthermore, reporter activity and *Dlx5/Dlx6* expression was reduced when *Dlx1/Dlx2* was knocked out in the mouse developing telencephalon (Zerucha et al., 2000). Additionally, loss of *Dlx2* resulted in reduced *Dlx1* expression in mice(Eisenstat et al., 1999). Taken together, this suggests *Dlx2* can regulate the expression of *Dlx1*, *Dlx5* and *Dlx6* whereas the expression of *Dlx5* and *Dlx6* may require the activity of both *Dlx1* and *Dlx2*.

During forebrain development, many factors interact at *Dlx* CREs to regulate temporal and region-specific *Dlx* expression. For example, *Ascl1* (previously *Mash1*) is a pro-neural factor that is involved in the specification and differentiation of ventral telencephalon progenitors(Yun et al., 2002). This transcription factor was identified to bind directly to the I12b enhancer and when the site was mutated, reduced enhancer activity resulted, suggesting *Ascl1*

is important in regulating expression of *Dlx1/Dlx2* in mice (Poitras et al., 2007). Additionally, knockdown of *ascl1* in zebrafish resulted in reduced expression of *dlx1a*, *dlx2a* and *dlx5a*, further supporting this factor as an important *Dlx* regulator (MacDonald et al., 2013). Another important neural factor that interact on *Dlx* CREs is the retinoblastoma protein which regulates the G1-S phase checkpoint during cell division and appears essential for proper maturation and migration of telencephalic interneurons by regulating expression of *Dlx1/ Dlx2* through direct binding of the I12b enhancer (Ghanem et al., 2012).

Less is known about trans-acting regulatory elements controlling *Dlx* gene expression in the developing face. The myocyte enhancer factor family2 member *Mef2c* is one of the few factors identified to directly bind to the enhancer upstream of *Dlx6* to activate *Dlx6* expression in lower jaw and posterior palate development (Verzi et al., 2007). This is also true in zebrafish where the ortholog *mef2ca* is required for *dlx6a* expression (Miller et al., 2007). Recently, the chromatin modifier *Kat6a*, identified in patients affected with congenital abnormalities including cleft palate and heart defects. Importantly, this modifier was found to regulate *Dlx5* expression by changing access to the locus via histone acetylation (Vanyai et al., 2019). Loss of *Kat6a* resulted in reduced expression of *Dlx5* and downstream targets leading to cleft palate of the lower jaw among other deformities in mice. Zebrafish *kat6a* is also important in pharyngeal segment identity, presumably also through regulation of *dlx5a* (Crump et al., 2006; Miller et al., 2004).

1.3.3 Signaling molecules regulating *Dlx* expression

Several signaling pathways have been found to influence *Dlx* expression, however the mechanisms are still largely unknown. Sonic Hedgehog (Shh) was found to induce expression

of *Dlx2* in the developing mouse telencephalon *in vitro* and *in vivo*, potentially through expression of a non-coding RNA molecule *evf2* (Feng et al., 2006). Shh also plays a role in regulating *dlx5a/dlx6a* expression during dorsal-ventral patterning of the zebrafish pharyngeal arches through the receptor Smoothened (Swartz et al., 2012). FGFs and BMPs are essential for proper expression of *Dlx1* and *Dlx2* in the first pharyngeal arch mesenchyme (Tucker et al., 1998, 1999). Dissected mouse mandibles were induced to express *Dlx2* when exposed to beads soaked in FGF8, but not BMP4 (B. L. Thomas et al., 2000). In a similar experiment, Park and colleagues demonstrated that FGF8 and FGF9 were able to induce I12a reporter activity in the mouse mandible but BMP4 antagonized FGF8 effects(Park et al., 2004). Lastly, Endothelin-1 (*Edn1*) is a signal produced by the ventral pharyngeal arch epithelia and is able to induce *Dlx5/Dlx6* expression to establish ventral fate in neural crest cells of the first pharyngeal arch (Clouthier et al., 2010; Coffin Talbot et al., 2010; Vieux-Rochas et al., 2010).

1.3.4 Downstream targets of *Dlx* genes

Due to the role of *Dlx* genes in the development of GABAergic interneurons, many of the known gene targets of *Dlx* transcription factors are involved in neuronal differentiation and GABA expression. Indeed, *Dlx1*, *Dlx2* and *Dlx5* are all found to be able to induce *in vitro,* the expression of GAD65, an essential component of GABA synthesis (Stühmer et al., 2002). Additionally, knockdown of *dlx2a* or *dlx5a* resulted in reduction in the expression of *gad65* in zebrafish (MacDonald et al., 2013). *Dlx1/Dlx2* were also shown to regulate the migration of cortical interneurons through direct repression of the Semaphorin (*Sema3*) receptor neuropilin2 (*Nrp2*)(Le et al., 2007). The interaction of *Sema3/Nrp2* is a repulsive guidance cue that mediates the sorting of tangentially migrating interneurons. Loss of *Dlx1/Dlx2* resulted in ectopic *Nrp2*

expression leading to accumulation of interneurons in the subventricular zone of the ganglionic eminences in which interneurons originate. Neurite outgrowth is also regulated by *Dlx1/Dlx2* activity through repression of *Pak3* (Cobos et al., 2007). Finally, *Wnt5a* is a direct target of *Dlx2* and *Dlx5*, and transplantation of wild-type (WT) neuronal precursors into a *Dlx2* or *Dlx5* null host was enough to prevent GABAergic interneuron differentiation through downregulation of *Wnt5a* (Paina et al., 2011).

Dlx genes are able to affect the morphogenesis of the jaws and palate through regulation of a few key signals and transcription factors. In the lower jaw, *Dlx5/Dlx6* induces the expression of *Hand2* and *Gsc* to define the ventral domain of the lower jaw (Depew et al., 1999). Oropharyngeal patterning also requires regulation of *Fgf10* signaling through *Dlx5* activity (Sugii et al., 2017).

1.4 Function of *Dlx* genes in craniofacial development

1.4.1 Overview of neural crest cells

Neural crest cells (NCC) are a population of transient embryonic cells that can differentiate into diverse derivatives and thus are often referred to as cells of the "fourth germ layer"(Sauka-Spengler & Bronner-Fraser, 2008). The introduction of the neural crest delineate vertebrates from other metazoans since this population provides key cells of paired sensory organs, craniofacial skeleton and peripheral nervous system. It may also be a driving force in expanding the vertebrate taxa by facilitating predatory behaviours (Gans & Northcutt, 1983). Development of NCC begin during gastrulation until late organogenesis. This process requires

intrinsic and extrinsic signals that govern their induction, specification, migration, and terminal differentiation.

1.4.2 NCC induction and specification

The ectoderm is the outer-most embryonic germ layer and forms the neural plate at the most dorsal aspect of the vertebrate embryo during gastrulation. The neural plate will produce the neural tube and central nervous system. Lateral and ventral to the neural plate is the non-neural ectoderm which will produce the epidermis and associated glands. The area between these two regions is called the neural plate border, the origin of the neural crest. Cells at the border are exposed to at least three major signaling pathways: intermediate levels of BMP from the neural ectoderm and antagonists from the underlying paraxial mesoderm; Notch signaling to promote neural crest formation and restriction to the neural plate border and canonical Wnt signaling (Deardorff et al., 2001; Endo et al., 2002; Lewis et al., 2004; Marchant et al., 1998). These inductive signals lead neural plate border cells to express a set of transcription factors including *Zic1*, *Msx1*, *Msx2*, *Dlx3*, *Dlx5*, *Pax3* and *Pax7*(McLarren et al., 2003; Sauka-Spengler & Bronner-Fraser, 2008). The combined expression of these transcription factors gives neural plate border cells the competency to become NCC. The prospective NCC will then express another set of transcription factors known as neural crest specifiers (or neural crest markers). These markers include *Sox9*, *Sox10*, and *Foxd3* and will guide the events involved in specifying NC fate including delamination, changing cell shape, motility and signaling competency involved in migration and differentiation (Sauka-Spengler & Bronner-Fraser, 2008).

During the above processes, the embryo continues through gastrulation into neurulation where the neural plate folds downwards to form the neural tube and bringing the two neural

plate borders together above the tube (Fig. 1.2). At this point, the neural plate border cells are neural crest precursors, having gone through induction and specification but are not migratory until the precursors segregate from the neural tube and the non-neural ectoderm encases the underlying structures.

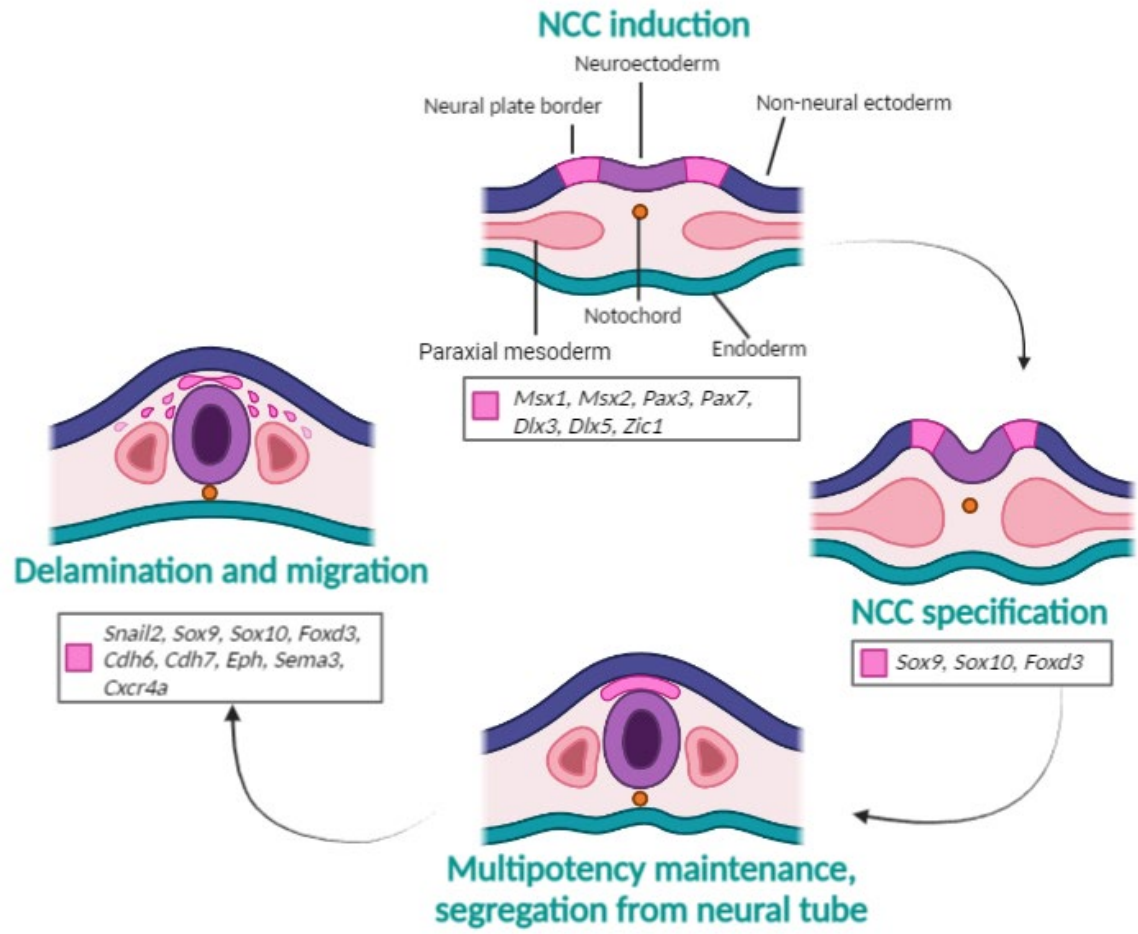

Figure 1.2. Schematic of neural crest cell formation from induction to migration.

Neural crest cells (pink) express different markers at different key points of formation, indicated by boxed genes.

1.4.3 NCC possess axial identity based on associated rhombomere

As the vertebrate nervous system continue to develop, the NC cell cycle is arrested and factors are expressed to both maintain multipotency and prevent apoptosis (Sauka-Spengler & Bronner-Fraser, 2008). Additionally, NCC will begin to express certain transcription factors that will bestow positional identity based on their location along the AP axis of the neural tube (Fig. 1.3). This positional information is related to the development of transient segments of the neural tube within the hindbrain region known as rhombomeres (Lumsden & Krumlauf, 1996; Minoux & Rijli, 2010). Rhombomeres are established through the expression of transcription factors such as *Hox* genes. Different paralogs of these genes are induced through varying concentrations of retinoic acid and FGF or Wnt (Dupé & Lumsden, 2001; Maves et al., 2002; Nordström et al., 2002). The combinatory effect of different levels of signals and transcription factors result in seven rhombomeres (r1-r7). With regards to NCC, the rhombomeres characterize migration streams and delineate the type of cell the NCC will ultimately become. NCC from the diencephalon and midbrain contribute to the frontonasal epidermis and mesenchyme respectively. NCC from r1, r2, r4 and r6 are known as cranial NCC (CNCC) and are the cells that become the bone, connective tissue, neurons and glia of the face (Schilling & le Pabic, 2014). Posterior to the last rhombomere, are NCC of the trunk which will migrate around and between somites to become part of the epidermis, connective tissue, neurons, glia of the trunk in addition to the enteric nervous system.

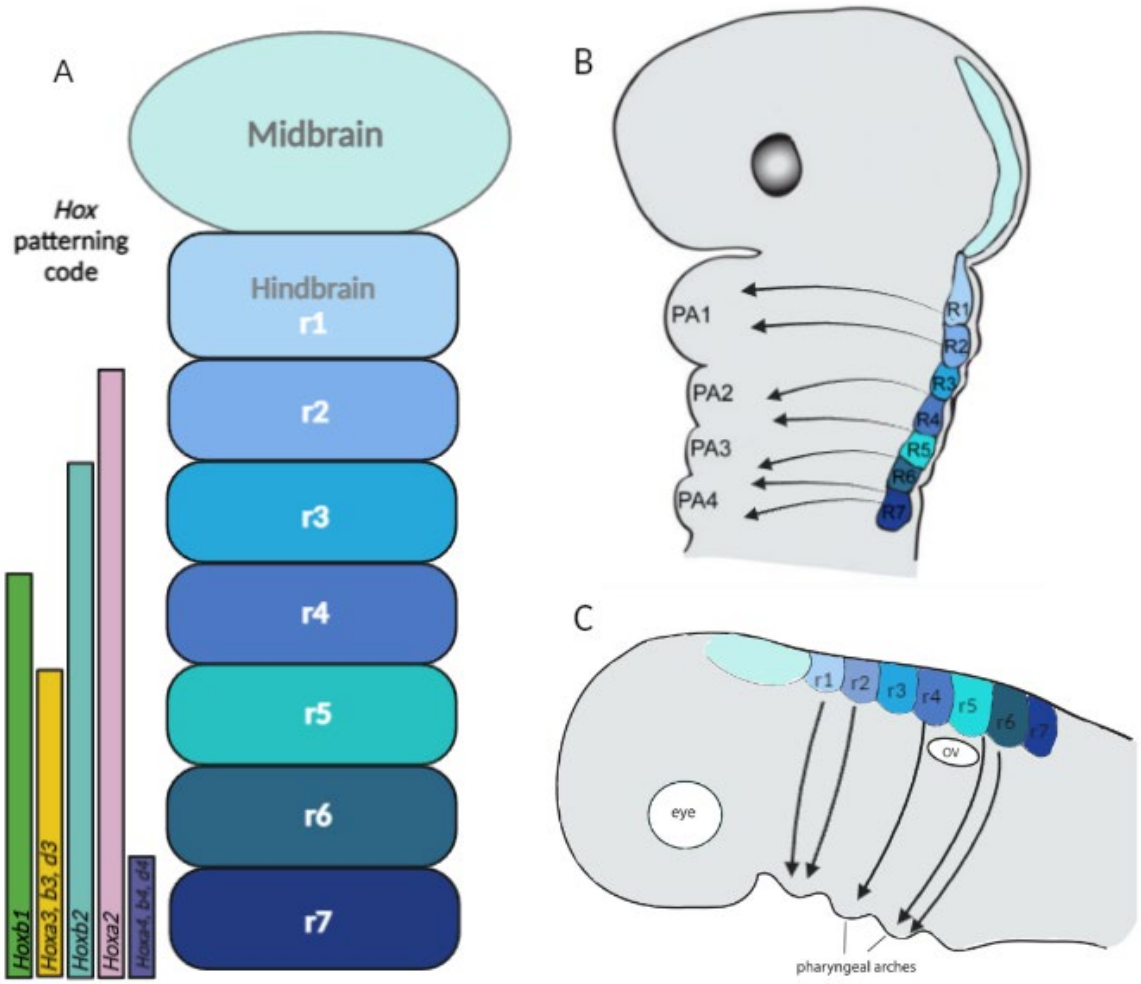

Figure 1.3. NCC are bestowed axial identity based on associated rhombomere (r1-r7) through expression of *Hox* genes.

(A) Vertebrate rhombomeres and *Hox* patterning code. This organization is conserved among vertebrates including mouse (depicted here) and zebrafish (expressing orthologs of *hox* genes in schematic). **(B-C)** Axial identity of NCC determines which pharyngeal (PA) to reside in mouse **(B)** and zebrafish **(C)**. (A and B adapted from (Kindberg & Bush, 2019)).

1.4.4 CNCC delamination and migration

From their position above the neural tube, all NCC will undergo delamination, epithelial-to-mesenchyme transition (EMT), and migrate to their final destination. Interestingly, the process of delamination and migration differ slightly based on NCC axial identity and species. Generally, CNCC will delaminate and undergo *en masse* EMT to migrate all at once to their destination whereas trunk NCC undergo EMT individually, delaminating and migrating in progressive waves (Taneyhill & Padmanabhan, 2014; Thiery et al., 1982). Delamination is the process where cells or groups of cells will separate from surrounding cells and is required for EMT which itself is a process that describes stationary cells becoming migratory. EMT requires the dismantling of various cellular junctions present between neighboring NCC and junctions of NCC with other ectoderm cells (neural tube below and non-neural ectoderm above), as well as cytoskeletal rearrangements that allow for migration (Thiery & Sleeman, 2006). This process is triggered by changes in extracellular signals such as TGF-β and FGF. Furthermore, elevated BMP and inhibition of Wnt signaling have recently been identified as additional signals to initiate EMT (Maj et al., 2016; Piacentino et al., 2021). These changes and the expression of neural crest specifiers previously mentioned (*Snail2*, *Sox9*, *Sox10*, *Foxd3*, etc) lead to changes in cell adhesion allowing EMT to proceed. For example, *Snail2* expression is shown to mediate the switch from N-cadherin to Type II Cadherins (eg: *Cdh6*, *Cdh7*) to weaken cell-cell connections (Batlle et al., 2000; Ikenouchi et al., 2003).

Once EMT is completed, NCC possess the ability to migrate. In zebrafish, CNCC begin migration at 12 hours post fertilization (hpf) and by 16hpf, cells have accumulated in transient groupings ventro-rostral from the dorsal neural tube known as pharyngeal arches (Schilling & Kimmel, 1994). Cells at each rhombomere will migrate all at once creating three streams of

CNCC: the first stream is from r1/2 to populate the first pharyngeal arch; CNCC from r4 will migrate to the second arch and CNCC from r5/6 will reside in the third arch (Kulesa et al., 2004; Piotrowski et al., 1996)(Fig. 3c). A combination of repulsive signals including Ephrin, Sema3 and BMP regulators confine CNCC to their streams and prevent mixing. Attractive signals from the endoderm and optical stalk such as the chemokine *Sdf1a* and the receptor *Cxcr4a* expressed by CNCC guide CNCC towards the pharyngeal arches(Killian et al., 2009).

1.4.5 Derivatives of pharyngeal arches

Prior to CNCC migration, the pharyngeal arches (PA) are already being segmented by the endoderm and induced to grow laterally from the developing pharynx by migrating paraxial mesoderm (Graham, 2008; McKinney et al., 2020). Veitch and colleagues demonstrated that PA can form without NCC but associated structures of the arches will be absent (Veitch et al., 1999). The number of PA can differ between organisms however the structures, in particular of the first two PA are similar and regulatory circuits are conserved. Amniotes possess five PA: the first PA is called the mandibular arch; the second PA the hyoid arch and the remaining three are broadly termed posterior PA (Fabik et al., 2021).

The first arch of amniotes will be split into two regions: the dorsal and proximal region will form the upper maxilla and the ventral, distal region the mandibles. The cartilage structures formed by the first PA are called the quadrate (maxillary) and Meckel's cartilage (mandibular). The quadrate will eventually undergo endochondral ossification to form the orbital, lateral skull wall, alisphenoid and incus bone of the middle ear (Rodríguez-Vázquez et al., 2018; Woronowicz & Schneider, 2019). NCC surrounding the quadrate will also form the maxilla, zygomatic and squamous part of the temporal bone through intramembranous ossification. The

Meckel's cartilage can be further broken into three regions from distal to proximal axis to form part of the dentary bone, jawbone or mandible, and malleus of the middle ear respectively, through endochondral ossification (Bhaskar et al., 1953; Shimo et al., 2004; Svandova et al., 2020).

The second arch produces cartilage that will undergo endochondral ossification to form the stapes. It is also the site of Reichert's cartilage that is continuous with the ear capsule and will form the temporal bone and horns of the hyoid which help attach the jaw to the neck and supports the tongue (Rodríguez-Vázquez et al., 2006).

Teleosts such as zebrafish possess seven arches: the first two are again the mandibular and hyoid arches and the remaining five are called branchial/gill arches that produce structures that help gill function (Kimmel et al., 2001; Yelick & Schilling, 2002). Similar to amniotes, the first arch can be broken into two regions producing the palatoquadrate (homolog of the quadrate) of the upper jaw and the Meckel's cartilage of the lower jaw (Fig. 1.4). The hyoid arch produces the hyosympletic cartilage in the dorsal region, which helps attach the jaw to the neurocranium and the ceratohyals and basihyal of the ventral region that help stabilize the jaw.

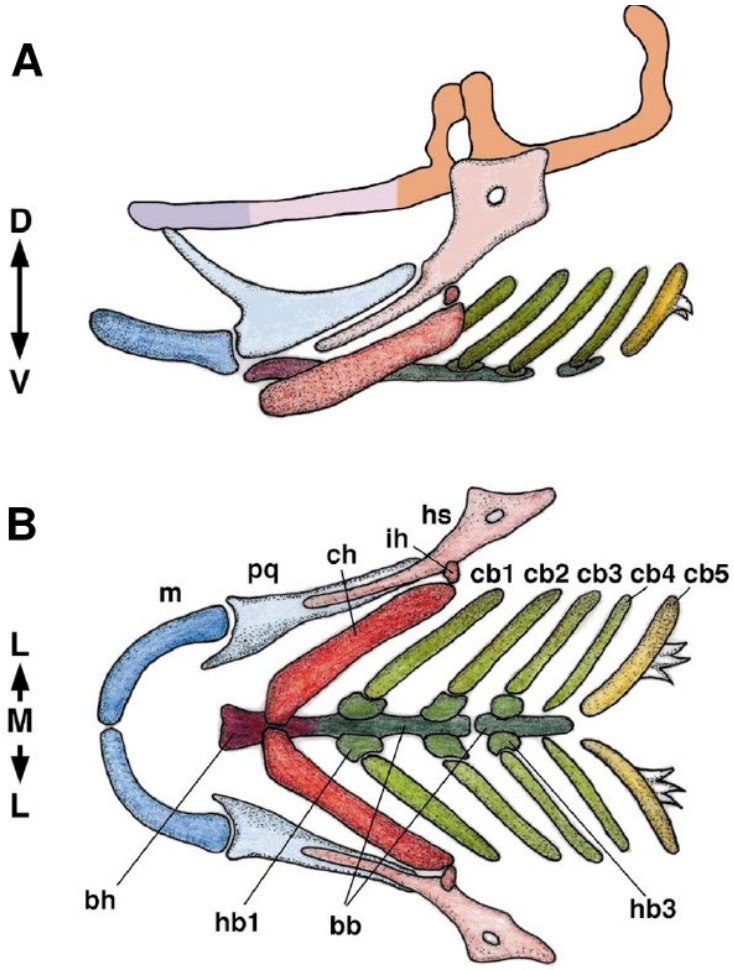

Figure 1.4. Cartilage structures of the teleost face.

(A) The neurocranium and pharyngeal skeleton in lateral view. **(B)** The paryngeal skeleton in ventral view. Abbreviations: bb,basibranchials; bh, basihyal; cb1-5, ceratobranchials; ch, ceratohyal; hb1, hypobranchial; hs, hyosympletic; ih, interhyal; m, Meckel's cartilage; pq, palatoquadrate. Figure from Kimmel et al., 2001.

1.4.6 Neural crest differentiation in the mandibular and hyoid arches

NCC are arrested from cell cycle progression and maintain multipotency until they reach their destination (Baggiolini et al., 2015). Once in the pharyngeal arches, CNCC are exposed to signals that play a role in cell fate choice. Wnt signaling is one such mechanism that is key in regulating the choice between differentiation into chondrocytes to produce cartilage, or osteoblasts to produce bone (Hartmann, 1993; for review see MacDonald et al., 2009). Inhibition of canonical Wnt signaling through deletion of the effector molecule β-catenin in NCC resulted in compete agenesis of cranial bones, absent maxilla, mandibles, and stapes. Ectopic cartilage structures also formed. These results suggest canonical Wnt signaling is required to balance osteogenesis and chondrogenesis (Brault et al., 2001; Day et al., 2005; Goodnough et al., 2014). In zebrafish, Wnt signaling is also important in chondrogenic fate decision. Knockdown of *fzb* or *frzd7a,* which are both able to bind to Wnt molecules, result in lack of lower jaw structures and loss of chondrocytes in ethmoid plate (Kamel et al., 2013). Wnt9a appears crucial for chondrogenic proliferation by regulating expression of *sox9a* (Curtin et al., 2011). Additionally, *wnt5b* appears to be important in regulating chondrocyte polarity affecting the shape of Meckel's cartilage in addition to regulating endochondral ossification (Ling et al., 2017). FGF signaling is also involved in regulating chondrogenic/osteogenic fate. Mutations in FGF receptors resulting in constitutive activity leads to premature loss of cranial sutures due to precocious osteogenesis (craniosynostosis) whereas reducing FGF increases chondrogenic proliferation (Burke et al., 1998; Sarkar et al., 2001; Wilkie, 1997). However, FGF8 is also able to induce chondrogenesis through activation of Sox9 expression. Thus, FGF influence on NCC fate choice is likely temporal and context-dependent (John et al., 2011; Walshe & Mason, 2000). Finally, a third important family of signaling molecules involved in NCC fate

choice is the TGF-β superfamily. TGF-β promotes proliferation of CNCC and loss of TGF-β signaling result in agenesis of both cartilage and bone structures (Iwata et al., 2010; Oka et al., 2008; Wurdak et al., 2005). BMPs are a member of the TGF-β superfamily and deletion of *Bmp2* was found to downregulate *Sox9* expression in the mandibular process demonstrating a requirement for BMP signaling in chondrogenesis (Chen et al., 2019).

The transcription factor and NCC marker *Sox9* is essential for chondrogenesis. Loss of *Sox9* results in embryonic lethality prior to cartilage development in the mouse and murine ES cell lines fail to differentiate into chondrocytes (Bi et al., 1999; Mori-Akiyama et al., 2003). The zebrafish mutant *jellyfish* (*jef*) is a hypomorphic mutant for *sox9a* and lacks most of the cartilage elements in the face (Yan et al., 2002). The *jef* mutant also exhibited significant reductions in the expression of a collagen *col2a1*. Collagen is an important component of cartilage and is produced by chondrocytes. *Sox9* appears able to regulate expression of this collagen in addition to *Col11a2* by binding directly to specific enhancers (Bell et al., 1997; Fang et al., 2010; Lefebvre et al., 1997).

CNCC can also differentiate into osteoblasts through the activity of Runx2, the master regulator of osteoblast differentiation. Deletion of this transcription factor results in agenesis of all ossified bone. Knock-out in NCC results in mice with severely hypoplastic mandible, maxilla, premaxilla, and nasal bones in addition to mineralization defects (Komori et al., 1997; Otto et al., 1997; Shirai et al., 2019). One downstream molecule regulated by Runx2 is *Osterix (Sp7*) which is a transcription factor required for osteoblast fate (K. Nakashima et al., 2002). Interestingly, Osterix is a co-activator that can partner with Dlx5 to initiate expression of ossifying genes (Hojo et al., 2016).

Ossification of the facial skeleton of mammals occurs through two processes. Intramembranous ossification is the primary mechanism wherein CNCC will differentiate into osteoblasts directly to form bone (Berendsen & Olsen, 2015). This process forms some of the bones of the neurocranium and viscerocranium. Other structures however are formed through endochondrial ossification which describes a process of cartilage replacement by invading osteoblasts, forming the base and posterior skull. In contrast, the zebrafish facial skeleton exhibit three types of ossification. Intramembraneous ossification produces the skull and opercular bones, similar to mammalian skeletogenesis where this ossification is important for the cranial vault and dentary. The second process is endochondrial ossification which is further broken into two types: 1) Type I where osteoblasts lay down a bone matrix following degradation of cartilaginous matrix to produce the ceratohyals and 2) Type II where ossification and calcification zones are absent and instead cartilage template is replaced by adipose cells. This latter process forms the hyomandibula, ceratobranchials and ethmoid plate (Weigele & Franz-Odendaal, 2016; Witten & Huysseune, 2009). Finally, the third type of ossification is perichondral ossification where bone is formed in the perichondrium, a dense layer of connective tissue that surrounds cartilage, and is the process that describes osteoblasts aggregating on the surface of cartilaginous template of the hyomandibula and Meckel's cartilage to deposit bone matrix (Hall, 2015).

1.4.7 Role of *Dlx* in craniofacial development

The *Dlx* genes are involved in craniofacial development beginning shortly prior to migration from the dorsal neural tube where CNCC from the first two rhombomeres will express *Dlx2* (Santagati & Rijli, 2003). Additionally, cells from r2 will lose *Hoxa2* expression so that

CNCC from r1 and r2 will migrate together to populate the first pharyngeal arch. In zebrafish, other *dlx* paralogs will also be expressed as CNCC are migrating, such as *dlx5a* (Yu et al., 2021). Once in the first pharyngeal arch, *Dlx* expression appears to provide patterning information along the dorsal-ventral and proximal-distal axes (Santagati & Rijli, 2003). *Dlx2*/*Dlx1* positive cells aggregate in the dorsal and proximal regions and *Dlx5*/*Dlx6* positive cells found more ventral and distal although overlapping of expression areas exist in the intermediate regions. This expression pattern is mediated by signals such as Edn1 and FGF8/9 in addition to transcription factors such as Mef2c as described in previous sections (1.3.2, 1.3.3).

Abnormal expression of *Dlx* paralogs within the craniofacial anlage result in severe consequences. Deletion of *Dlx2* in mice lead to loss and abnormal morphology of maxillary structures, clefting of the secondary palate and other malformations resulting in embryonic lethality (Qiu et al., 1995). Mice lacking *Dlx1* presented with only some of the changes observed in *Dlx2* mutants suggesting these paralogs may be compensatory or redundant in some regions of the first and second arch derivatives (Qiu et al., 1997). Supporting this reasoning, compound *Dlx1*/2 mutants die at birth and have exacerbated defects relative to both single mutants. Similarly, reduction of *dlx1a*, *dlx2a* or both paralog expression by morpholino-mediated knockdown resulted in deformities of first and second arch derivatives (Sperber et al., 2008). Loss of both paralogs presented with the most severe phenotype, much like compound mutants in the mouse. Additionally, reduced *dlx1a*/*dlx2a* expression led to increased NCC apoptosis and abnormal expression of downstream patterning genes involved in proper chondrogenesis.

While the consequence of *Dlx1*/*Dlx2* perturbations were defects in dorsal and proximal craniofacial structures, deletion of *Dlx5* in mice resulted in exencephaly and death shortly after birth (Acampora et al., 1999; Depew et al., 1999). Non-exencephalic mutants present with

dysmorphology of proximal structures of the mandibular component of PA1. In particular, the Meckel's cartilage is shortened and does not connect correctly with the middle ear, leading to an ectopic intramemranous bone by P0. Additional morphological defects were apparent in the otic and nasal capsules which led to sensory impairments. Loss of *Dlx5* also led to a shortened soft palate and absence or dysmorphology of muscles that help with the function of the soft palate such as swallowing or sucking, through dysregulation of FGF10 signaling (Sugii et al., 2017). Interestingly, knockdown of *dlx5a* or in the *dlx5a* hypomorphic mutant in zebrafish only resulted in mild defects of the intermediate domain (jaw joint, second arch joint, opercle, branchiostegal bones), in contrast to the phenotypes observed in mice (Talbot et al., 2010).

The compound null mutant for *Dlx5*/*Dlx6* in mice revealed the most severe craniofacial phenotype wherein neonates die shortly after birth, are usually exencephalic and those that had a formed head presented with a complete loss of the Meckel's cartilage due to homeotic transformation to a secondary maxillary (Beverdam et al., 2002; Depew et al., 2002; Merlo et al., 2002; Robledo et al., 2002). Other craniofacial defects include fused or dysmorphic inner and middle ear cartilages, severe patterning defects of cranial floor cartilages and reduced ossification of cartilage structures (Robledo et al., 2002).

Despite the above observations on *Dlx*/*dlx* gene function during craniofacial development, little is known about how each paralog affects development of craniofacial structures. This is particularly true in the case of mammalian studies since loss of one or more *Dlx* genes lead to embryonic or early lethality.

1.5 Nervous system development and *Dlx* genes

1.5.1 Induction and neurulation

The vertebrate nervous system begins development during gastrulation when the three germ layers are produced. Cells on the surface of the embryo will actively migrate to the center through a small invagination or opening called the blastopore. The ectoderm is induced to a neural fate through the activity of three factors secreted by the dorsal blastopore lip, called the shield in zebrafish and the node in the mouse (Spemann & Mangold, 1923; Beddington, 1994; Oppenheimer, 1953; Ozair et al., 2013). These proteins are Noggin, Chordin and Follistatin, all three which antagonize BMP activity. Activity of these antagonists help create a BMP gradient where the neural plate will develop under low BMP conditions.

Through interactions with the neighboring epidermis and signals from the organizer, patterning of the neural plate results in a wider portion of the neural plate at the anterior end and the posterior becoming narrower (Cox & Hemmati-Brivanlou, 1995; Niehrs, 1999; Ozair et al., 2013). The wider portion will become the brain while the narrow portion will become the spinal cord. Two processes occur to form the neural tube from the neural plate: primary neurulation in which neural plate cells proliferate, fold and invaginate into the body to form hollow tube; and secondary neurulation where an aggregate of mesenchyme cells form a solid cord that subsequently hollow out (Harrington et al., 2009). In many vertebrates, both processes are used: primary neurulation at the anterior and secondary neurulation more posterior (Catala et al., 1995; Lowery & Sive, 2004). In zebrafish, some controversy exists whether primary neurulation occurs at the anterior since zebrafish neurectoderm first forms the neural keel, a solid rod of cells before forming a lumen and tube (reviewed in Lowery & Sive, 2004). However, the neural keel is not made of mesenchymal cells and recent studies have identified hallmarks of primary

neurulation during formation of zebrafish forebrain such as presence of the hingepoint (Werner et al., 2021).

1.5.2 Organization and regionalization of the embryonic brain

After the anterior portion of the neural tube is formed, patterning to segment the structure into three primary vesicles is already underway. These three vesicles, from anterior to posterior, are the prosencephalon (forebrain), mesencephalon (midbrain) and rhombencephalon (hindbrain). By the time the neural tube is fully formed, secondary vesicles are present to segment the prosencephalon into the telencephalon and diencephalon, while the rhombencephalon is divided into the metencephalon and mylencephalon (Purves et al., 2001).

Telencephalon

Shortly after neural tube closure, the telencephalon is further divided into the dorsal, pallial domain and the ventral, subpallial region through opposing gradients along the dorsoventral axis(Ulloa & Briscoe, 2007). Wnt and Bmp molecules from the dorsal midline and paramedial neuroectoderm opposes a Shh gradient from the anterior mesendoderm and later, the rostroventral telencephalon. Independent of Shh activity, the transcription factor *Foxg1* is important for the specification, survival, proliferation, and patterning of the ventral telencephalon. Deletion of *Foxg1* in mice or knockdown of *foxg1* in zebrafish result in loss of ventral precursors (Danesin et al., 2009; Duggan et al., 2008; Martynoga et al., 2005; Xuan et al., 1995). Fgfs are required for ventral telencephalic development: increased apoptosis of subpallial cells were observed when Fgf signaling was blocked and deletion of *Fgf* receptors result in failure to generate ventral telencephalon structures (Gutin et al., 2006; Shanmugalingam et al., 2000; Shinya et al., 2001; Walshe & Mason, 2000). The ventral

telencephalon or the subpallium consist of the ganglionic eminences from which GABAergic interneurons arise such as the medial ganglionic eminence that will become the future pallidum (involved in the limbic system) and the lateral ganglionic eminence that will become the future striatum. The amygdala also arises from this portion of the telencephalon.

The dorsal telencephalon domain also requires Fgfs and Foxg1 activity since loss of either affect the size of the dorsal telencephalon (Paek et al., 2009). Wnt signaling is also necessary and sufficient to produce mature dorsal identities in chick and mice where loss or gain of β-catenin function result in loss or gain of dorsal telencephalic cell identities and structures (Backman et al., 2005; Gunhaga et al., 2003). The effect Wnt signaling has on shaping dorsal telencephalon identity is in part due to regulating *Pax6* expression (Gunhaga et al., 2003). The dorsal telencephalon is divided into four domains that will develop into the neocortex (dorsal pallium), hippocampus (medial pallium), piriform cortex (lateral pallium) and components of the amygdaloid complex (ventral pallium) (Medina et al., 2004; Puelles et al., 2000).

Diencephalon

The diencephalon lies posterior to the telencephalon and is divided into three segments known as prosomeres. Signals including Wnt, Shh, Fgf and Bmp are critical for inducing and maintain prosomere identity (López-Bendito & Martini, 2020). Prosomere 1 (P1) which abuts the midbrain, will develop into the pretectum, and parts of the ventral tegmental area and substrantia nigra (Borostyánkoi-Baldauf & Herczeg, 2002; Garcia-Lopez et al., 2004). These areas are important in oculomotor and visuomotor functions as well as motor control and head orientation reflexes. Prosomere 2 is anterior to P1 and will produce the habenula and pineal

body in mature brains (Garcia-Lopez et al., 2004; Hikosaka, 2010). Finally, prosomere 3 the most anterior and ventral segment and will develop into the prethalamic nuclei and prethalamic eminence.

Mesencephalon

The midbrain region is defined by two borders: the diencephalon-mesencephalon boundary and the midbrain-hindbrain boundary. The diencephalon-mesencephalon boundary is produced via repressive interaction between *Pax6* expressed throughout the diencephalon and *En/Pax2* which are markers of the midbrain (Matsunaga et al., 2000; Walther & Gruss, 1991). The midbrain-hindbrain boundary through interaction between the midbrain *Otx2* and the hindbrain *Gbx2* transcription factors (Shamim & Mason, 1998; Simeone et al., 1992). With these two boundaries established, the midbrain is divided into two domains through a dorsoventral gradient of Shh from the floorplate (Echelard et al., 1993; Ericson et al., 1996; Nomura & Fujisawa, 2000). The transcription factors *Pax3* and *Pax7* are also highly expressed in the roofplate to establish the tectum domain whereas the ventral domain delineates the tegmentum domain (Matsunaga et al., 2001). The tectum will become the optic tectum in birds, fish and amphibians or the superior colliculus in mammals. The tegmentum becomes several structures including a portion of the reticular formation, the substantia nigra and ventral tegmental area.

1.5.3 Organization and regionalization of zebrafish telencephalon

In mammalian telencephalon development, a process known as evagination occurs describing the bilateral expansion of telencephalic hemispheres with neural wall enclosing a

centrally located ventricle (Fig. 1.5a). Thus, the proliferative regions of the brain, the ventricular and subventricular zone are located in the center of the brain. In ray-finned fish including zebrafish however, a separate process called eversion is used in telencephalon development. In eversion, the midline dorsal pallium rolls outwards laterally, resulting in the ventricles being pulled outwards from the middle of the two hemispheres and surrounding the outer dorsal layers of the telencephalon (Nieuwenhuys & Meek, 1990; Northcutt & Braford, 1980; Wullimann, 2009). Consequently, proliferative regions of the brain are found in the center of the telencephalon and surrounding dorsal regions. The partial eversion hypothesis proposed by Wullimann (2004) suggest that medial pallium and dorsal pallium are everted but not the lateral and ventral pallium, through anatomical and marker expression data (Wullimann & Mueller, 2004)(Fig. 1.5b). This hypothesis also suggests that despite anatomical locations differing, zebrafish possess analogous structures to mammalian brains such as the lateral ganglionic eminences being analogous to the teleostean dorsal subdivision of dorsal subpallium near the center ventricle.

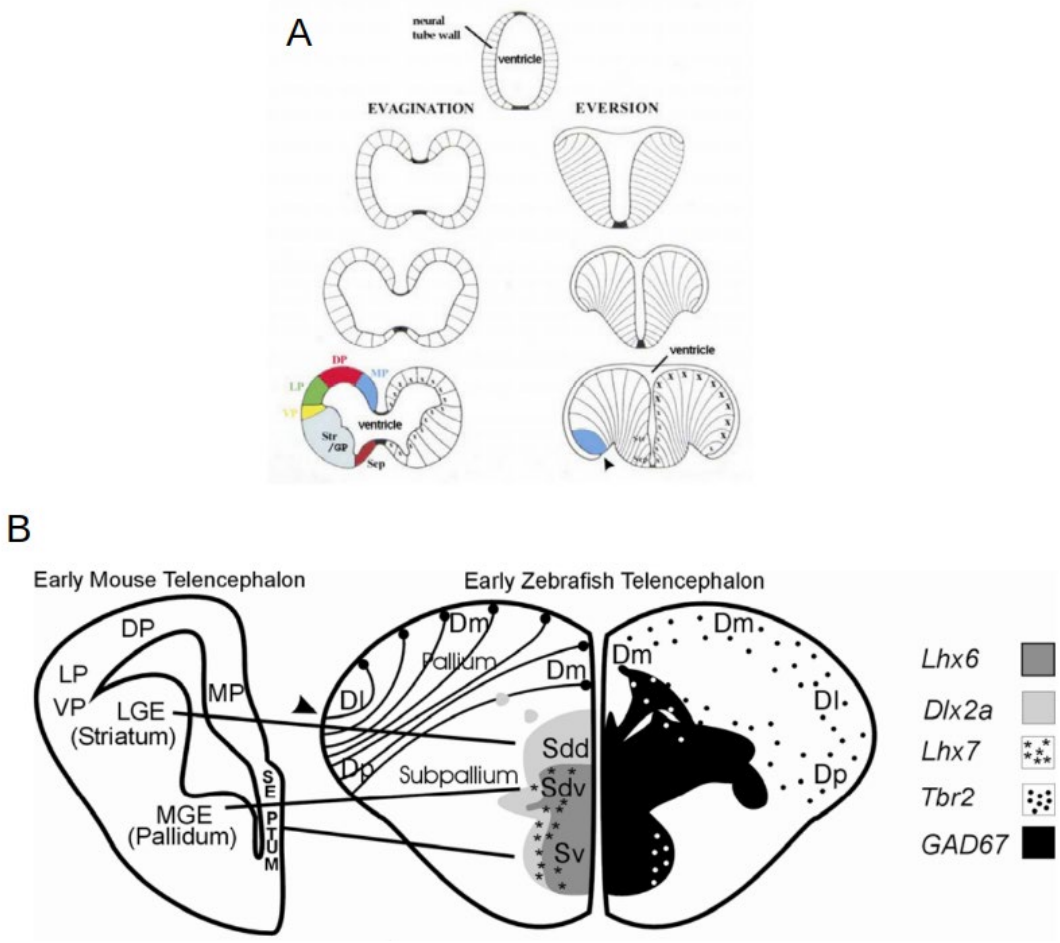

Figure 1.5. Regionalization and organization of the teleost telencephalon.

(A) Mammalian telencephalon arise through a process known as evagination where the two lobes of the brain balloon out from the ventricle. Teleostean telencephalon undergo eversion instead where the midline dorsal pallium fans out resulting in altered topology of telencephalon regions. **(B)** Analogous structures between mouse telencephalon and zebrafish. Expression of certain markers of telencephalic regions were used to identify analgous regions. Figure adapted from Wullimann, 2009.

1.5.4 GABAergic interneuron development

Gamma-aminobutyric acid (GABA) is the main inhibitory neurotransmitter in the vertebrate central nervous system. Once released into the synaptic cleft, the neurotransmitter will open inhibitory ion channels on the post-synaptic membrane. Production of GABA from glutamate requires the activity of two enzyme isoforms: glutamate decarboxylase (GAD)67 and GAD65. The two isoforms are encoded by the genes *Gad1* and *Gad2* respectively. While these two enzymes are often co-expressed, the subcellular localization of expression differs: GAD67 is usually in the cytoplasm and synthesize GABA for cell metabolism whereas GAD65 is found in axon terminals, responsible for GABA synthesis in an activity-dependent manner (Pinal & Tobin, 1998).

Cells that express GABA in the mammalian brain originate from transient subdivisions of the subpallium called the ganglionic eminences. There are three ganglionic eminences (GE) based on their location: medial (MGE), caudal (CGE) and lateral (LGE) which all give rise to GABAergic interneurons although the destination and subtyping of these neurons differ based on their origin (Laclef & Métin, 2018). The main GABAergic interneurons produced in the MGE are parvalbumin and somatostatin expressing neurons whereas calretinin, VIP, reelin subtypes originate mostly from the CGE and LGE (Butt et al., 2005; Corbin et al., 2003; Flames et al., 2007; Fogarty et al., 2007; Xu et al., 2004, 2008). As such, each area of the GE express similar and unique transcription factors that may play a role in specifying different types of GABAergic interneuron subtypes. Expression of *Ascl1* and *Dlx* paralogs are observed in all three GEs where *Ascl1* is found in the ventricular and subventricular zones to aid in neurogenesis and *Dlx* paralogs are expressed in both neurogenic areas and regions of differentiating progenitors (Casarosa et al., 1999; Long et al., 2009; Petryniak et al., 2007; Potter

et al., 2009; Yun et al., 2002). In contrast, cells from the MGE also express *Nkx2.1*, *Lhx6* and *Sox6* whereas cells from the CGE and LGE express *Prox1*, the serotonin receptor *5-HT3a*, the orphan nuclear receptor *Nr2f2* and *Sp8* (Azim et al., 2009; Butt et al., 2008; Grigoriou et al., 1998; Kanatani et al., 2008; Miyoshi et al., 2015; Tricoire et al., 2010).

As these neurons are undergoing differentiation, they are also leaving the GEs to enter other parts of the brain via tangential migration. In tangential migration, neurons move parallel to the surface of the brain (Hatten, 2003). Tangential migration out of the GEs mostly occurs through two streams (Lavdas et al., 1999; Wichterle et al., 1999). The first is a superficial route through the marginal zone and the second is a deeper path overlapping with the SVZ. There is a third route that a smaller fraction of neurons takes through the subplate. For all three tracts, neurons will colonize the cortex homogenously (Marín & Rubenstein, 2001). Since GABAergic neurons from the GE all take the same routes out towards the cortex, similar molecular processes are used regardless of GE of origin, such as Sema3/ Nrp interactions (Marín et al., 2001; Tamamaki et al., 2003). At some point, neurons will switch from tangential migration to radial migration, to enter and integrate into cortical layers of the cortical plate (Lim et al., 2018). Mechanisms behind this switch and what cues are involved to determine which cortical layer each neuron integrates into is still unknown however neuronal activity appears to be critical in normal laminar layer distribution (Bortone & Polleux, 2009; de Marco García et al., 2011). Once in the correct laminar layer, GABAergic will complete differentiation and maturation, which may take up until post-natal ages.

Unlike the developing mammalian brain, zebrafish brains do not possess GEs. Instead, gene expression data suggest the dorsal subdivision of the dorsal subpallium is analogous to the LGE while the ventral subdivision of the dorsal subpallium is the teleostan MGE (Mueller &

Wullimann, 2009). The expression of *gad67 i*s observed in these areas located near the ventricles, one of the proliferative zones of the zebrafish brain during development and as adults (Mueller & Wullimann, 2009; Pellegrini et al., 2007; Zupanc et al., 2005). GABA expression is observable by 2dpf, overlapping with areas expressing gad67 except near the ventricles, suggesting GABA expression occurs only in post-mitotic cells (Mueller et al., 2006; Mueller & Wullimann, 2009). Furthermore, GABA expressing neurons also migrate tangentially from the region near the ventricles outwards and then radially, similar to amniote GABAergic interneuron migration tracts. Zebrafish brains also possess many of the same GABAergic interneuron subtypes including calretinin, somatostatin and parvalbumin.

1.5.5 Calretinin expressing GABAergic interneurons

Calretinin (CR) is a calcium binding protein first identified in the retina (Schwaller, 2014). About 10-30% of GABAergic interneurons express CR, representing a heterogenous group according to cell morphology such as bipolar or multipolar cell bodies (Kubota et al., 1994; Tamamaki et al., 2003). Some CR-expressing neurons also co-express other markers of GABAergic interneurons such as vasoactive intestinal polypeptide, cholecystokinin, neuropeptide Y and somatostatin (Cauli et al., 2014; Gonchar & Burkhalter, 1997; Wang et al., 2004). Additionally, CR expressing neurons also exhibit a range of firing potentials further highlighting the heterogeneity of this group (Karagiannis et al., 2009; Wang et al., 2002). As previously mentioned, most CR expressing neurons derive from the CGE with a smaller population originating in the dorsal MGE (Fogarty et al., 2007; Xu et al., 2004). These two

populations can also be classified as different CR neurons: VIP-bipolar neurons from the CGE and SOM-Martinotti neurons from the MGE.

1.5.6 Development of somatosensory systems of the peripheral nervous system

The peripheral nervous system (PNS) describes all the nerves and ganglia outside the brain and spinal cord (central nervous system, CNS), connecting the CNS to the body's limbs and organs. The PNS is divided into two systems: the somatic nervous system that controls voluntary movements through communication between sensory systems, CNS and motoneurons and the autonomic nervous system that regulates smooth muscle and glands without conscious input. The autonomic nervous system is itself divided into two systems: the sympathetic nervous system controlling "flight or fight" responses, and the parasympathetic system controlling "rest and digest" functions. NCC contribute to the entire PNS, forming cranial placodes with neuroectoderm and neuroepithelial cells to create the somatic nervous system, neurons of the dorsal root ganglia (somatic and sympathetic) and other sympathetic ganglia, and finally Schwann cell precursors, a derivative of NCC, make up the parasympathetic system ganglia (Baker & Bronner-Fraser, 2001; Dyachuk et al., 2014; Espinosa-Medina et al., 2014; Ladher et al., 2010).

The development of cranial placodes into sensory systems used by the somatic nervous system is well characterized. There six placodes shared among all vertebrates: the adenohypophyseal placode that produces the anterior pituitary; the lens placode generating the lens of the eye; the otic placode that forms inner ear structures, the sensory hair cells and the vestibulocochlear ganglion involved in vestibular stimuli sensation; the olfactory placode that generates the olfactory and vomeronasal epithelia; the epibranchial placode that lie dorsal to

pharyngeal arches to give rise to viscerosensory neurons including ganglia of the face, glossopharyngeal, vagal nerves and somatosensory neurons that mediate touch, temperature and pain sensation from skin; and finally the profundal and trigeminal placodes giving rise to subpopulation of somatosensory neurons of the profundal and trigeminal ganglia (Baker & Bronner-Fraser, 2001; Schlosser, 2010). Fish and amphibians possess a seventh placode called the lateral line placode that generates the hair cells and supporting cells of neuromasts, the sensory organs of the lateral line and neurons innervating those organs.

All cranial placodes derive from cells in the preplacodal area (PPA), a narrow band of non-neural ectoderm at the border between the neural plate and epidermis (G. F. Couly & le Douarin, 1987; G. Couly & le Douarin, 1990; Schlosser & Ahrens, 2004). The preplacodal area is also more anterior to the developing neural crest although the two cell populations are in close proximity (Schlosser, 2014). FGF ligands are important for the induction of PPA, but the origin and specific ligands are dynamic since FGFs are expressed in mesoderm, ectoderm and endoderm contacting the presumptive PPA and the types of ligands differ temporally and by species (Schimmang, 2007). Diversification of the PPA to generate different placodes is thought to be through different dosage and interactions between different FGFs from any of the three germ layers, and WNT from the hindbrain as morphogenesis of the neural tube continues. In particular, the otic placode appears to require WNT expression as demonstrated in mouse and chick where lower levels of β-catenin or increased antagonism of WNT signaling result in otic cell loss, but increased β-catenin activation leads to enlarged otic placodes at the expense of the epibranchial placode (Freter et al., 2008; Ohyama et al., 2006). BMP signaling is also involved in diversification of PPA ectoderm, as demonstrated in chick and zebrafish where inhibiting Bmp inhibits formation of epibranchial placodes (Begbie et al., 1999; Holzschuh et al., 2005).

Preplacodal ectoderm and NCC are not only closely positioned during neural tube formation, but the two populations also migrate together in a chase-and-run interaction. NCC may spatially constrict placodal formation (Bailey et al., 2006; Grocott et al., 2012; Theveneau et al., 2013). This interaction, mediated through SDF1/CXCR4 chemoattraction and subsequent contact inhibition through N-cadherin and cell polarity changes, was demonstrated to help subdivide the PPA and is particularly important for formation of epibranchial placodes. Ablation of premigratory NCC completely abolishes epibranchial cell movements and formation of placodes whereas blocking either SDF1 in preplacodal ectoderm or CXCR4 in NCC arrests NCC migration and ultimately prevents formation of epibranchial placodes. NCC is also involved in the formation of the lens placode by expressing TGF-β ligands to repress lens identity (Bailey et al., 2006; Grocott et al., 2012).

Once placodes are established, NCC continue to interact with placodal cells to form ganglia that innervate placodal sensory cells. Ablation of NCC in the chick lead to misplaced epibranchial ganglia with projections that fail to connect to hindbrain demonstrating the critical role NCC play in organization of central connections from placode to brain (Begbie & Graham, 2001). This is likely due to abnormalities in NCC migration since disrupting Nrp/Sema interactions or the interaction between the EGF receptor Errb4 and neuregulin leads to misplaced ganglia in the chick and mouse (Golding et al., 2004; Osborne et al., 2005; Schwarz et al., 2008). Ganglion condensation in the trigeminal ganglia is also dependent on NCC interaction with placode cells (Shiau et al., 2008). Finally, NCC-derived glia are also important for axonal pathfinding of the lateral line ganglia, are closely associated with neuromasts after development and may regulate the number of neuromasts deposited (Collazo et al., 1994; D. T. Gilmour et al., 2002; Grant et al., 2005; López-Schier & Hudspeth, 2005).

1.5.7 The posterior lateral line

The lateral line is a sensory system found in aquatic vertebrates including fish and amphibians that detect water motion and pressure in relation to the body in order to aid in navigation and behaviours such as shoaling, predator and prey detection and mating (Dijkgraaf, 1963; Montgomery et al., 2000). This system consists of a series of neuromasts connected by the lateral line ganglion which project into the medial octavolateralis nucleus of the hindbrain (Butler & Maruska, 2016). From this nucleus, ascending projections are made into the ventrolateral portion of the midbrain torus semicircularis that processes mechanosensory information. Neuromasts consist of hair cells that can transduce water vibrations into a chemical signal via microtubule-rich kinocilium bending into actin-rich stereocilia, which then activate ion channels (Fig. 1.6A). Support cells and mantle cells contribute to the structure of the neuromast. Each hair cell of a neuromast is independently innervated by afferent and efferent fibers. The lateral line is divided into two systems: the anterior lateral line that connects neuromasts of the head and the posterior lateral line (PLL) that describes the system of neuromasts along the trunk and tail of the organism. The PLL has been extensively studied in zebrafish and will be one of the foci of this thesis.

After the lateral line placode has migrated to a position just posterior of the otic placode, it is divided into two where the anterior portion develops into the PLL ganglion and the posterior half becomes the lateral line primordia that will migrate along the trunk towards the tail, depositing clusters of 20-30 cells at regular intervals of 5-7 somites (D. Gilmour et al., 2004; Ma & Raible, 2009; Metcalfe et al., 1985). This process begins at 19-25 hpf, neuromasts are recognizable by 48hpf and by 72hpf, the zebrafish larvae possesses around 12 neuromasts

representing the rudiments of three PLL that will continue to expand in number of neuromasts as the fish grows (Fig. 1.6B,C) (Ledent, 2002; Metcalfe et al., 1985). As adults, the total number of neuromasts may differ depending on the length and width of the fish body but all additional neuromasts will fall within one of three lines established as larvae forming vertical lines of neuromasts known as a stitch (Fig. 1.6D) (Ledent, 2002).

The migrating lateral line primordia exhibits pre-patterning where cells at the leading edge are unpatterned and become progressively specified closer to the trailing edge where cells are formed in clusters or rosettes called protoneuromasts before being deposited (Ghysen & Dambly-Chaudière, 2007; Lecaudey et al., 2008). This polarization is possible through an anterior to posterior gradient of Wnt and Fgf signals where Wnt is high in the leading (posterior) edge to maintain a population of progenitors as the primordia migrates and Fgf is highest at the trailing (anterior) edge to mediate protoneuromast formation (Aman & Piotrowski, 2008; Lecaudey et al., 2008; Nechiporuk & Raible, 2008). This bipartite gradient also influences changes in chemokine receptor expression, cell adhesion dynamics and cell polarity to allow for collective migration and protoneuromast deposition(Dambly-Chaudière et al., 2007; David et al., 2002; Hava et al., 2009). Growth cones from the lateral line ganglion follow the migration of the primordia, innervating protoneuromasts as they are deposited (Metcalfe et al., 1985).

Expansion of the lateral line as the fish grows larger is possible through development of intercalary neuromasts from latent progenitors deposited from the migrating primordia between protoneuromasts and through budding of established neuromasts to form accessory neuromasts (E. D. Thomas et al., 2015). Formation of intercalary neuromasts is regulated by Schwann cells from a nearby lateral line nerve in addition to Wnt and Fgf signaling (Lush & Piotrowski, 2014). Budding of accessory neuromasts from primary neuromasts forming a stitch is also regulated

by Wnt signaling but innervation is also required for proper stitch formation and maintenance since accessory neuromasts are innervated by the same nerve as the primary neuromast (Grant et al., 2005; Wada et al., 2013). Neuromasts can also regenerate following physical insult or exposure to heavy metals or aminoglycoside antibiotics through Schwann cell activity (Ceci et al., 2014; Sánchez et al., 2016).

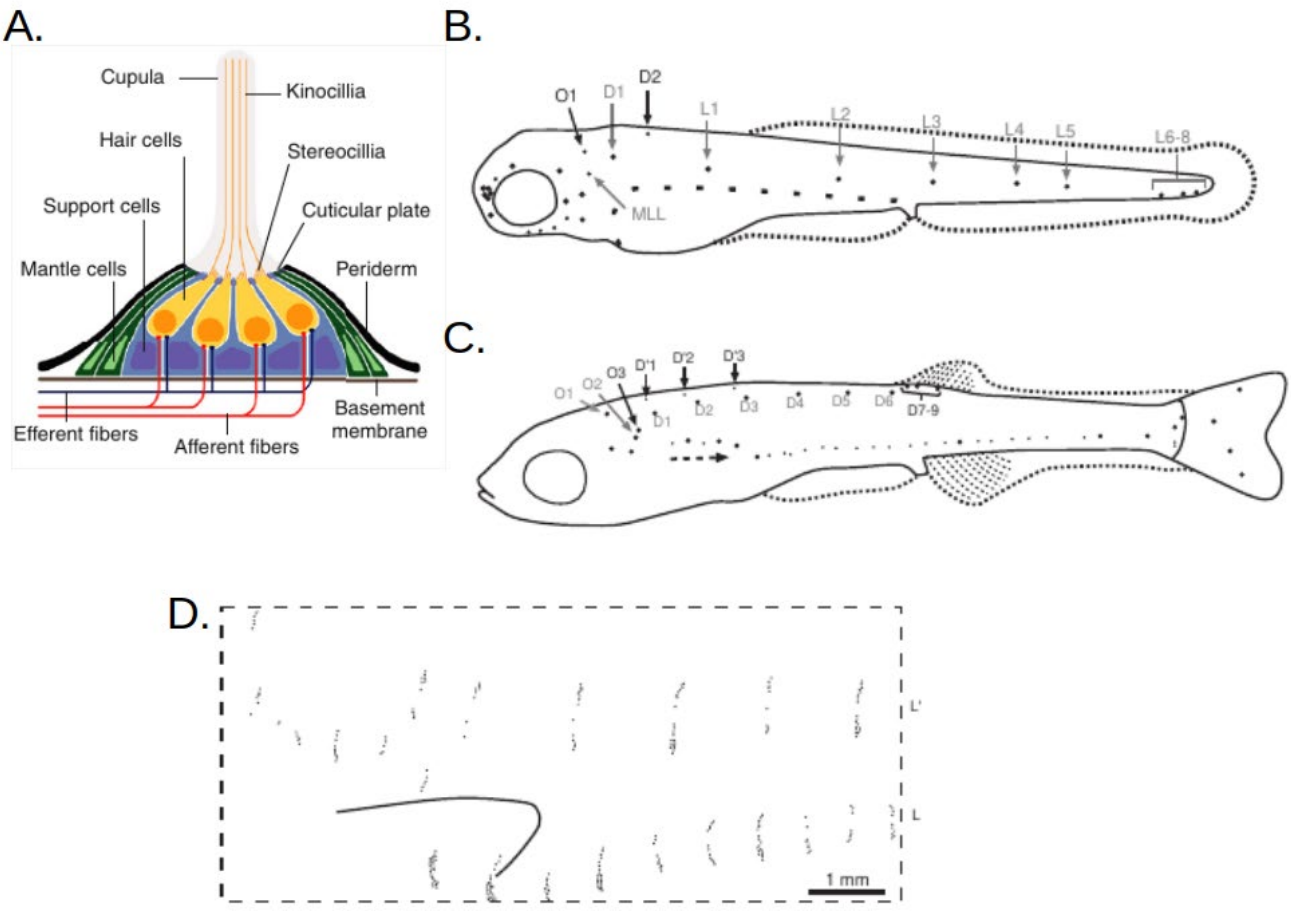

Figure 1.6. The lateral line is a system of neuromasts that become more elaborate along the trunk of the body as the fish grows.

(A) Schematic of a neuromast which is made of sensory hair cells (yellow), surrounded by support cells (purple) and mantle cells (green). Upon encountering vibrations in water, kinocilia will bend to move the shorter stereocilia, opening ion channels (adapted from Ma and Raible, 2009). **(B)** The rudimentary lateral line is present by 3dpf. O, D and L neuromasts represent different lateral line branches. **(C)** O, D and L PLL systems become more elaborate in juvenile fish. D) Part of the PLL system in an adult fish demonstrating stitch formation of the L and L' lines (adapted from Ledent, 2002)

1.5.8 Role of *Dlx* in the nervous system

Brain

The *Dlx* paralogs *Dlx1*, *Dlx2*, *Dlx5* and *Dlx6* are expressed in distinct and overlapping regions of the ganglionic eminences where *Dlx1* and *Dlx2* are expressed in the proliferative ventricular zone, *Dlx5* and *Dlx6* expressed in the mantle zone of migrating and differentiating neurons, and all four paralogs expressed in the subventricular zone (Bulfone et al., 1993; Simeone et al., 1994) (Fig. 1.7). There is also a temporal sequence of *Dlx* expression: *Dlx*, *Dlx1* and *Dlx5* then *Dlx6* with the latter two expressed in more differentiated neural progenitors (Eisenstat et al., 1999; J. K. Liu et al., 1997; Zerucha & Ekker, 2000). Thus, loss of *Dlx* expression generally result in alterations in GABAergic interneuron population and distribution in the brain, with some differences based on the *Dlx* lost. For example, knock-out of *Dlx1* does not result in embryonic lethality but rather in an age-dependent and location dependent loss of Gad67+ neurons in the neocortex and hippocampus but not in the olfactory bulb, thalamic reticular nucleus and hypothalamus where *Dlx1* is also expressed (Cobos et al., 2005). This reduction is correlated with decreases in the number of cortical interneurons making somatostatin, calretinin but not Parvalbumin. Knock-out of *Dlx2* also result in mild consequences to forebrain development in mice although homozygotes do die shortly after birth due to craniofacial abnormalities (Qiu et al., 1995). In contrast, knock-out of both *Dlx1* and *Dlx2* result in early post-natal lethality and abnormal proliferation, migration and differentiation of striatal neurons from the LGE possibly due to blocking proper cell-cell communication via Notch signaling (Anderson et al., 1997; Yun et al., 2002). Additionally, these mutants had a complete block in differentiation of GABAergic and dopaminergic interneurons in the olfactory bulb (Bulfone et al., 1998). The severity of phenotypes observed in double *Dlx1*/*Dlx2* knock-

out mutants but mild neural consequences in *Dlx1*$^{-/-}$ or *Dlx2*$^{-/-}$ suggest functional redundancy between these paralogs. Yet, the specific loss of certain subtypes of GABAergic neurons in the somatosensory cortex and hippocampus of *Dlx1*$^{-/-}$ mice also suggest GABAergic subtypes have differential *Dlx* requirements during development.

Deletion of *Dlx5* result in early postnatal lethality with profound cranial structure abnormalities including exencephaly making study of *Dlx5*$^{-/-}$ brains and other neural consequences difficult (Acampora et al., 1999; Depew et al., 1999). In intact brains, disorganization of OB cell layers and impairment of GABAergic interneuron differentiation and differentiation of dopamine neurons were observed (Levi et al., 2003; Long et al., 2003). Using neural stem cells from *Dlx5*$^{-/-}$ brains and culturing them into neurospheres, Perera and colleagues were able to further determine that loss of *Dlx5* does not affect proliferation nor apoptosis but did reduce differentiation into neurons, supporting the idea that *Dlx5* fulfills a function during later neurogenesis (Perera et al., 2004).

Simultaneous deletion of *Dlx5* and *Dlx6* leads to exencephaly of the anterior brain similar to *Dlx5* loss (Depew et al., 2002; Robledo et al., 2002). However, the brains of these dysmorphic mice exhibit normal telencephalic patterning, including preservation of normal *Dlx1* and *Dlx2* expression in the ventricular and subventricular zones of the LGE and MGE(Wang et al., 2010). However, tangential migration of interneurons was affected where cells of the superficial migratory stream was poorly formed and did not migrate as far into the neocortex compared to WT siblings. Furthermore, when cells from *Dlx5*/6$^{-/-}$ MGE were transplanted into a WT host, these cells produced significantly fewer parvalbumin neurons and the parvalbumin neurons that were produced had more neurites that were shorter demonstrating a role of *Dlx5*/6 in parvalbumin neuron differentiation.

The effect of *dlx1a*, *dlx2a*, *dlx5a* and *dlx6a* is less known in zebrafish brain development. Similar to the mouse, the above *dlx* paralogs and an additional paralog, *dlx2b* (through teleost-related duplication event) are expressed in distinct and overlapping regions of the zebrafish brain between 24 hpf and 48hpf (MacDonald et al., 2010). Additionally, *dlx1a, dlx2a* and *dlx2b* are expressed closer to the ventricle, which is proliferative and likely analogous to the mammalian subventricular zone whereas *dlx5a* and *dlx6a* are expressed outside the ventricular zone where more differentiated neurons are found, similar to mammalian *Dlx5*/*Dlx6* expression (MacDonald et al., 2010; Wullimann & Mueller, 2004). Knockdown of *dlx1a/dlx2a* and *dlx5a/dlx6a* also lead to reductions in expression of *gad1b*, the zebrafish ortholog of *Gad1*, suggesting loss of function of zebrafish *Dlx* orthologs may result in reductions of GABAergic neuron numbers (MacDonald et al., 2013). Furthermore, lineage tracing experiments demonstrated some cells that expressed *dlx1a/dlx2a* co-express somatostatin or calretinin whereas some cells that expressed *dlx5a/dlx6a* are parvalbumin positive, supporting the idea certain *dlx* paralogs are more associated with certain subtypes of GABAergic interneurons (Solek et al., 2017). Expression of all four *dlx* paralogs in the brain persist into adulthood where transcripts are detected in the telencephalon and periventricular hypothalamus of the midbrain in addition to almost all neurogenic niches of the adult zebrafish brain suggesting a role in constitutive proliferation (Mendes et al., 2020).

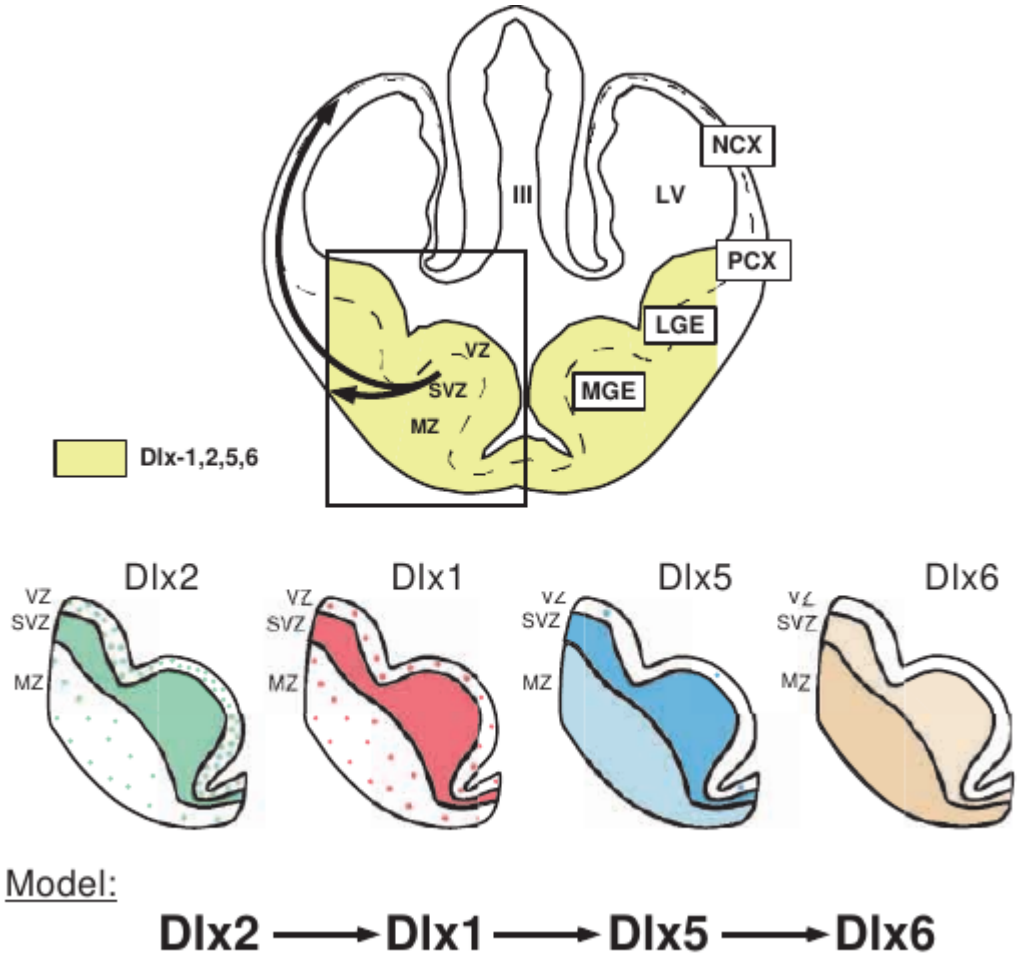

Figure 1.7. Expression of Dlx genes in the developing mouse telencephalon.

Dlx paralogs are expressed in overlapping and distinct regions of the ganglionic eminences following a temporal sequence. Figure from Panganiban and Rubenstein, 2002.

Sensory systems

Some evidence suggest *Dlx* activity is involved in development of various sensory systems of the PNS. *Dlx5* is involved in forming the neural plate border and as such is involved in subdividing the early embryonic ectoderm to help form the PPA(Yang et al., 1998). Loss of *Dlx5* in the mouse leads to abnormalities in otic placodogenesis, development of the otic vesicle and structural defects in components of the inner ear required for vestibular sensation (Acampora et al., 1999; Depew et al., 1999). Furthermore, loss of an enhancer regulating *Dlx5* expression in mice result in deafness and abnormal locomotion characterized by rapid circling and head shaking due to structural defects in semicircular canals (Johnson et al., 2018). Loss of *Dlx2* in mice was shown to affect trigeminal ganglia arborization where nerves that enter the mandibular arch made abnormal connections towards the lateral surface of the proximal mandibular arch instead (Qiu et al., 1995). Knockdown of *dlx2a* in zebrafish resulted in loss of trigeminal sensory ganglia, potentially due to reduced NCC survival (Sperber et al., 2008).

1.6 CRISPR-Cas9 mediated genome editing

The clustered regularly interspaced short palindromic repeat (CRISPR)-Cas genome editing system was initially discovered over 30 years ago in *E. coli* but the function of these repeated sequences would not be known until much later after discovery in a number of other bacteria and archaea genomes as a type of immune system against bacteriophages and archaeal viruses (Ishino et al., 1987; Mojica et al., 1993, 2005). At the same time, several other genes were identified in hyperthermophilic archaea as associated with CRISPR called Cas (CRISPR-associated) genes and were thought to work with CRISPR to function as acquired immunity akin to RNAi systems in eukaryotes (Jansen et al., 2002; Makarova et al., 2002, 2006). In

general, the process of CRISPR-Cas genome editing requires three steps: 1) invading phage DNA is identified and fragmented by Cas protein; 2) the fragments are inserted into the CRISPR locus as spacers; 3) the CRISPR locus is transcribed with the new phage-derived fragment (pre-crRNA) which is processed into the crRNA before binding to Cas protein to allow the protein-RNA complex to cleave foreign DNA (Ishino et al., 2018).

Two classes of CRISPR-Cas systems were subsequently described based on the effector proteins involved: class 1 are systems with multi-subunit effector proteins of 4-7 cas proteins whereas class 2 are systems using single multidomain Cas proteins (Burstein et al., 2016; Shmakov et al., 2017). It is the latter class that is used in most genome editing strategies due to the relatively few components required- a single Cas protein that is both capable of binding the crRNA and induce double-strand breakage of DNA. Of the different Class 2 Cas proteins, Cas9 is the most commonly used since it is the best studied multidomain effector protein.

Much work has been done since the discovery that CRISPR-Cas systems (in particular, CRISPR-Cas9) can be used to edit genomes to make the process as simple and targeted as possible (Jinek et al., 2012). In this simplified system, only the Cas9 protein and a synthetic "guide-RNA" consisting of a fusion of the crRNA and transactivating crRNA is required. The guide-RNA will bind to the Cas9 protein and by base complementarity, will direct the enzyme to the DNA target of interest. This system has been used extensively in many models including zebrafish, as a more efficient alternative to previously common methods of genome editing such as zing finger nuclease or transcription activator-like effector nucleases (W. Y. Hwang et al., 2013; Jao et al., 2013; Ota et al., 2014).

1.7 Statement of inquiry

The *dlx* genes are clearly crucial to development of various tissues based on the high conservation observed among vertebrates yet understanding how each paralog influences development is still largely unknown. Majority of previous analysis on Dlx function was performed in mice however knock-out of individual or combinatory *Dlx* genes usually resulted in embryonic or early lethality. Therefore, the overall purpose of my thesis is to explore the role of each *dlx* paralog of interest (*dlx1a, dlx2a, dlx5a* and *dlx6a*) during development of the craniofacial and nervous system in zebrafish. Analysis in zebrafish may be particularly useful since embryos develop *ex utero*, an extensive molecular toolbox is available for use and the model is highly amenable to genome editing. To fulfill this goal, three specific aims will be addressed:

First, what is the cross-regulatory consequence of *dlx* paralog loss on the expression of the remaining *dlx* genes of interest during early zebrafish development (1-3 days post fertilization)? This aim will probe the similarities and differences underlying *dlx* expression between zebrafish compared against knowledge gleaned from mouse studies.

Second, I aim to identify how loss of each *dlx* paralog of interest affect craniofacial development. Specifically, I will determine if any gross anatomic changes occur, and identify the molecular mechanisms underlying those changes.

Third, I will explore the effect of *dlx* loss during nervous system development. Specifically, I will focus on the impact on calretinin neuron distribution in the brain during larval and adult ages. Additionally, I will describe consequences of *dlx* loss on the PLL in zebrafish to further substantiate the role of *dlx* function in the sensory nervous system.

Chapter 2

Materials and Methods

2.1 Animal care and husbandry

All experiments were conducted following protocols approved by the University of Ottawa Animal Care Committee. Adult zebrafish were housed in circulating water at 28.5˚C with a 14hr light cycle. Embryos were collected from natural spawning and raised in E3 embryo media at 28.5˚C. Phenylthiourea (final concentration of 0.003%) was added at 24-26hpf to prevent development of pigmentation when required. Larvae older than 5dpf were housed in petri dishes in system water and fed a diet of rotifers or pulverized flake food twice daily. A water change was performed prior to each feed.

2.2 CRISPR-Cas9 mutagenesis

For each *dlx* gene, multiple guide-RNAs (sgRNAs) were designed to target the 5'UTR or the first exon and 3'UTR or last exon using CHOPCHOP (Montague et al., 2014). Templates for sgRNA transcription were generated by annealing gene specific oligonucleotides containing T7 promoter sequence, the 20-base pair target site, and a complementary region of 80 bp constant oligonucleotide (Gagnon et al., 2014; Varshney et al., 2015). The MAXIscript T7 kit (Life Technologies) was used to synthesize sgRNA from oligonucleotide templates following manufacturer protocols. Cas9 protein (New England Biolabs) and at least two sgRNAs targeting the 5'UTR and 3'UTR (final concentration of 20ng/µL each) were injected together with 0.1% phenol red (Sigma) into 1-2cell stage embryos. Potential founders were identified using PCR on gDNA from pooled 3dpf embryos after crossing with WT. Deletion of target gene was also confirmed by sequencing gDNA of individual F1 heterozygous fish. Table 1 lists the sequences for sgRNAs templates. Table 2 lists the primers used for genotyping and expected amplicon size.

Table 1 sgRNA sequences for generating *dlx* mutants

Mutant	sgRNA 1 (5'-3')	sgRNA 2 (5'-3')
dlx1a	GGACCAATCAGAGAGCACCT	GGTCCCCTGAACTGGGCCAT
dlx2a	GGCAATGATCAACGTGGCAT	GGAAACGCTTTCGGCCCCTA
dlx5a	GGCTATTACAGCCCTGCCGG	GGCTCTCGATATAATGGCAT-
dlx6a	GGGAGCCGGAATGGAGACAG	GGCAGGTACGGACTGTGGTG and GGCGTGTCAATGGTCGACAA
inter56	GGCGTGTCAATGGTCGACAA	GGCTCTCGATATAATGGCAT
dlx5i6	GGGAGCCGGAATGGAGACAG	GGCAGGTACGGACTGTGGTG

Table 2. Primers for genotyping *dlx* mutants

Target	Forward sequence (5'-3')	Reverse sequence (5'-3')	Product size
dlx1a WT	CCTATGCGTCTCGGTCCATT	CGTAGTGCGTCGACAAAAGC	740
dlx1a mutant		GTGTTTCTTCTCCGGTGCGA	320-350
dlx2a WT	GCATGAAACACATGGAAACCGA	AGTCTCCACCTCACCCCTCA	629
dlx2a mutant	TTGCTGACGCGACATTGC	CAAGTCCCAGGAATCGCCG	130-160
dlx5a WT	ATCAAGAACCAGGCGCATCT	GAGCCCACACAGAGATAGCA	498
dlx5a mutant		CCCTTTTCAGCTCTCCACGAT	290-310
dlx6a WT	GGAGGCTCAAGACTCGTCAA	TTGCTGACATACGACGGGG	429
dlx6a mutant		AAAACGATTCGCTTCCTGTC	200-250
inter56 WT	AGCTACATGCCCGGCTATTC	GGACAAGATGCGGCTCTATTC	796
inter56 mutant		ATAGCCCCCAACCTACAAGC	350-400
dlx5i6 WT	GGAGGCTCAAGACTCGTCAA	TTGCTGACATACGACGGGG	429
dlx5i6 mutant		CCCTTTTCAGCTCTCCACGAT	200-230

2.3 Whole mount RNA in situ hybridization (WISH)

Antisense mRNA probes were labelled with digoxygenin-dNTP (Roche, #11277073910) and synthesized from PCR fragments or cDNA clones: *dlx1a*, *dlx2a*, *dlx5a, dlx6a, sox9a* (Akimenko et al., 1994; Chiang et al., 2001; Ellies et al., 1997; Stock et al., 1996). Vectors containing cDNA clones were linearized with B*am*H1 or *Eco*R1 (Thermo Fisher) and the antisense riboprobes were synthesized with either T3 or T7 RNA polymerase as required (Thermo Fisher). PCR primers with T3 (forward) or T7(reverse) polymerase binding sites were used to generate RNA probes for *foxd3*, *col11a2*, *wls* and *wnt5b* (Table 3).

Embryos under 72hpf were manually dechorionated prior to overnight fixation in 4% PFA/PBS at 4°C. Whole mount RNA *in situ* hybridization (WISH) was performed on age-matched mutant and wild-type embryos per probe and genotype following previously described protocols (Thisse & Thisse, 2008). At least two trials per probe and mutant at each time point were performed. Images presented are representative of 15-30 larvae per time point and genotype unless otherwise indicated.

Table 3. Primers for *in situ* hybridization RNA probe generation

Target	Forward sequence (5'-3')	Reverse sequence (5'-3')
foxd3	AATTAACCCTCACTAAAGGCTCAGTGGAATC TGCGAGT	TAATACGACTCACTATAGCCATTTCGATACCGCT GCTG
col11a2	AATTAACCCTCACTAAAGAGACCTCGTTTGT GCTCCTC	TAATACGACTCACTATAGACGGGCTCCAAAAAC AGTGA
wls	AATTAACCCTCACTAAAGCGGATGGAGCTTC GATCACC	TAATACGACTCACTATAGCATTGCGCAGGCAGT AATCC
wnt5b	AATTAACCCTCACTAAAGGTGACCCTCATCG TCTGCAA	TAATACGACTCACTATAGCATTGCGCAGGCAGT AATCC

2.4 Alcian blue, alizarin red staining and morphometrics

Alcian blue and alizarin red staining in 5dpf larvae was performed following established protocols (Walker & Kimmel, 2009). For staining in 14dpf larvae, the following modifications were used: larvae were fixed with 2% PFA for 1.5hrs at room temperature (RT) then washed in 10mM Tris, pH 7.5/10mM $MgCl_2$ for 15 min prior to 0.04%/10mM $MgCl_2$ alcian blue staining overnight. Stepwise rehydration with 80%, 50%, 25% ethanol/100mM Tris for 15 min. Samples were then washed in 0.5% KOH for 15min and then bleached with 3% H_2O_2/0.5%KOH for 15min. Rinsed with 35% saturated $NaBO_4$ for 15min, digested with 1% Trypsin in saturated $NaBO_3$ for 15min. Washed with 10% glycerol/0.5% KOH until samples are saturated before staining overnight with 0.01% alizarin, pH7.5. Washed with 50% glycerol/0.1% KOH until saturated and a second wash overnight before storage and/or imaging in 70% glycerol/H2O.

Measurements were made using ImageJ of each side of the Meckel's cartilage, palatoquadrate, and ceratohyal for each imaged animal in the ventral position. The measurements were then averaged to account for left or right skewing during positioning of the larvae and then averaged again for each genotype.

2.5 BrdU treatment

At 52hpf or 5dpf, *dlx5i6*$^{+/-}$*; sox10:GFP* incrossed larvae were treated with either 10mM BrdU (Sigma B5002) or 15mM BrdU respectively with 10% dimethysulfoxide in system water following established protocols (Ling et al., 2017; Verduzco & Amatruda, 2011). Larvae were then washed three times with system water and recovered for 4 hours at 28.5˚C in system water. At 4 hours post treatment (hpt), all treated larvae were euthanized with tricaine on ice before decapitation below the yolk ball. Heads were fixed in 2% PFA/PBS for 30 minutes at room

temperature in 96 well plates and the posterior portion lysed for genotyping in 10ul 0.05mM NaOH. After PFA fixation, samples were washed with 1xPBS and then stored in 100% methanol at -20˚C until genotypes were identified.

2.6 Vital dye staining

For acridine orange staining, live embryos at 2dpf and 3dpf were stained with 10ug/mL of acridine orange (3, 6-Bis(dimethylamino) acridine hydrochloride zinc chloride double salt; Sigma-Aldrich) in system water for 30 minutes in the dark at RT (~23˚C). Larvae were washed three times with system water prior to imaging.

To stain neuromasts, larvae (3dpf), juveniles (1-2months) or adults (3+months) were incubated with 0.005% DASPEI (2-(-(Dimethylamino) styryl)-N-ethylpyridinium iodide; Biotium) in system water for 15 min, 30 minutes, or 1 hour respectively. Fish were washed twice with system water and allowed to recover in fresh system water for up to 5 minutes before imaging.

2.7 Neuromast regeneration

Prior to treatment, fish body length was recorded and transferred to numbered static tanks. Neuromasts were stained and imaged to record pre-treatment neuromast number and distribution. To degenerate neuromasts, fish were incubated with 0.001% gentamycin sulfate (Sigma, G-3632) with system water in static tanks overnight at 28.5˚C. For the next two days, complete water changes occurred twice daily along with regular feeding with standard diet food (van Trump et al., 2010). At 48 hpt, fish were stained with DASPEI and imaged to confirm

neuromast degeneration. Fish were stained and imaged once more at 72 hpt to observe neuromast regeneration.

To analyze neuromast regeneration, neuromasts for each posterior lateral line was counted for each fish from images taken prior to gentamycin treatment and three days after treatment. The difference in neuromast number per line between post- and pre- gentamycin treatment was calculated and graphed.

2.8 Immunohistochemistry

For BrdU staining, samples were rehydrated step-wise in 75%/50%/25% methanol/PBST then washed in PBST before permeabilized with 10mg/mL proteinase K for 20 minutes (56hpf) or 40 minutes (5dpf). Samples were then post-fixed with 4% PFA/PBS for 20 minutes followed by 2N HCl for 30 minutes (56hpf) or 1 hour (5dpf) for antigen retrieval. All samples were blocked with 10% FBS/PBST for 1 hour at RT

For microtubule organizing center (MTOC) staining, larvae were euthanized in excessive tricaine and then fixed in 4% PFA/PBS overnight at 4°C. Samples were washed with PBST then cut below the yolk ball for greater antibody penetration and easier manipulation imaging. Samples were then digested with 10mg/mL proteinase K for 30 minutes and then washed 3 times 15 minutes with 0.1% PBS-TritonX (PBSTr) before blocking with 10% FBS/ 0.5%PBSTr for 2 hours at RT.

For staining of neuromasts and hair cells in 3dpf larvae, larvae were euthanized in tricaine and fixed in 4% PFA/PBS overnight at 4C. The following day, larvae were washed in PBST, 2x10 min then washed 2x 10min with PBSTr. To increase permeabilization of antibodies, larvae were incubated in 1% tritonX-100 in 1xPBS for 8 hours at RT. The next day,

samples were blocked in 10%FBS/PBSTr for 2 hours at RT. Alexa Fluor 594-phalloidin was treated as a secondary antibody for this procedure.

For all staining in larvae (intact or not), samples were incubated with primary antibodies in 1%FBS/PBST or 1% FBS/PBSTr overnight at 4°C after blocking. Samples were washed the next day 3x 15min with PBST or PBSTr and then incubated with secondary antibodies in 1%FBS/PBST or PBSTr overnight at 4°C. Samples were washed the next day 3x 15 min in PBST prior to mounting for imaging.

For calretinin neuron labeling, size-matched adult (4 months – 1.5 years) mutant-WT sibling pairs were euthanized and decapitated. Adult brains were dissected the same day and fixed in 4% PFA/PBS at 4°C overnight. Following fixation, all samples were washed with 1x PBS twice prior to treatment with 15% sucrose-PBS until saturated. Samples were then incubated with 30% sucrose-PBS overnight at 4°C before mounting into cryo-moulds with OCT compound (Tissue-Tek VWR) and frozen in liquid nitrogen. Samples were sectioned at 14-18um using the CM3050S cryostat (Leica) in triplicate. Slides were labelled in a code to prevent bias during staining and cell counting. After immunohistochemistry, 50µL of VECTASHIELD PLUS Antifade Mounting Medium with DAPI (Vector Laboratories, H-2000) was added to each slide, cured for 30-45 minutes and sealed with nail polish. Stained slides were stored up to 1 month at 4°C.

A list of antibodies and the concentrations used can be found in Table 4 below.

Table 4. Antibodies used for immunohistochemistry

Host	Target	Supplier information	Dilution
Mouse	Acetylated tubulin	Millipore Sigma, T7451	1:200
Mouse	BrdU	Life Technologies, B35128	1:400
Mouse	Calretinin	Swant, 6B3	1:400
Rabbit	GFP	Life technologies, A11122	1:500
Goat (IgG H+L) Alexa 488	Mouse	Life Technologies, A11001	1:1000 or 1:300
Goat (IgG H+L) Alexa 594	Mouse	Life Technologies, A11005	1:1000
Goat (IgG H+L) Alexa 488	Rabbit	Life Technologies, A11008	1:1000
Goat (IgG H+L) Alexa 594	Rabbit	Life Technologies, A11012	1:300
N/A	AlexaFluor 594-Phalloidin	Thermo Fisher Scientific, A12381	3:100

2.9 RNA extraction, cDNA synthesis and RT-qPCR

Total head RNA was extracted from 2dpf and 3dpf *dlx5a*$^{-/-}$ and WT sibling larvae with TriZol (Invitrogen, Thermo Fisher) according to manufacturer's protocol. A pool of 20-25 embryos was used for each timepoint from three different crosses to generate three biological samples. After precipitation, all RNA were analyzed for purity and integrity through gel electrophoresis and using the NanoDrop 1000 spectrophotomerter (Thermo Fisher Scientific). Samples with absorbance of 1.95-2.1 and clear 18S and 28S bands were used for cDNA synthesis. For cDNA synthesis, 750ng of RNA was used for iScriptTM cDNA Synthesis Kit

(Life Science Research, Bio-Rad) following manufacturer's protocol. RT-qPCR was performed in triplicate with 1:4 cDNA diluted in nuclease-free water and using SsoFastTM EvaGreen® Supermix (Bio-Rad) on the Bio-Rad CFX96 instrument. Table 5 lists primers for *sox9a*, *col11a2*, *wnt5b*, *ror2* and *frzd7a*. Since primers for *wnt5b* had poor efficiency even after various parameters were altered during optimization, two primer pairs were used to corroborate results. For reference genes, *ef1a* and *r18s* were used (Kalyn & Ekker, 2021; McCurley & Callard, 2008). Primer efficiencies through standard curve using serial cDNA dilutions for all targets were between 89%-118%. Analysis of fold changes was performed using Microsoft Excel.

Table 5. Primers used for qRT-PCR

Target	Forward sequence (5'-3')	Reverse sequence (5'-3')	Amplicon size
sox9a	GCGTCCAGCATGGGAGAAGT	GCCTCTCGTTTCAGATCCGC	125 bp
col11a2[1]	GATATTCGGAAGAAGCGGAGG	CGCAAAACATCTACTGGATCTG	101 bp
wnt5b-1	GAGGGTGAGCTTTCCACCTG	GTTCACGAGCGTCCACAAAC	139 bp
wnt5b-2	TATTGGAGAGGGGGCGAAGA	ATATGCATGACACGGCCGAA	114 bp
ror2[2]	GAGGATTACAACTGGAGCTCAT	AGCCTCAATCTCTTCAGACTCG	106 bp
frzd7a	GACAAATTCAGCGACGACGG	CCCGCTGAGAGAAACCATGT	149 bp

[1] (Mukherjee et al., 2021)

[2] (Young et al., 2014)

2.10 Swimming activity

Initial characterization of *dlx5a*$^{-/-}$ and *dlx5i6*$^{-/-}$ swimming phenotype was carried out by recording individual adult fish (3+ months old) swimming in a static tank while placed inside a white polystyrene foam box. Fish were allowed to acclimate in the white environment for 10

mintutes before 3 minute long videos were made. The number of spins and turns per fish were quantified twice and averaged. Counts were performed by two individuals independently.

More detailed behavioural observations were recorded using the ZebraLab software and the ZebraCube tracking system (ViewPoint Life Science). Individual fish were transferred into a static tank and allowed to acclimate in the ZebraCube by freely swimming for 10 minutes followed by a 6 minute recording period. Parameters analyzed were total distance travelled and inactive duration.

2.11 Imaging

To capture otic vesicle morphology in 4dpf larvae, fish were anesthetized with 0.2 mL of 0.4% tricaine and positioned in 3% methylcellulose (Millipore Sigma, M0262). Images were acquired with Nikon SMZ1500 using NIS-Elements F software. The same camera and software were used to capture in situ hybridization results.

For capturing vital dye labeling, fish were anesthetized with 0.2 mL of 0.4% tricaine, positioned in either system water or 3% methylcellulose and visualized using the Zeiss Axiozoom with Apotome microscope and Zen Black software.

Immunohistochemistry performed in whole mount larvae were mounted on either petri plates coated with 1% agarose or glass slides with 1% agarose. Holes were created in the agarose with Pasteur pipettes and samples were positioned in the holes with 1% low-melt agarose. Visualization of labeling was performed using either the Zeiss LSM880 confocal with Zen Black software or Nikon A1R MP confocal with NIS Elements software. Capturing MTOC labeling was exclusively performed on the latter confocal.

The Olympus FV1000 BX61 confocal and Fluoview software was used to capture calretinin labelling on sectioned brain tissue.

2.12 Cell counting

ImageJ was used for all cell counting analyses. To analyze number of CR+ cells in a brain region, total number of positive cells were counted for each tissue slice per region and then averaged by how many sections were counted per brain. Means were then averaged again for each genotype and normalized to WT.

2.13 MTOC analysis

After z-stacks were obtained, specific images within a stack were used to create traces of Meckel's cartilage cells using Krita digital painting software (KDE). The images to make traces were chosen because it captured majority of Meckel's cartilage cells. Once traces were made, cells were divided into five areas (top, bottom, left, right, center) based on relative position from the midline. The position of MTOC was recorded based on these traces.

2.14 Statistical analysis

Graphs and statistical analysis were performed using GraphPad Prism v9. For average cartilage lengths, Brown-Forsythe and Welsh One-way ANOVA with Tukey's multiple comparisons test was used. All other statistics used two-tailed unpaired t-test with Welch correction and Holm Sidak method. When data was less than 10 individual points, it is presented

as mean ± standard deviation, otherwise mean ± SEM was used. For all tests * $p<0.05$; ** $p<0.001$; *** $p<0.0001$.

Chapter 3

Results

3.1 Cross regulation of *dlx* genes in larval zebrafish

Results from Sections 3.1.1 – 3.1.6 were published in Yu et al., 2021 (Yu EPY., Perin S., Saxena V and Ekker M. 2021. Novel cross-regulation interactions between *dlx* genes in larval zebrafish. *Gene.* **801** 145848.)

3.1.1 Mutants generated by CRISPR-Cas9 are fertile and viable as adults

All mutants were made by injecting at least two gRNAs targeting the 5' or first exon and 3' UTR simultaneously into 1-2cell stage embryos. Fish with germline mutations were identified by crossing with WT and progeny were genotyped using PCR using primers flanking the gRNAs or within the gene. Heterozygotes were then incrossed and progeny monitored for survival and genotyped at 3 months old, revealing homozygotes are viable and produced at Mendellian ratios. Homozygous fish did not have gross morphological or behavioural defects except in *dlx5a* wherein mutants display swim abnormalities (Emily Yu, Sofia Perin, Hadeel Al Hadi and Marc Ekker, unpublished observations). All homozygous fish are fertile and progeny from in-crosses are also viable.

3.1.2 *dlx1a* and *dlx2a* may not have compensatory roles in gene activation of downstream *dlx* paralogs until 72hpf

Previous work in mice and zebrafish have shown that deletion or knockdown of *Dlx1*/*dlx1a* or *Dlx2*/*dlx2a* independently result in only mild phenotypes, while perturbations of both *Dlx1*/*dlx1a* and *Dlx2*/*dlx2a* lead to severe neurological and craniofacial phenotypes (Anderson et al., 1997; Cobos et al., 2005; Qiu et al., 1995). These results suggested that *Dlx1/dlx1a* and *Dlx2/dlx2a* may be functionally redundant. Based on this assumption, it was expected that *dlx1a* expression in *dlx2a*$^{-/-}$ or *dlx2a* expression in *dlx1a*$^{-/-}$ would increase compared to WT to compensate for the activity of the missing paralog. However, this was largely not observed by WISH in *dlx1a* and *dlx2a* mutants at 24-72hpf (Fig. 3.1). Staining for *dlx1a* in *dlx2a*$^{-/-}$ larvae appears similar in intensity to WT at 24hpf and 72hpf whereas the staining for *dlx2a* in *dlx1a* mutants appear equal or slightly decreased in 24hpf and 48hpf larvae.

Interestingly, at 72hpf, there may be an increase in *dlx2a* expression in *dlx1a*$^{-/-}$. If the paralogs have compensatory action, it may also be expected that their region of expression would expand to encompass the missing paralog. While *dlx1a* and *dlx2a* are expressed in mostly overlapping regions in the telencephalon, diencephalon and branchial arches, *dlx2a* extends more ventrally in the subpallium (MacDonald et al., 2010). Based on the similarity in staining regions, it is unlikely *dlx1a* expression region is expanded in *dlx2a*$^{-/-}$.

In mice, the expression of *Dlx1* in *Dlx2* mutants is reduced in the ganglionic eminences (Eisenstat et al., 1999). While expression of *dlx1a* was comparable to WT in *dlx2a*$^{-/-}$ at 24hpf and 72hpf, the expression of *dlx1a* was reduced in the *dlx2a* mutants at 48hpf, recapitulating this previously described relationship.

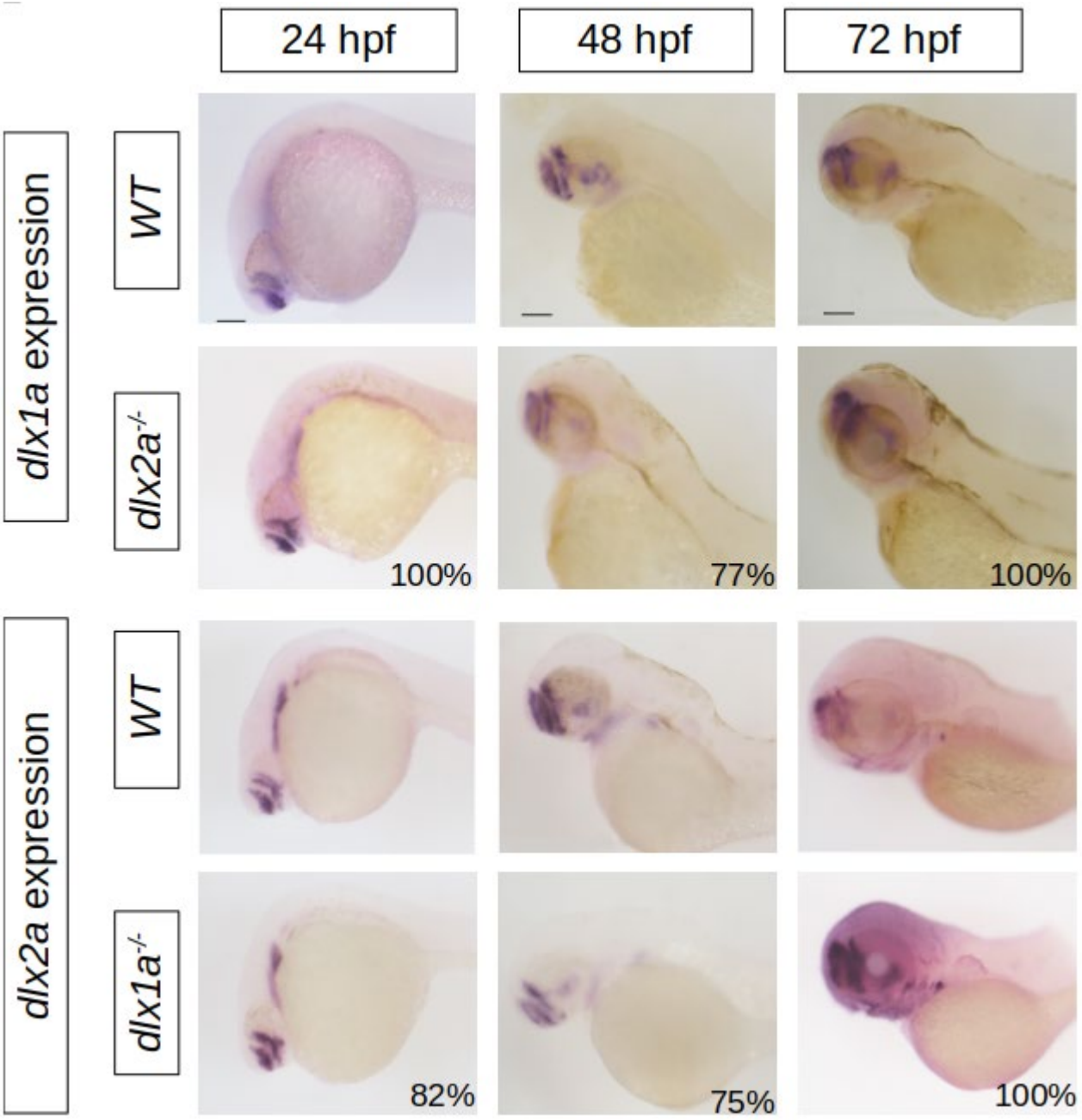

Figure 3.1. Expression of dlx1a in dlx2a$^{-/-}$ and expression of dlx2a in dlx1a$^{-/-}$ by WISH.

In situ results does not suggest compensation is occurring until 72hpf in *dlx1a*$^{-/-}$. Expression of both paralogs are found in the telencephalon, diencephalon and branchial arches. Percentages indicate how often the phenotype was observed. Scale = 100µm.

3.1.3 Regulation of *dlx2a* expression may be mediated by Dlx5a and Dlx6a

The expression of *dlx2a* but not *dlx1a* was increased in *dlx5a*$^{-/-}$ at 24hpf and 72hpf and all time points in *dlx6a*$^{-/-}$ (Fig. 3.2-3.3). There may be increased expression of *dlx2a* in 48hpf *dlx5a*$^{-/-}$ larvae but the differences are minute compared to other stages. Based on previous work, *Dlx2/dlx2a* was shown to be important for regulating *Dlx5/dlx5a* expression, potentially through activity of the CREs within *Dlx5/6* locus (Zerucha et al., 2009). Our results suggest an additional layer of regulation wherein a feedback mechanism may exist to control the amount of *dlx2a* expressed via activity of Dlx5a and/or Dlx6a.

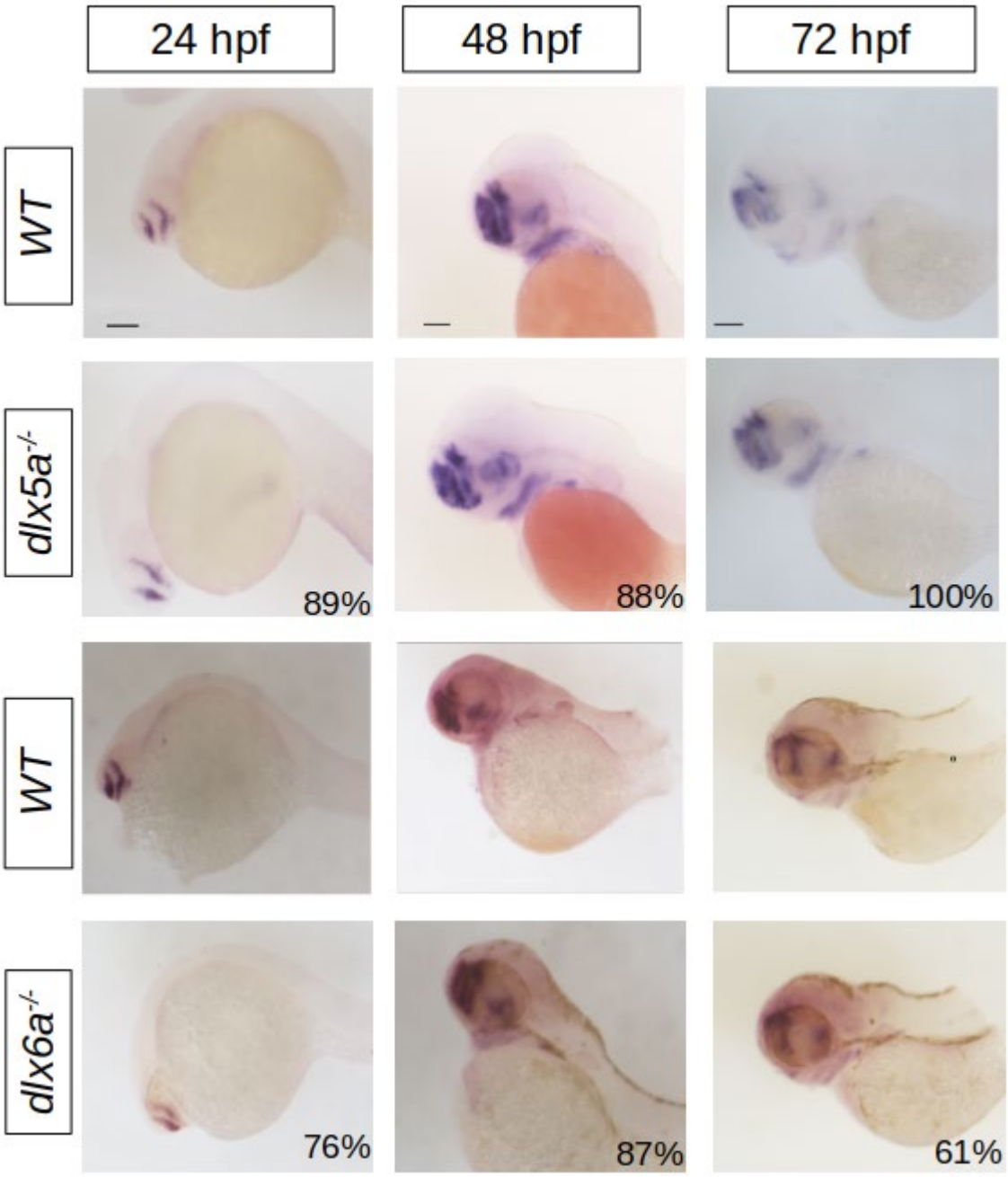

Figure 3.2 Expression of dlx1a in dlx5a$^{-/-}$ and dlx6a$^{-/-}$ larvae at 24hpf – 72hpf.

Little change in staining intensity were observed compared to WT for all samples. Staining of *dlx1a* in the telencephalon, diencephalon and branchial arches in mutants and WT are at near equal levels. Percentages indicate how often the phenotype was observed. Scale = 100µm.

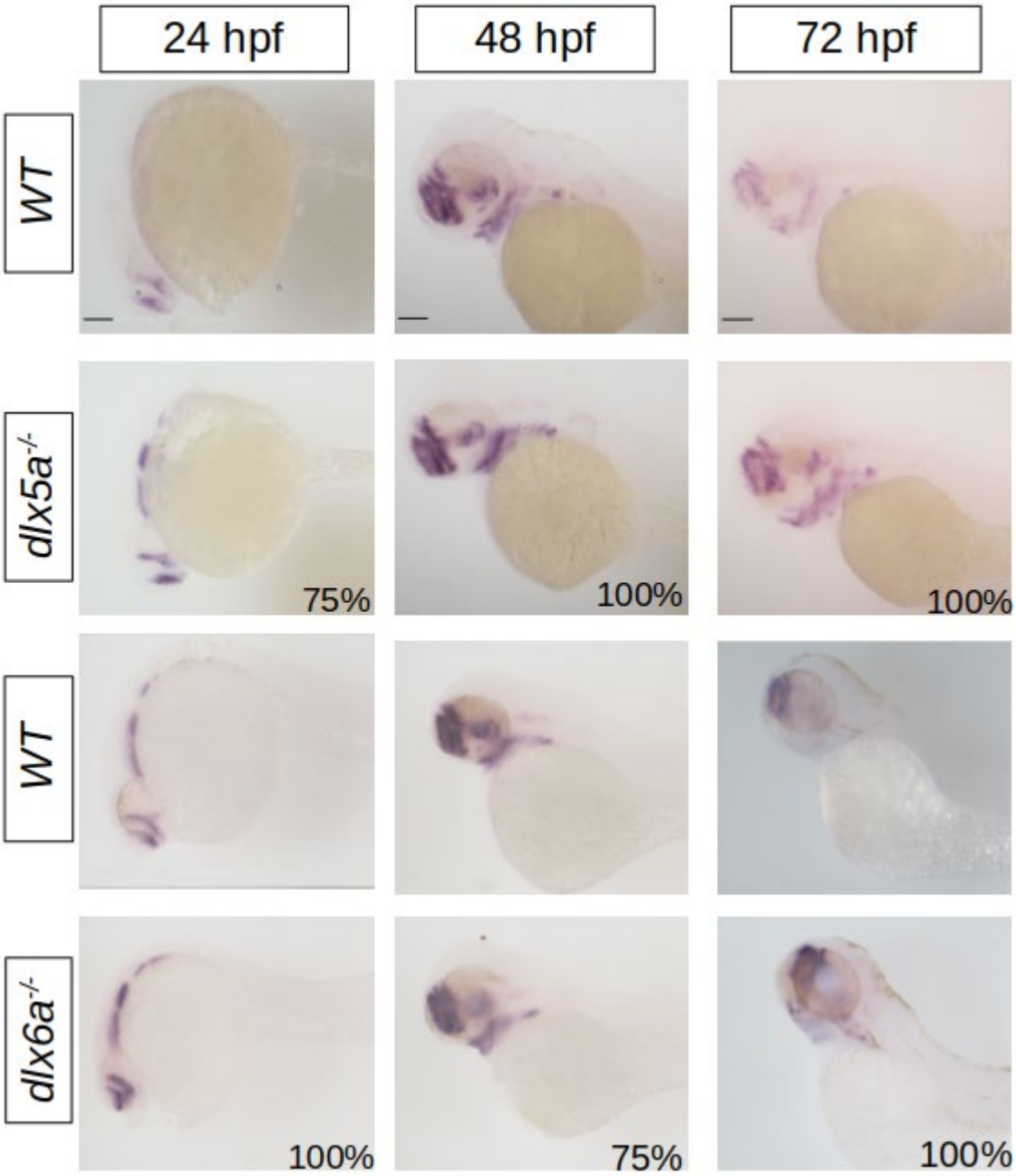

Figure 3.3 Expression of dlx2a is increased in dlx5a$^{-/-}$ and dlx6a$^{-/-}$ larvae.

Expression of *dlx2a* is present in telencephalon, diencephalon and branchial arches. Staining for *dlx2a* is most increased in branchial arches in mutants whereas increases in *dlx6a* mutants appears global. Percentages indicate how often the phenotype was observed. Scale = 100µm.

3.1.4 Diminished expression of *dlx5a* in *dlx2a*$^{-/-}$ suggests Dlx2a is required for maintenance but not initiation of *dlx5a* expression

It was previously shown that knock down of *dlx2a* in zebrafish led to reduced *Dlx5/dlx5a* expression, indicating potential cross regulation (MacDonald et al., 2013). It was therefore expected that *dlx5a* would be expressed at lower levels or absent in *dlx2a* mutants. Surprisingly, *dlx5a* was still expressed at near WT levels in the telencephalon, diencephalon and branchial arches of *dlx2a* mutants at 24hpf and 48hpf (Fig. 3.4). However, the expression of *dlx5a* is reduced to near undetectable levels by 72hpf. This suggests that *dlx2a* may not be required for initial *dlx5a* expression but is involved in the maintenance of expression in later development in zebrafish.

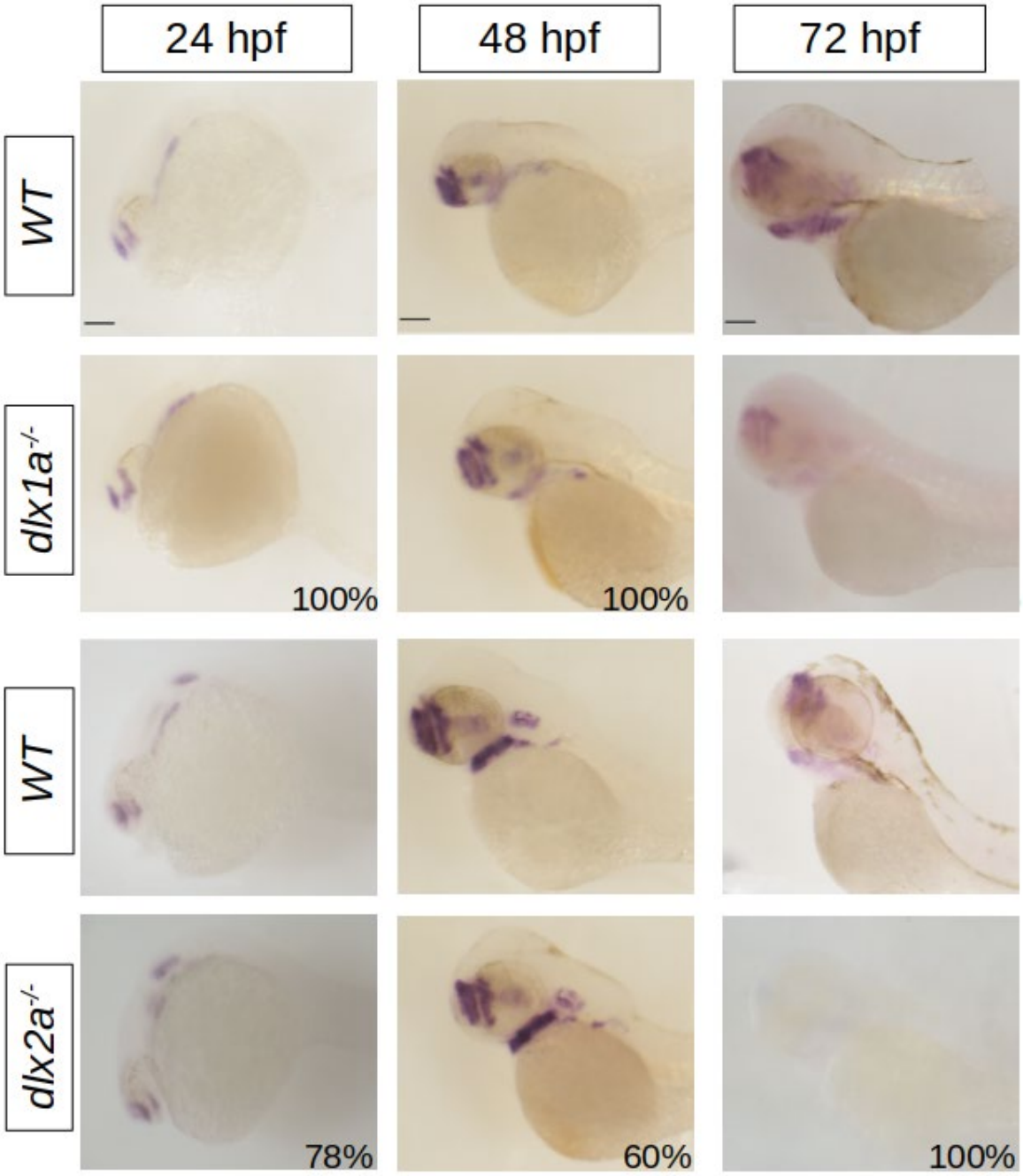

Figure 3.4. Expression of dlx5a in dlx1a$^{-/-}$ and dlx2a$^{-/-}$ larvae.

Expression of *dlx5a* is present in 24hpf-72hpf WT and 24-48hpf mutants in the telencephalon, diencephalon, branchial arches, otic placode and pectoral fin bud. Percentages indicate how often the phenotype was observed. Scale = 100µm.

3.1.5 Dlx5a is necessary for the expression of *dlx6a*

Deletion of *dlx5a* abolished expression of *dlx6a* at all stages of development analyzed, suggesting *dlx5a* regulates the expression of *dlx6a* (Fig. 3.5). Furthermore, the expression of *dlx5a* in the *dlx6a* mutants at 48hpf and 72hpf appears increased, especially in the diencephalic regions (hypothalamus and prethalamus). This increased *dlx5a* expression in the absence of Dlx6a suggests a potential feedback mechanism exists to regulate *dlx5a* expression and/or Dlx5a may compensate for Dlx6a in these brain regions.

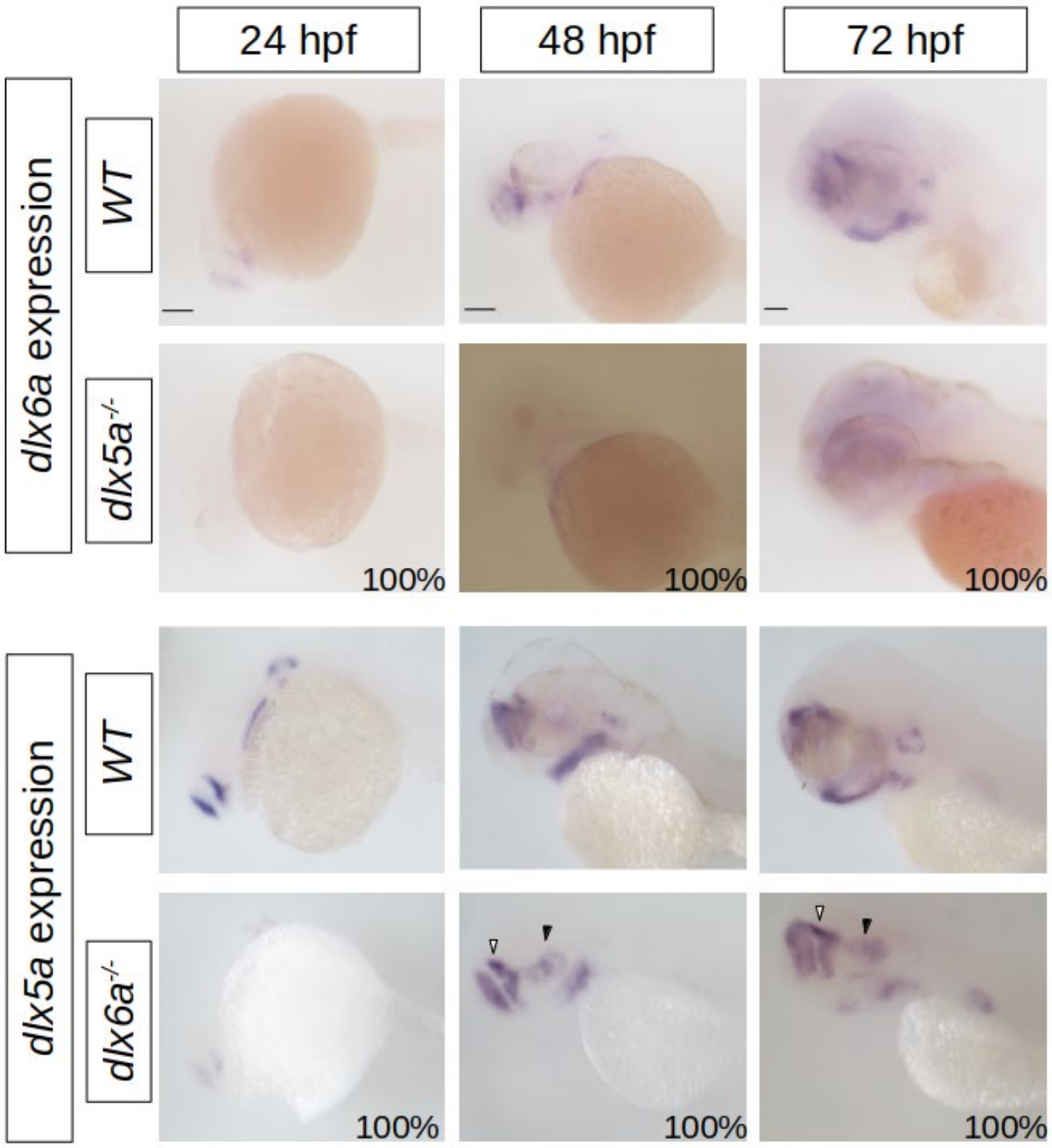

Figure 3.5. Expression of dlx6a in dlx5a$^{-/-}$ and dlx5a in dlx6a$^{-/-}$ larvae.

Expression of *dlx6a* is severely reduced in the absence of Dlx5a whereas the expression of *dlx5a* appears increased in 48hpf and 72hpf, especially in the prethalamus (outlined arrow) and hypothalamus (black arrowhead). These observations suggest *dlx5a* regulates the expression of *dlx6a*. Percentages indicate how often the phenotype was observed. Scale = 100µm.

3.1.6 Persistent *dlx5a* and *dlx6a* expression in *inter56*$^{-/-}$ suggests alternative or compensatory CRE activity

Interestingly, expression of *dlx5a* and *dlx6a* was still observed in *inter56* mutants at all time points investigated in the telencephalon, diencephalon and branchial arches, where normal *dlx5a* and *dlx6a* expression is expected (Fig. 3.6). While the expression of *dlx6a* is increased compared to controls, the expression of *dlx5a* may be weaker in 24hpf mutants and then increases to WT levels by 48hpf and 72hpf. The persistent expression of these paralogs in the absence of the intergenic enhancers may still be regulated by Dlx2a since *inter56*$^{-/-}$ have increased *dlx2a* expression at all time points. These results further suggest an alternative mechanism to activate *dlx5a* and, possibly *dlx6a* expression and consequently, in the absence of previously described regulation pathways. An alternative CRE may be active in the brain of these mutants due to the absence of i56i and i56ii activity, and this alternative CRE may be triggered in response to reduced amounts of Dlx5a.

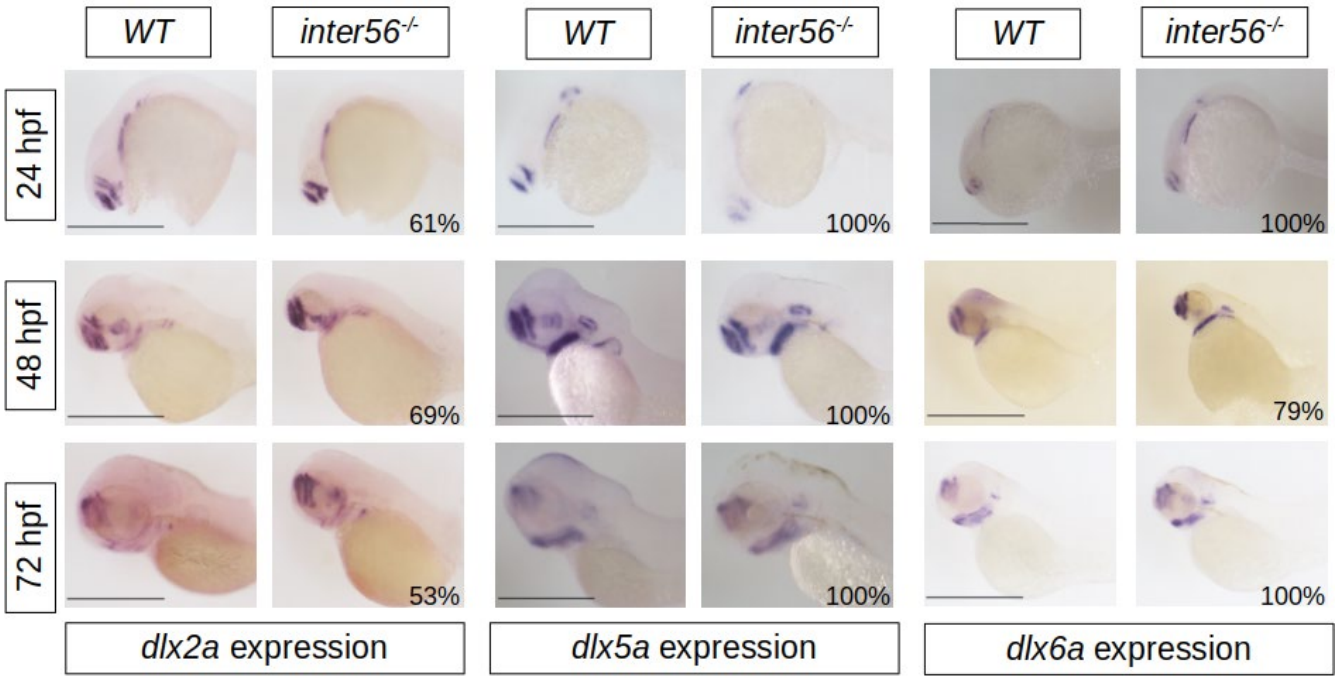

Figure 3.6. Expression of dlx2a, dlx5a and dlx6a in inter56$^{-/-}$ larvae.

Staining for *dlx2a* is darker suggesting greater expression in mutants at all time points in all areas where *dlx2a* expression is expected. The expression of *dlx5a* appears to increase from 24hpf to 48hpf to meet WT levels. Expression of *dlx6a* appears increased in all stages analyzed. Percentages indicate how often the phenotype was observed. Scale = 500µm.

3.2 Effect of *dlx* loss during craniofacial development in the zebrafish

3.2.1 Morphology of adults

Not only are *dlx* mutants all viable and fertile, no severe or consistent morphological craniofacial defects were observed in adults. All fish can feed on a standard diet of rotifers, brine shrimp and flake food.

3.2.2 Length and shape of PA1 and PA2 structures are altered in *dlx* mutants at 5dpf

Compared to WT (146±2.4 μm), *dlx2a*$^{-/-}$ (117.2±7.9 μm), *dlx5a*$^{-/-}$ (78.2±2.0 μm), *dlx5i6*$^{-/-}$ (71.9±2.4 μm) and *dlx6a*$^{-/-}$ (131.5±3.4 μm) all had significantly smaller Meckel's cartilage (MC) structures (Fig 3.8, A). Importantly, *dlx5a*$^{-/-}$ and *dlx5i6*$^{-/-}$ MC are shorter compared to all other *dlx* mutants as well. For the palatoquadrate (PQ), *dlx1a*$^{-/-}$ (167.6±2.1), *dlx2a*$^{-/-}$(132.4±8.5), *dlx5a*$^{-/-}$(80.6±5.8 μm) and *dlx5i6*$^{-/-}$(78.7±4.7 μm) were shorter compared WT (187±2.76 μm) (Fig 3.8, B). Once again, *dlx5a*$^{-/-}$ and *dlx5i6*$^{-/-}$ larvae had the shortest PQ among all mutants. Additionally, *dlx1a*$^{-/-}$ and *dlx2a*$^{-/-}$ PQ were also significantly different from each other. Compared to WT (179.8±2.9 μm), the ceratohyal (CH) of *dlx2a*$^{-/-}$ (139.3±10.6 μm), *dlx5a*$^{-/-}$ (104.6±1.3 μm) and *dlx5i6*$^{-/-}$ (98.4±1.2 μm) were shorter (Fig 3.8, C). Again, *dlx5a*$^{-/-}$ and *dlx5i6*$^{-/-}$ had the smallest structures of all mutants.

In analyzing the ventral images, the MC of *dlx5a*$^{-/-}$ and *dlx5i6*$^{-/-}$were often wider and did not protrude as far distally compared to WT. Thus, a final measurement was performed to analyze the width/length ratio of the MC finding that only *dlx5a*$^{-/-}$ and *dlx5i6*$^{-/-}$ mutant larvae possessed smaller ratios, at 0.33± 0.08 and 0.31±0.08 respectively compared to 0.44±0.08 in WT (Fig 3.8, D).

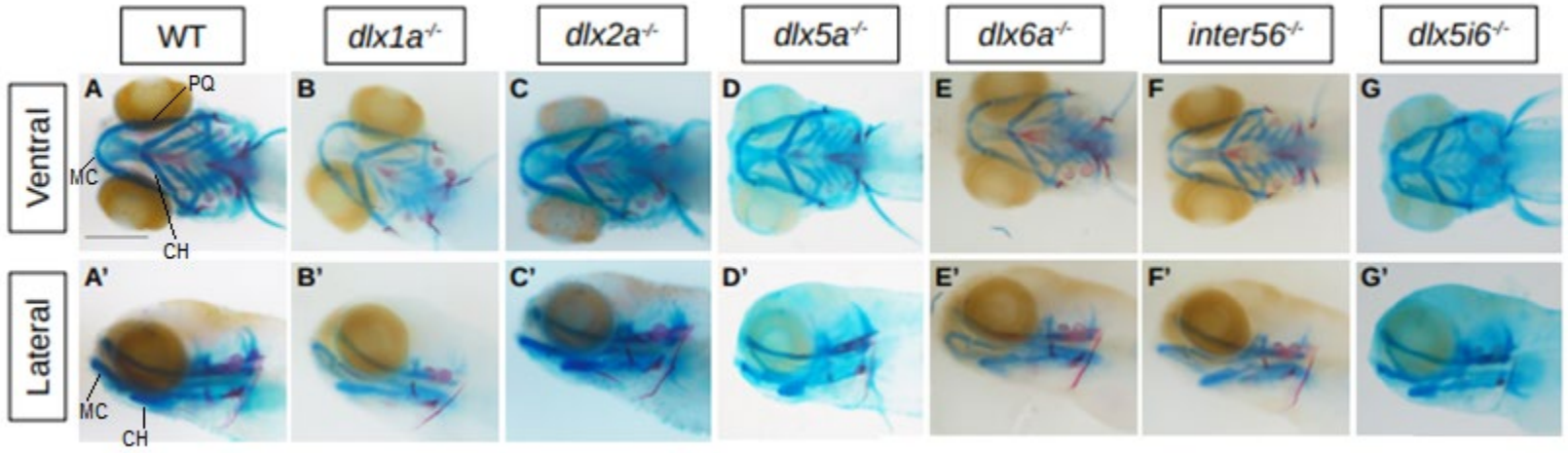

Figure 3.7 Alcian blue and alizarin red staining in 5dpf zebrafish.

Alcian blue and alizarin red staining to visualize cartilage and calcified bone respectively in 5dpf WT and *dlx* mutant larvae in the ventral (A-G) and lateral (A'-G') positions. Scale = 150μm. Abbreviations: CH- ceratohyal; MC- Meckel's cartilage; PQ- palatoquadrate.

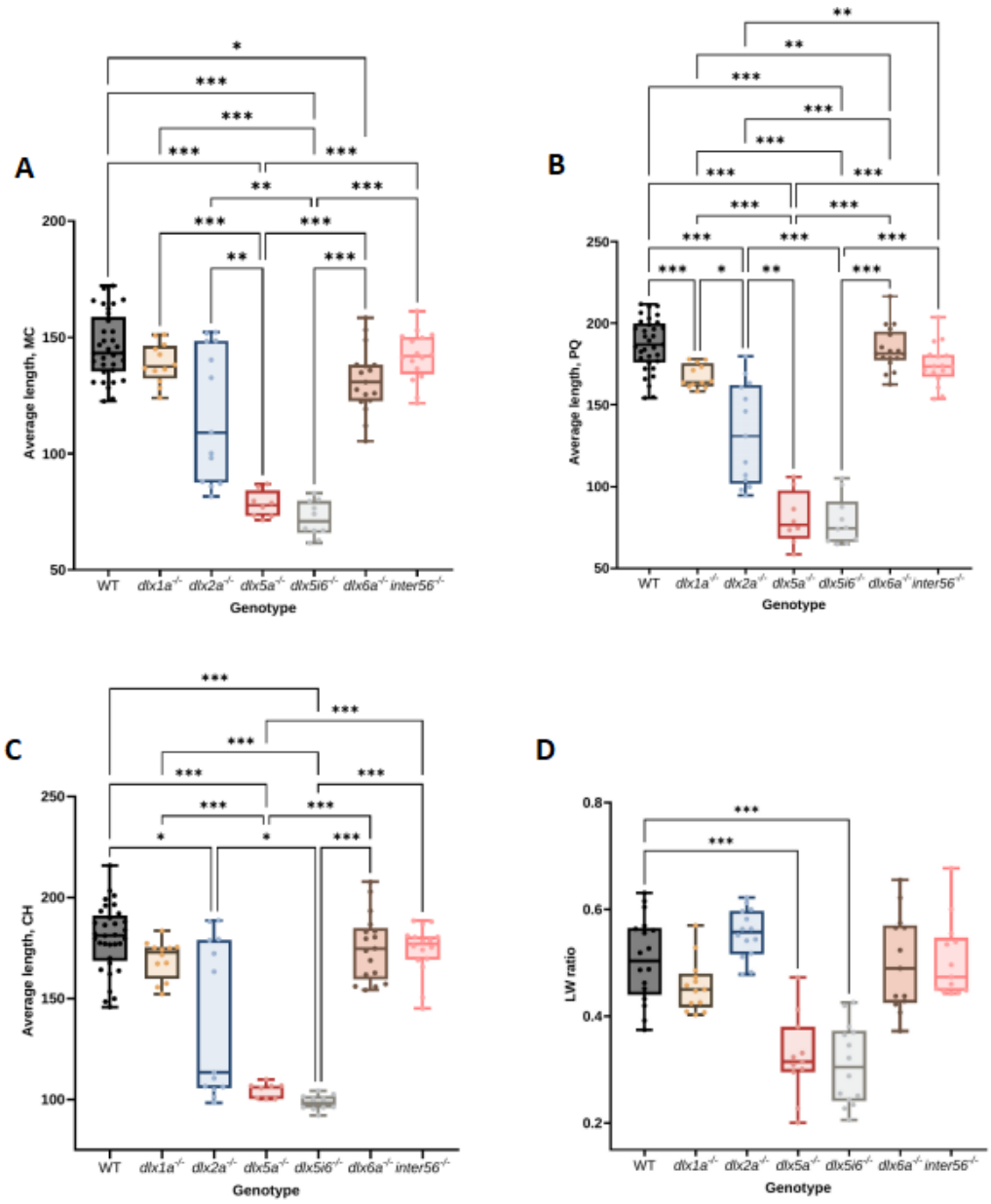

Figure 3.8. Measurements of average MC (A), PQ (B) and CH (C) structures and length/width ratio of the MC (D).

All morphometric data show analyzed structures in *dlx5a*$^{-/-}$ and *dlx5i6* $^{-/-}$ are all shorter and the MC is wider and shorter (smallest ratio). Measurements made from WT (n=33), *dlx1a*$^{-/-}$ (n=12), *dlx2a*$^{-/-}$(n=14), *dlx5a*$^{-/-}$ (n=8), *dlx5i6*$^{-/-}$(n=13), *dlx6a* $^{-/-}$ (n=17) and *inter56*$^{-/-}$ (n=16) larvae. All data represented as mean ± SEM. One-way ANOVA with Tukey's multiple comparisons test was performed. * $p<0.05$, ** $p<0.001$; ***$p<0.0001$. No asterisk indicates comparison was not significant.

3.2.3 Measurements of PA1 and PA2 structures in 14dpf larvae

Since adult fish did not possess overt morphological changes to jaw structures, it was possible the differences observed at 5dpf would be rescued as larvae develop. Thus, measurements were also performed at 14dpf (Fig. 3.9, A-G).

This analysis found that the MC was significantly shorter in *dlx5a*$^{-/-}$ *(*128.3±2.78 μm) and *dlx5i6*$^{-/-}$ (140±3.2 μm) larvae compared to WT (160.8±2.2 μm) (Fig. 3.10, A). The size of the MC in *dlx5a*$^{-/-}$ and *dlx5i6*$^{-/-}$ larvae were also significantly different compared to *dlx2a*$^{-/-}$ (156±2.4 μm) as well. In fact, *dlx5a*$^{-/-}$ MC is different from all other mutants, suggesting *dlx5a* is very important for the size of the MC.

The PQ was also significantly smaller in *dlx5i6*$^{-/-}$ mutant larvae (178±3.3 μm) compared to WT (198.7±2.3 μm) and *dlx2a*$^{-/-}$ mutant larvae (202.9±4.2 μm) but *dlx5a*$^{-/-}$ PQ was not significantly different compared to WT or any other mutants (Fig 3.10, B). Interestingly, the PQ of *dlx1a*$^{-/-}$ mutants (172.7±2.9 μm) was also significantly smaller compared to WT and *dlx2a*$^{-/-}$ mutants. Finally, the PQ of *inter56*$^{-/-}$ mutants (180.3±3.4 μm) was also smaller compared to *dlx2a*$^{-/-}$ but not WT. The PQ of *dlx2a*$^{-/-}$ did not differ from WT.

The last structure analyzed was the CH. This is the only PA2 structure of interest and surprisingly, many differences were identified compared to WT and between mutants (Fig 3.10, C). The CH of *dlx1a*$^{-/-}$ mutants were again significantly smaller (162.6±1.9 μm) compared to WT (186.8±3.2 μm) and *dlx2a*$^{-/-}$ mutants (201.1±3.5 μm). This group was also smaller compared to *dlx5a*$^{-/-}$, *dlx6a*$^{-/-}$ and *inter56*$^{-/-}$ mutants. The CH of *dlx5i6*$^{-/-}$, *dlx6a*$^{-/-}$ *and inter56*$^{-/-}$ mutant larvae were also smaller compared to *dlx2a*$^{-/-}$ but not compared to WT. Finally, *dlx2a*$^{-/-}$ mutant CH was found to be significantly larger compared to WT.

The LW ratio of the MC was also measured once more in *dlx* mutants finding that *dlx5a*$^{-/-}$ and *dlx5i6*$^{-/-}$ larvae still possessed shorter and wider MC, having the smallest ratios at 0.58±0.03 and 0.52±0.02 compared to 0.75±0.01 in WT (Fig 3.10, D). Compared to the other mutants, *dlx5a*$^{-/-}$ and *dlx5i6*$^{-/-}$ LW ratios were also significantly different. Interestingly, the ratio between *dlx1a*$^{-/-}$ and *dlx2a*$^{-/-}$ mutant larvae were also different.

Based on measurements made of craniofacial structures at 5dpf and 14dpf, *dlx5a*$^{-/-}$ and *dlx5i6*$^{-/-}$ larvae are consistently in a separate group from other mutants, possessing the shortest MC at both time points and with MC that are wider and shorter compared to WT. Additionally, *dlx5i6*$^{-/-}$ larvae present with similar expression of other *dlx* genes compared to *dlx5a* suggesting these mutants may have similar genetic network expression (Fig 3.11). For these reasons, the two mutant lines will be considered the same for the duration of section 3.2 and will be collectively called *dlx5a* mutants.

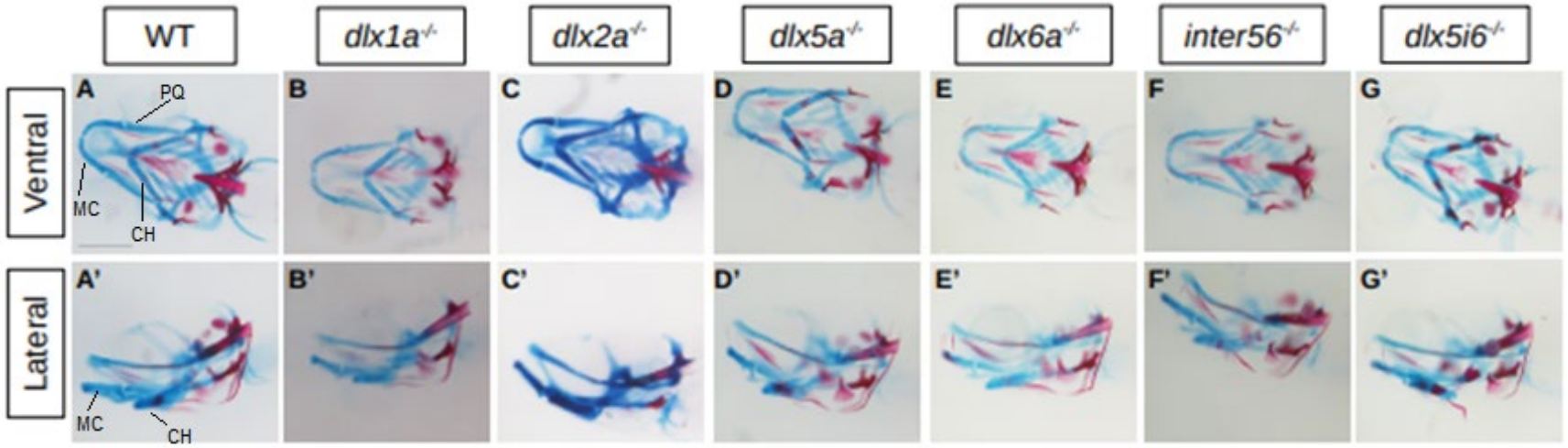

Figure 3.9. Alcian blue and alizarin red staining in 14dpf larvae.

Alcian blue and alizarin red staining to visualize cartilage and calcified bone respectively in WT (A) and *dlx* mutants (B-G) in the ventral and lateral positions at 14dpf. Note MC in *dlx5a* and *dlx5i6* mutants appear wider and more retracted compared to WT. At this age, more bone structures are visible, and the CH is undergoing endochondral ossification. Teeth are also visible in all *dlx* mutants from the last ceratobranchial. Scale = 150µm. Abbreviations: CH- ceratohyal; MC-Meckel's cartilage; PQ- palatoquadrate.

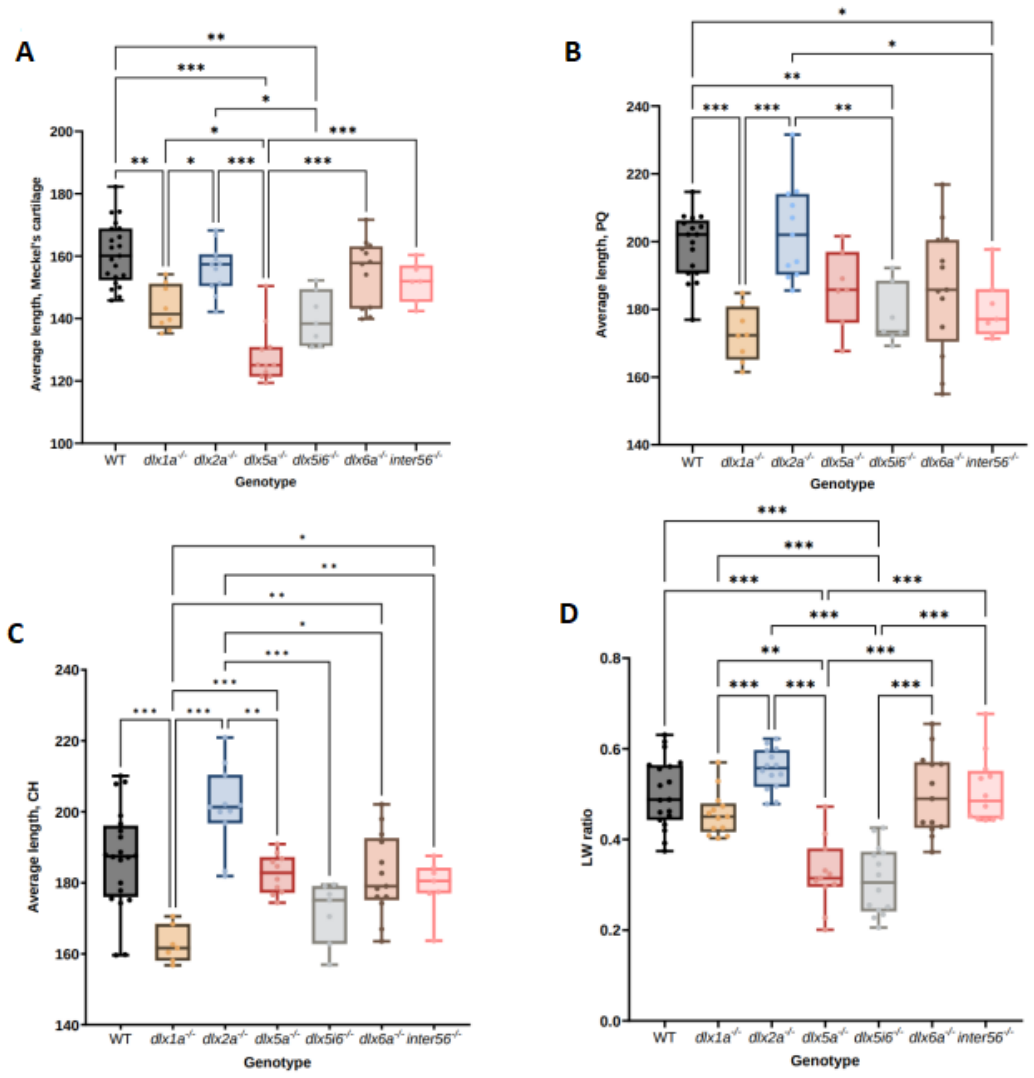

Figure 3. 10. Morphometric analysis of MC, PQ, CH and LW ratio of MC in 14dpf larvae.

(A) Average length of MC in 14dpf show *dlx5a*$^{-/-}$ and *dlx5i6*$^{-/-}$ larvae still have the shortest structures but *dlx1a*$^{-/-}$ larvae also have shorter MC at this timepoint. **(B)** Average length of PQ showing *dlx1a*$^{-/-}$, *dlx5i6*$^{-/-}$ and *inter56*$^{-/-}$ PQ are shorter compared to WT. **(C)** Average length of CH shows *dlx1a*$^{-/-}$ now have the shortest structure. **(D)** LW ratio of MC showing *dlx5a*$^{-/-}$ and *dlx5i6*$^{-/-}$ larvae continue to have the smallest ratio indicating wider MC. Data presented as mean ± SEM from measurements on at least 8 animals each genotype One-way ANOVA with Tukey's multiple comparisons test was performed. * $p<0.05$, ** $p<0.001$; ***$p<0.0001$. No asterisk indicates comparison was not significant.

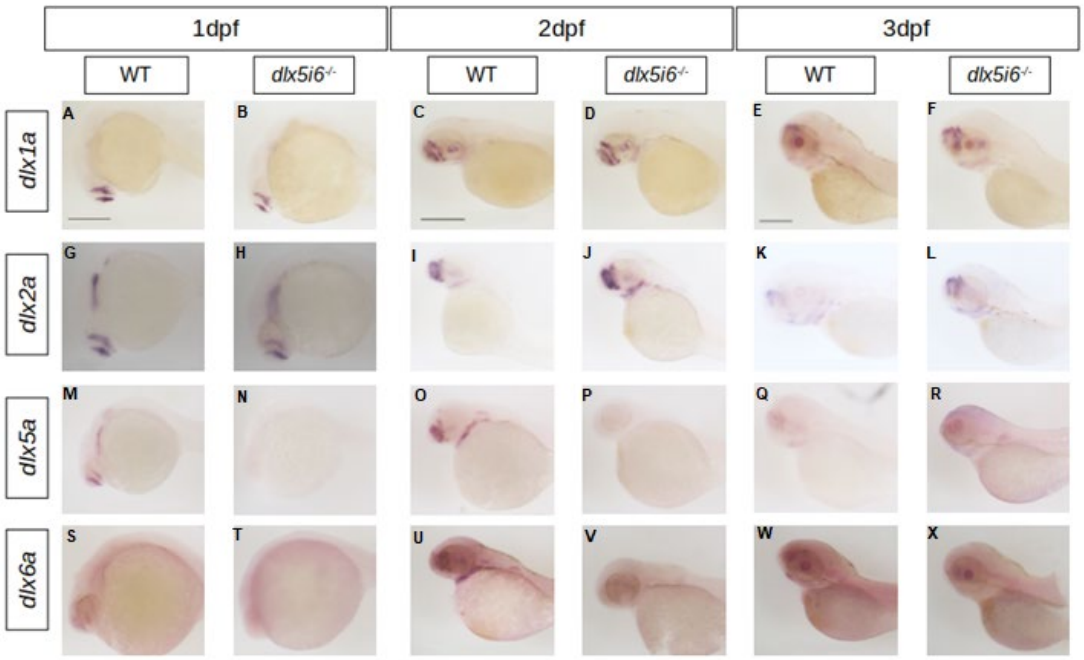

Figure 3.11. Expression of *dlx* genes in *dlx5i6*$^{-/-}$ larvae from 1-3dpf. (A-F) Larvae were stained for *dlx1a* expression showing similar staining intensity between WT and mutants. (G-L) Staining for *dlx2a* suggests increased expression by 2dpf and 3dpf in *dlx5i6*$^{-/-}$ larvae, similar to observations in *dlx5a*$^{-/-}$ previously described. (M-R) Staining for *dlx5a* expression demonstrates no transcripts for *dlx5a* was produced in *dlx5i6*$^{-/-}$ larvae at all time points. (S-X) Expression of *dlx6a* is absent in *dlx5i6*$^{-/-}$ larvae. Scale = 100μm.

3.2.4 Abnormal morphology of PA1 derivatives observed in *dlx5a* mutants is not due to increased *dlx2a* expression

From 3.1.3, the expression of *dlx2a* is increased in *dlx5a*$^{-/-}$ at 24-72hpf, thus a possible confounding factor is that craniofacial phenotypes observed in *dlx5a* mutants may be due to compensatory activity from Dlx2a. To investigate this possibility, compound mutants were created through mating *dlx2a*$^{-/-}$ with *dlx5a*$^{-/-}$ adults. Very few *dlx2a*$^{-/-}$*; dlx5a*$^{-/-}$ adults were recovered after heterozygous incrosses by tail clipping which may suggest larval lethality, however poor overall survival of all fish entered into the nursery at the time was observed. To circumvent poor survival, compound heterozygous fish were mated and progeny were genotyped at 5dpf. Alcian blue and alizarin red staining was performed on all genotyped larvae, revealing a variety of phenotypes that impacted the morphology of MC, CH and PQ, which were grouped into five classifications. (Fig 3.12). While the most severe phenotype was observed in double homozygous larvae, the MC continues to be malformed and shorter in *dlx2a*+/-*; dlx5a*$^{-/-}$ suggesting that even with one functional *dlx2a* and thus possibly less Dlx2 compared to *dlx5a*$^{-/-}$, a similar phenotype was present.

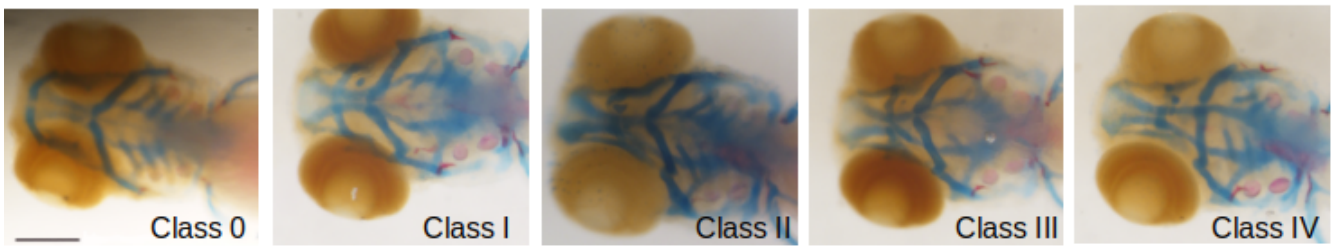

Class 0:
- Normal, sometimes M does not meet in the middle

Class I:
- Meckel's retracted and small/ more bent at middle
- CH still present and chevron shaped
- PQ shortened but shape is clear

Class II:
- Meckel's retracted and/or broken but still curved
- CH present and chevron shaped, may be thicker
- PQ shortened but shape is clear (still has elongated element)

Class III:
- Meckel's retracted and straight
- CH present and cheron shaped, may be thicker
- PQ shortened but shape is still clear/present

Class IV:
- Meckel's is missing or only a fragment present
- CH flat or inverted
- PQ is just a wedge or shortened but still elongated

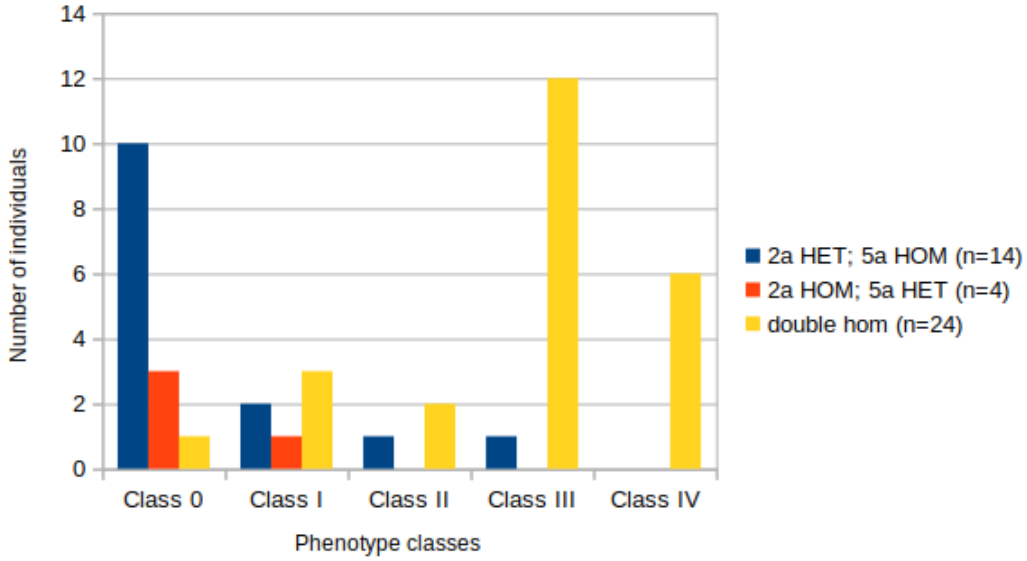

Figure 3.12. Craniofacial phenotypes observed in *dlx2a*$^{-/-}$; *dlx5a*$^{-/-}$ larvae at 5dpf.

(A) Examples of the variety and ranging severity of morphological changes to PA1 and PA2 derivatives. These phenotypes were grouped into 5 different classes. **(B)** Description of the five classes of phenotypes. **(C)** Distribution of phenotype classes in three compound mutant genotypes. Scale = 150µm.

3.2.5 Expression of neural crest and differentiation markers were altered in *dlx5a* mutants

One possible explanation to shorter and malformed PA1 derivative observed in *dlx5a* mutants may be that fewer NCC contribute to PA1 structures, either through defects in migration or differentiation. To test this, the expression of *foxd3*, *sox9a* and *col11a2* was assessed through WISH.

At 2 somite stage or 9hpf, induction of NCC at the neural plate border is underway, marked by expression of *foxd3* in cells at the border. However, expression domain of *foxd3* in the mutants is wider apart, indicating the border is further from the midline where the presumptive tube will form and may suggest possible defects in NCC positioning or migration as the embryo develops (Fig 3.13A, B). NCC continue to express *foxd3* as they migrate, beginning at 12hpf. Thus, *foxd3* expression in embryos at 10 somite stage or 14hpf, after the onset of NCC migration, was probed. In both WT and *dlx5a* mutants, staining was observed in similar regions suggesting overall migration as not affected (Fig 3.13C, D).

Another NCC marker assessed was *sox9a*. This transcription factor is present during NCC specification, migration and is essential for chondrogenic differentiation which begins at 48hpf. Expression of *sox9a* was similar between *dlx5a* mutants and WT at 48hpf, once again indicating migration was unaffected and that perhaps the onset of differentiation was unaffected (Fig 3.13E, F). However, at 72hpf, when many of the cartilaginous structures are being formed including the Meckel's cartilage, palatoquadrate and ceratohyal, there was more staining for *sox9a* in mutants compared to WT (Fig 3.13G, H). Additionally, the area of staining expands to cover entire cartilage structures in mutants rather than the distal tips observed in WT. These observations suggest more *sox9a* expressing cells were present in PA1 derivatives. Interestingly, RT-qPCR results indicate a statistically significant increase of *sox9a* expression in mutants at nearly 3.5 times more than WT while at 3dpf only a trend towards increased expression was observed (Fig 3.13M).

The expression of a *col11a2*, a collagen produced by chondrocytes in craniofacial structures was also investigated. At 48hpf, staining for *col11a2* does not differ between *dlx5a* mutants and WT (Fig 3.13I, J). However, by 72hpf, staining for *col11a2* is more intense in mutants compared to WT. These observations are partially supported by RT-qPCR where *dlx5a* mutants have a 1.3-fold increase of *col11a2* expression at 3dpf (Fig 3.12N).

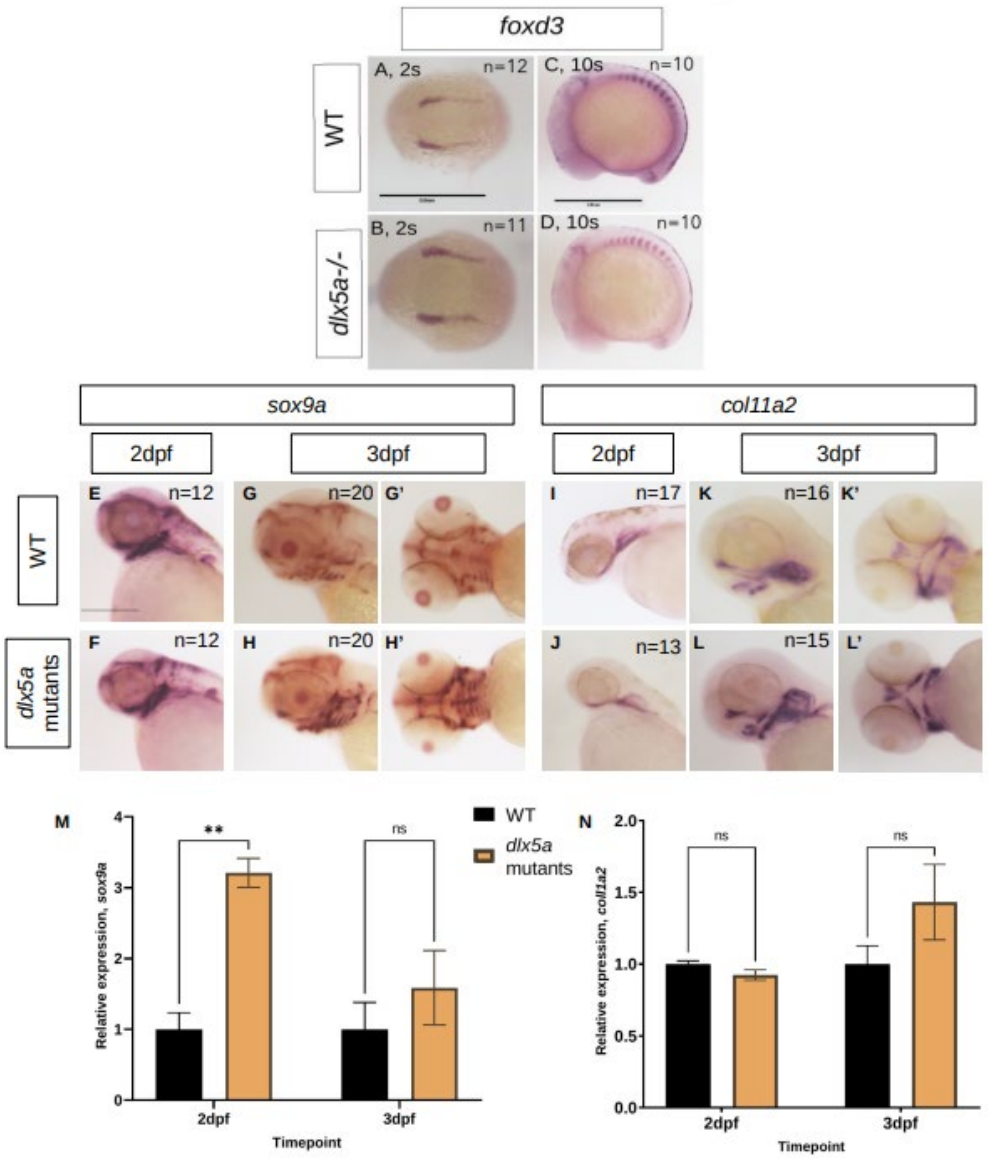

Figure 3.13. Expression of NC markers in *dlx5a* mutants during NC specification, migration and chondrogenesis.

(A-D) Expression of *foxd3* by WISH in mutants **(B, D)** and WT **(A, C)** at 2 somites and 10 somites when NC is being specified and during migration respectively. **(E-H)** Expression of *sox9a* in 2dpf and 3dpf mutants **(F, H)** and WT **(E, G)**. Lateral views **(E-H)** show expression of *sox9a* in the developing PA1 and PA2 structures. Ventral views **(G', H')** demonstrates that staining for *sox9a* is present throughout the cartilage structures. **(I-L)** Expression of *col11a2* by WISH in 2dpf and 3dpf larvae. (M-N) RT-qPCR for *sox9a* and *col11a2* demonstrating increases in expression of these two markers in mutants. All relative expression reported as mean ± SEM. ** $p<0.01$, ns: no significance. Scale = 100µm

3.2.6 Increased proliferation without changes in apoptosis was observed in *dlx5a* mutants

Results from *in situ* for *sox9a* and *col11a2* suggest either abnormal expression of these markers or more cells in craniofacial structures resulting in increased staining and expression. To resolve these two possibilities, BrdU pulse-chase experiment was performed to observe potential increases in cell proliferation in mutants. At 52hpf, *dlx5i6*$^{-/-}$*;fli1a:GFP* and labeled WT siblings were incubated with BrdU, chased for 4 hours and fixed at 52hpf for analysis revealing about twice as many BrdU+ cells in *dlx5i6*$^{-/-}$ compared to WT (Fig 3.14C- D, G). A similar experiment was also performed on 5dpf *dlx5i6*$^{-/-}$*; sox10:GFP* and labeled WT siblings, also revealing 2.2x more BrdU+ cells in the MC, suggesting that mutants exhibit increased proliferation (Fig 3.14 E-G).

It is possible increased proliferation is a mechanism to compensate for more apoptosis of NCC or chondrocytes. Therefore, acridine orange staining was performed to label any apoptotic cells at 48hpf and 72hpf. At both time points, *dlx5a* mutants and WT did not exhibit differences in number of fluorescent puncta in craniofacial regions but some mutants did have more labeled cells in the brain, indicative of more apoptosis in that organ (Fig 3.14 A, B).

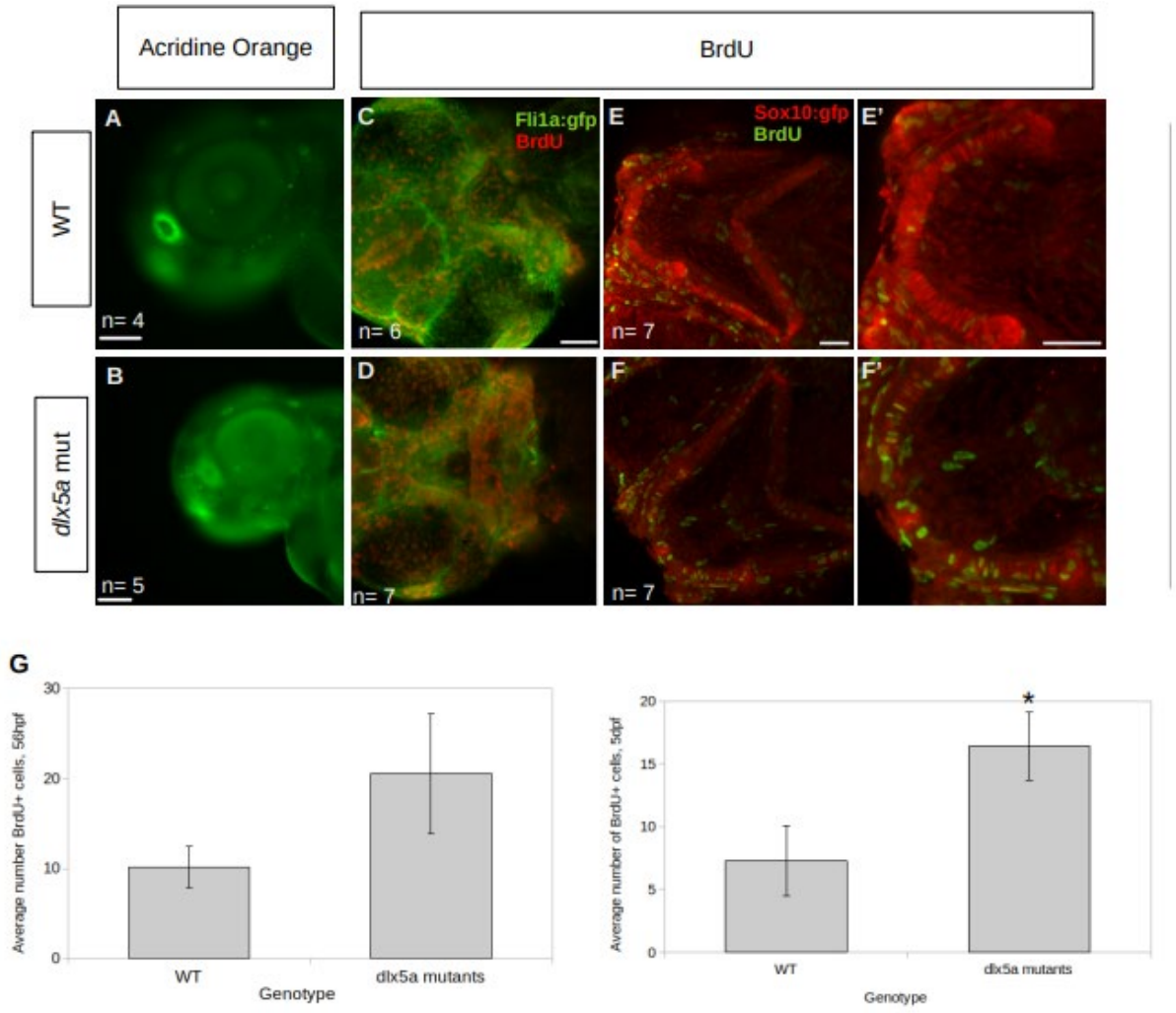

Figure 3.14. BrdU pulse-chase and acridine orange staining in *dlx5a* mutants.

(A-B) Acridine orange staining in 3dpf larvae showing no differences in number of stained puncta in the craniofacial region between *dlx5a* mutants and WT larvae. Scale = 100um. **(C, D)** BrdU pulse-chase at 56hpf showing increased number of BrdU+ cells in developing Meckel's cartilage. **(E-F)** BrdU pulse-chase at 5dpf also showing increased number of BrdU+ cells in the Meckel's cartilage. **(E', F')** are of the same animal as E and F with increased magnification. **(G)** The number of BrdU+ cells were quantified confirming increased numbers in 56hpf (left) and 5dpf (right). Scale for BrdU images = 50µm. * $p<0.05$ by one tail, unpaired t-test.

3.2.7 Wnt signaling defects were observed during MC development

It was previously reported that the characteristic arch of the MC is in part due to non-canonical Wnt activity (Ling et al., 2017). For example, loss of *wnt5b* in zebrafish resulted in shorter MC with smaller L/W ratios and inappropriate chondrocyte cell orientation at the midzone. Thus, expression of Wnt signaling components was investigated in *dlx5a* mutants. At 2dpf, expression of *wls*, a component involved in the trafficking of *wnt5b*, was expressed at similar levels between mutants and WT siblings (B. T. Wu et al., 2015a)(Fig 3.15a, b). However, the expression of *wnt5b*, a non-canonical Wnt expressed by NCC and surrounding mesoderm of PA1, was reduced at 2dpf (Fig 3.15e, f). Interestingly, by 3dpf, *wls* and *wnt5b* expression was increased in mutants relative to controls (Fig 3.15c, d, g, h). The expression of *wnt5b* was also assessed by RT-qPCR using two different primer sets, both demonstrating *wnt5b* has a trend of decreased expression at 2dpf in *dlx5a* mutants with a 0.6- or 0.4-fold expression (Fig 3.16 A, B). At 3dpf, the expression of *wnt5b* show a trend towards increased expression. The expression of two *wnt5b* receptors, *ror2* and *frzd7a* was also assessed by RT-qPCR, finding that in mutants, the expression of both receptors have a trend towards differential expression compared to WT (Fig 3.16 C, D).

One process governed by non-canonical Wnt signaling is regulation of cell polarity. To visualize this, 3dpf fish were stained with acetylated tubulin to label the microtubule organizing center (MTOC) and cell membranes with phalloidin (Fig. 3.17a, b). Within the MC, the polarity of the MTOC is split to either the left or right of the chondrocyte relative to the midline of the cartilage structure, which can be determined by dividing a cell into quadrants (Fig. 3.17c, left). This analysis revealed that the MTOC is positioned relatively equally in both WT and *dlx5a* mutants (WT: 41.8% right, 34.5% left; mutant: 34.5% right, 29.3% left). MTOC were also found in the top (WT: 7.3%, mutant:10.7%) and bottom (WT:12.7%, mutant: 16%) quadrants for both genotypes. However, most

strikingly, more cells were found with the MTOC in the center of the cell in mutants (20%) compared to WT (3.6%). Additionally, chondrocyte cell shape was rounder in mutants and did not exhibit the characteristic “stack of pennies” morphology. Both these results phenocopy *wnt5b* mutants, supporting a possible interaction between *dlx5a* activity and *wnt5b* function, potentially interfering with planar cell polarity during MC development.

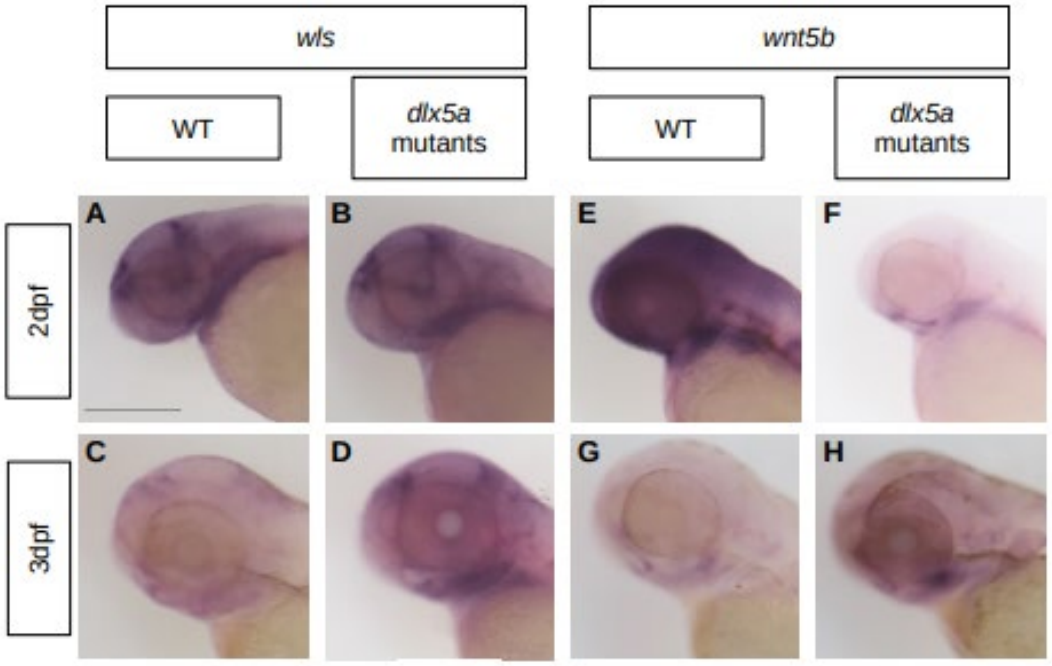

Figure 3.15. Expression of *wls* and *wnt5b* in *dlx5a* mutants at 2dpf and 3dpf.

(A-B) Expression of *wls* in 2dpf larvae showing similar staining intensities suggesting similar levels of expression. **(C-D)** Expression of *wls* in 3dpf larvae showing increased staining in *dlx5a* mutants. **(E-F)** Expression of *wnt5b* in 2dpf larvae. At the same time it took to stain *dlx5a* mutants, WT larvae became over-stained suggesting lowered expression in *dlx5a* mutants. **(G-H)** Expression of *wnt5b* in 3dpf larvae showing increased staining in *dlx5a* mutants compared to WT suggesting increased expression at this time. Scale = 100µm.

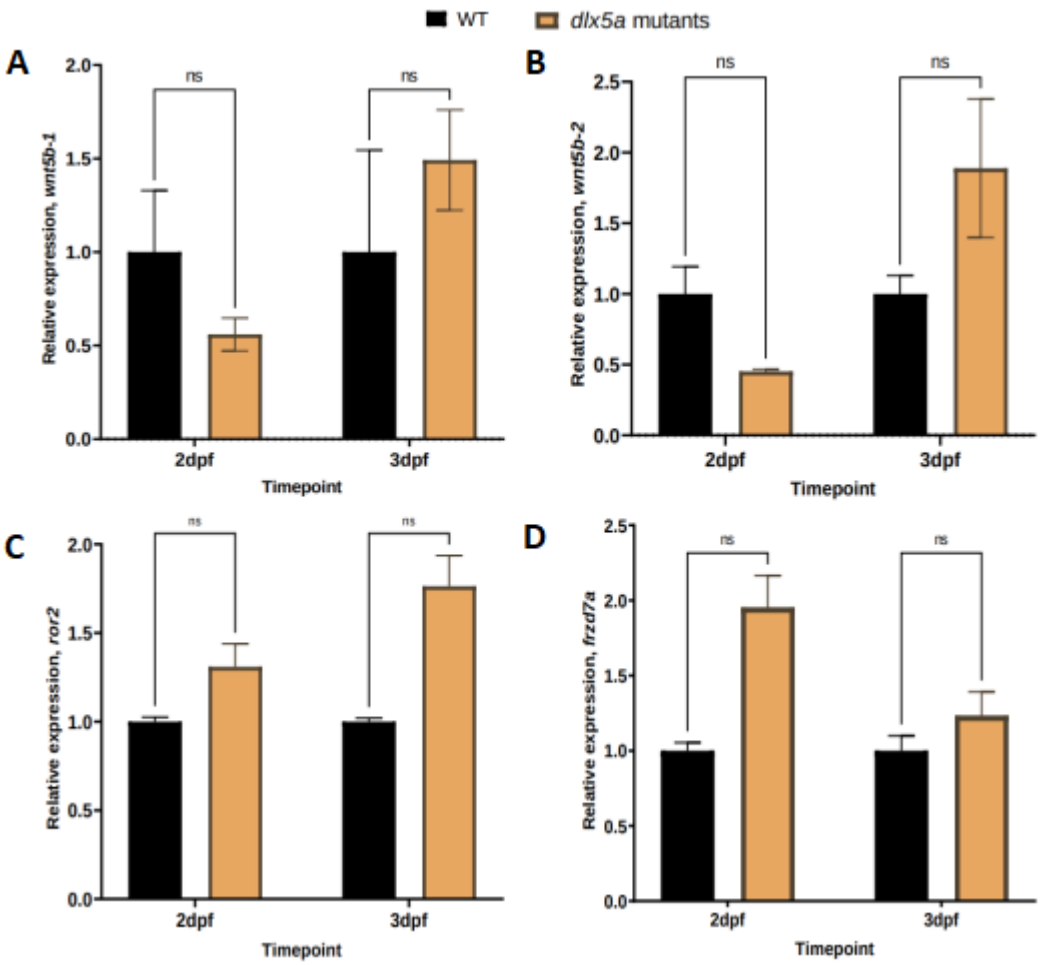

Figure 3.16. Expression of *wnt5b*, *ror2* and *frzd7*a by RT-qPCR

(A-B) RT-qPCR of *wnt5b* using two different primer sets showing decreased expression at 2dpf and increased expression at 3dpf. **(C)** Expression of *ror2* showing increased expression at both timepoints in *dlx5a* mutants. **(D)** Expression of *frzd7a* in *dlx5a* mutants is increased at 2dpf and 3dpf. All qPCR results reported as mean ± SEM from three pools of 20 larvae heads for each genotype. Ns: no significance using two-tailed, unpaired t-test with Holm-Sidak method.

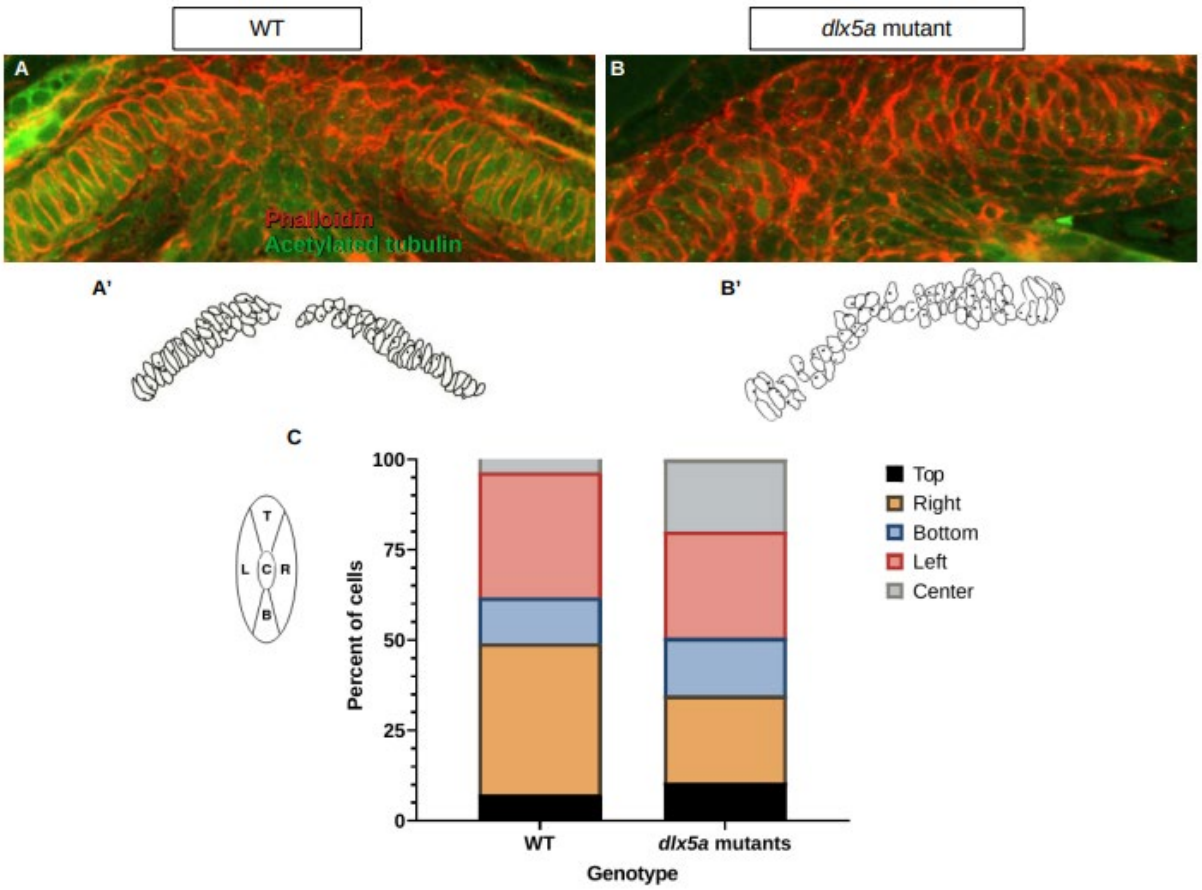

Figure 3.17. Positioning of microtubule organizing center (MTOC) is randomized in *dlx5a* mutant Meckel's cartilage at 3dpf.

(A, B) 3dpf larvae were stained with phalloidin and acetylated tubulin to label cell membranes and MTOC respectively in WT **(A)** and *dlx5a* mutants **(B).** Traces of Meckel's cartilage cells were made **(A', B')** to enable easier analysis. **(C)** A cell was divided into 5 regions (left schematic) relative to midline of Meckel's cartilage to determine MTOC localization which should be skewed equally to the left and right positions. Mutants displayed more randomization with greater number of MTOC in the top, bottom and center locations. A total of 4 WT animals representing 55 cells and 5 mutant animals representing 75 cells were analyzed.

3.3 Consequence of *dlx* gene loss on central and peripheral nervous system

Work described in sections 3.3.2 to 3.3.4 were partially performed by Hadeel Al Hadi under my supervision to fulfill her UROP placement and summer NSERC project requirements. Work described in Section 3.3.1 was partially performed by Jinane El Hage. Larval analysis described in Section 3.3.1 was performed by Emily Lam.

3.3.1 Distribution of calretinin expressing neurons in the telencephalon and midbrain

Calretinin (CR) expressing neurons are a heterogenous subpopulation of GABAergic interneurons(Cauli et al., 2014). Previous work in mouse *Dlx* mutants also suggested CR+ populations are altered in number and distribution (Cobos et al., 2005; Jones et al., 2011; Mao et al., 2009). Thus, to determine if the number of calretinin expressing neurons is reduced or if the distribution of these neurons is altered in *dlx* mutant fish, adult mutant and WT sibling brains were dissected, sectioned and stained for calretinin via immunohistochemistry. Similar sized sibling pairs were used and only brains similar in size to WT sibling were used for analyses.

In general, no significant differences were observed in any of the mutants compared to WT brains in any of the regions analyzed, likely due to large standard error observed in many samples (Figs 3.18, 3.19 and 3.20). In the dorsal telencephalon, majority of mutants had a trend of fewer CR+ neurons than WT (Fig 3.18). Only *dlx1a*$^{-/-}$ mutants showed a trend towards more CR+ neurons with a normalized average of 1.59±0.75 CR+ cells. In the ventral telencephalon, *dlx2a*$^{-/-}$ mutant brains showed a trend towards half as many CR+ neurons as WT (Fig 3.19). In contrast, *dlx6a*$^{-/-}$ mutant ventral telencephalon showed a trend towards increase in CR+ neurons with a normalized average of 1.42±0.13. These results suggest there are inconsistent differences within the telencephalon as a whole based on genotype and that perhaps specific *dlx* genes affect different subregions of the telencephalon.

For the optic tectum, observations were divided between the periventricular gray zone (PGZ) where majority of cell bodies are found and the outer layers of the optic tectum proper (TeO). In the PGZ, *dlx5a*$^{-/-}$, *dlx6a*$^{-/-}$ and *dlx5i6*$^{-/-}$ mutants displayed a trend towards fewer CR+ neurons with a normalized average of 0.69±0.21, 0.67±0.21, and 0.35±0.16 cells respectively (Fig. 3.20). In contrast, PGZ of *dlx1a*$^{-/-}$ mutant brains had a trend towards more neurons with a normalized average

of 1.55±0.34 CR+ cells. In the TeO, *dlx1a*$^{-/-}$ and *dlx5i6*$^{-/-}$ mutant brains had fewer neurons with normalized averages of 0.56±0.1 and 0.66±0.26 cells respectively. Interestingly, there was a significant difference observed in the number of CR+ neurons in 7dpf *dlx5a*$^{-/-}$ and *dlx5i6*$^{-/-}$ larval heads suggesting the trends observed in adult brains may reach significance with a larger sample size (Fig. A1). Taken together, there is a trend of fewer CR+ neurons in the entire optic tectum of *dlx5i6*$^{-/-}$ mutants.

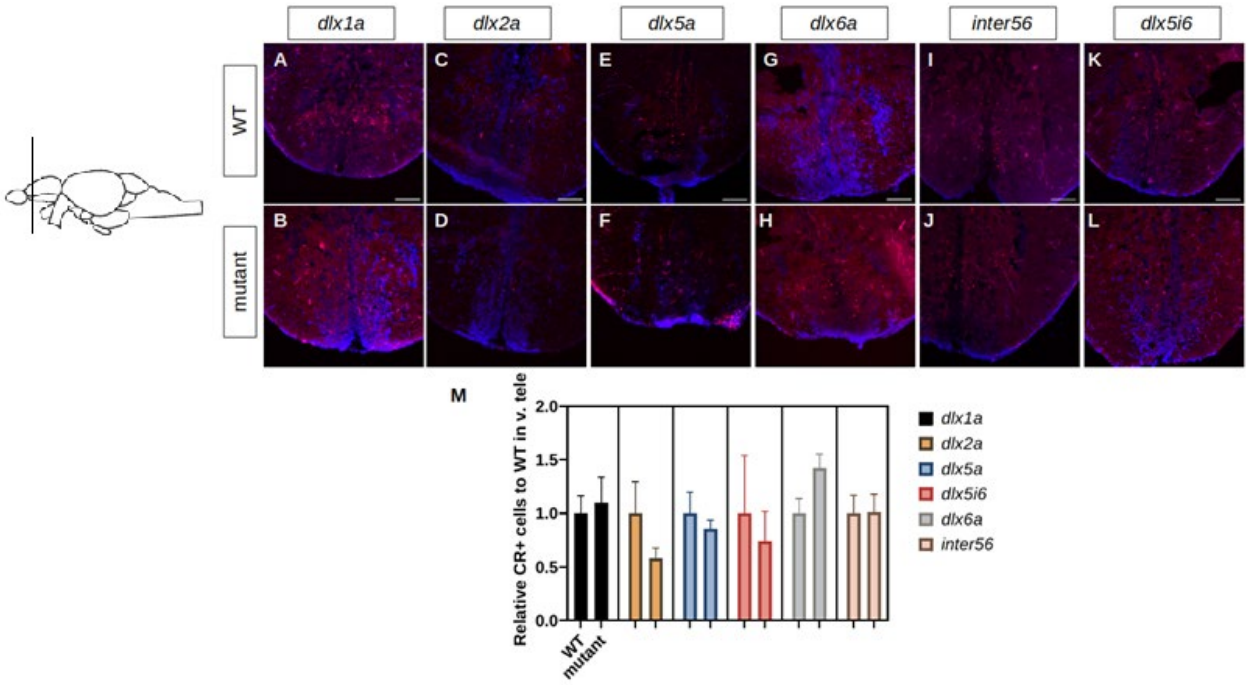

Figure 3.18. Number of CR+ neurons in the ventral telencephalon of adult *dlx* mutant brains.

(A-L) Transverse cryosections showing immunofluorescence of CR+ (red) and DAPI (blue) cells in dissected ventral telencephalon of WT or mutant sibling for each *dlx* gene. **(M)** Quantification of number CR+ cells in the ventral telencephalon of analyzed brains. All data are normalized averages presented as mean ± SEM. Images and data are representative of 3 brain pairs for *dlx1a*$^{-/-}$(p=0.737), *dlx2a*$^{-/-}$(p=0.245), *dlx5a*$^{-/-}$(p=0.537), *dlx6a*$^{-/-}$(p=0.09) and *inter56*$^{-/-}$ (p=0.963) groups. For *dlx5i6*$^{-/-}$, only two brain pairs were used. No significance was found using two-tailed unpaired t-test. Scale = 100μm.

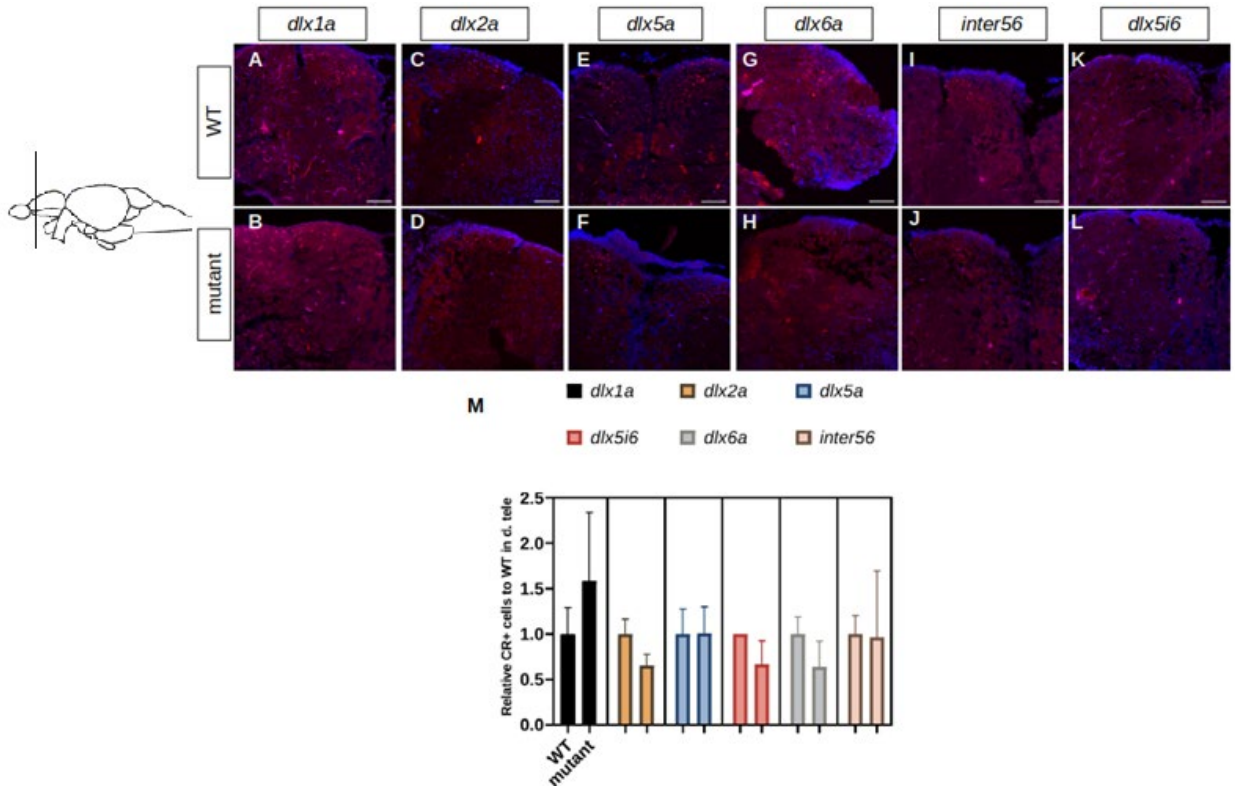

Figure 3.19. Number of CR+ neurons in the dorsal telencephalon of adult dlx mutant brains.

(A-L) Transverse sections of *dlx* mutant and WT sibling brains showing immunofluorescence of CR+ (red) and DAPI (blue) cells in one lobe of the dorsal telencephalon. **(M)** Quantification of number CR+ cells in the dorsal telencephalon of analyzed brains. All data are normalized averages presented as mean ± SEM. Images and data are representative of 3 brain pairs for *dlx1a*$^{-/-}$ (p=0.507), *dlx2a*$^{-/-}$ (p=0.168), *dlx5a*$^{-/-}$ (p=0.987) and *dlx6a*$^{-/-}$ (p=0.349) groups. For *dlx5i6*$^{-/-}$ and *inter56*$^{-/-}$, only two brain pairs were used. No significance was found using two-tailed unpaired t-test. Scale = 100μm.

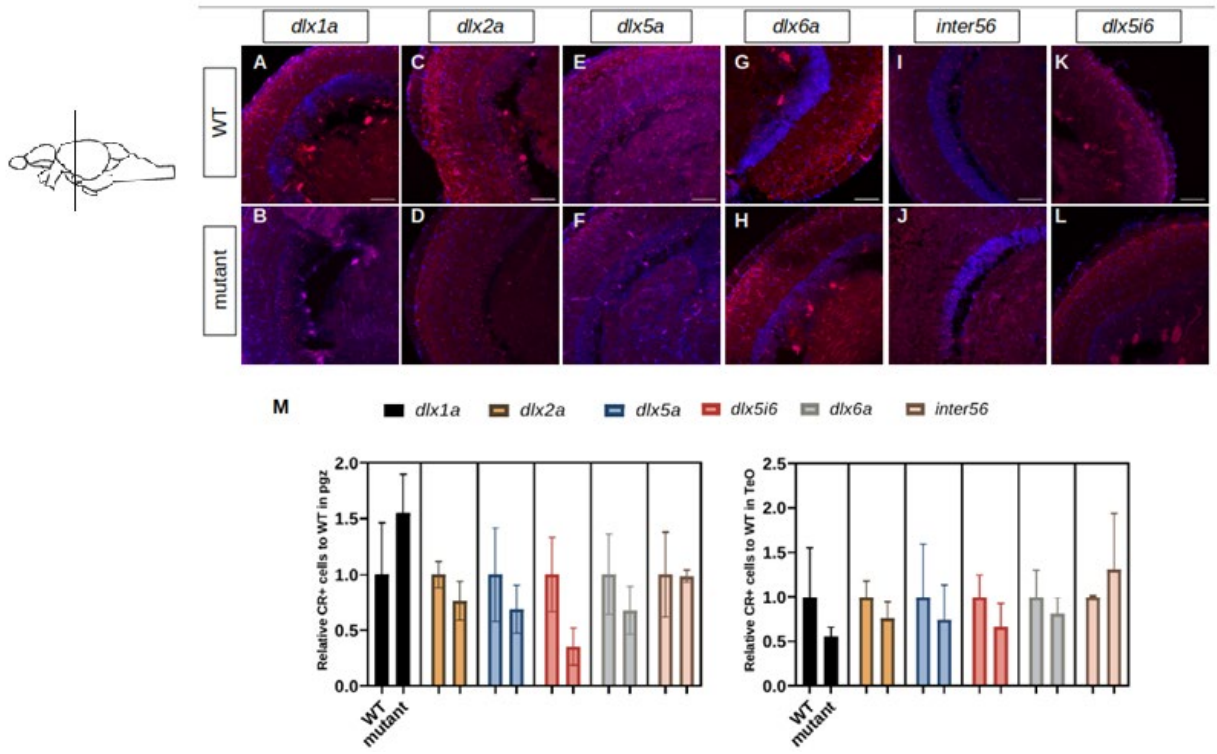

Figure 3.20. Number of CR+ neurons in the optic tectum of adult *dlx* mutant brains.

(A-L) Transverse sections of *dlx* mutant and WT sibling brains showing immunofluoresence of CR+ (red) and DAPI (blue) cells in one area of the optic tectum. **(M)** Quantification of number CR+ cells in the PGZ (left) and TeO (right) of analyzed brains. All data are normalized averages presented as mean ± SEM. Images and data are representative of 3 brain pairs for *dlx2a*, *dlx5a, dlx6a* and *dlx5i6* groups. P values for the pgz are as follows: *dlx2a*$^{-/-}$ (p=0.329), *dlx5a*$^{-/-}$ (p=0.445), *dlx6a*$^{-/-}$ (p=0.481) and *dlx5i6*$^{-/-}$ (0.133). For the TeO cortex, the p-values are : *dlx2a*$^{-/-}$ (p=0.403), *dlx5a*$^{-/-}$ (p=0.737), *dlx6a*$^{-/-}$ (p=0.622) and *dlx5i6*$^{-/-}$ (0.381). No statistical significance was found using a two-tailed t-test. No statistical analysis was performed for *dlx1a*$^{-/-}$ and *inter56*$^{-/-}$ groups since only two brains were used. Scale = 100µm.

3.3.2 Abnormal swim phenotype was observed in *dlx5a*$^{-/-}$ and *dlx5i6*$^{-/-}$ mutant adults

Unexpectedly, *dlx5a*$^{-/-}$ and *dlx5i6*$^{-/-}$ *mutant* fish were found to possess abnormal swim behaviours characterized by increased spinning and turning as they move. Importantly, these behaviours are not present in larvae or in juveniles under 1.5 months old. To characterize this behaviour, 3–8-month-old *dlx5a*$^{-/-}$ and WT siblings were recorded in 3-minute-long videos to observe the number of spins and turns that fish would make in that interval (Fig. 3.21). Mutants performed more changes in direction (turns) in a swim bout than WT siblings in addition to performing behaviours never observed in WT such as spinning during a swim bout.

Locomotor activity of *dlx5a*$^{-/-}$ mutants was further analyzed using the ZebraLab software. Mutants did not display significant differences in inactive duration or total swim distance. However, it is worth noting mutants displayed greater variation in these parameters (Fig. 3.22 A, B). Interestingly, traces of fish movement produced through ZebraLab also enabled the qualitative observation that mutants consistently displayed more activity in the center of the tank compared to the characteristic thigmotaxis observed in WT siblings (Fig 3.22 C, D).

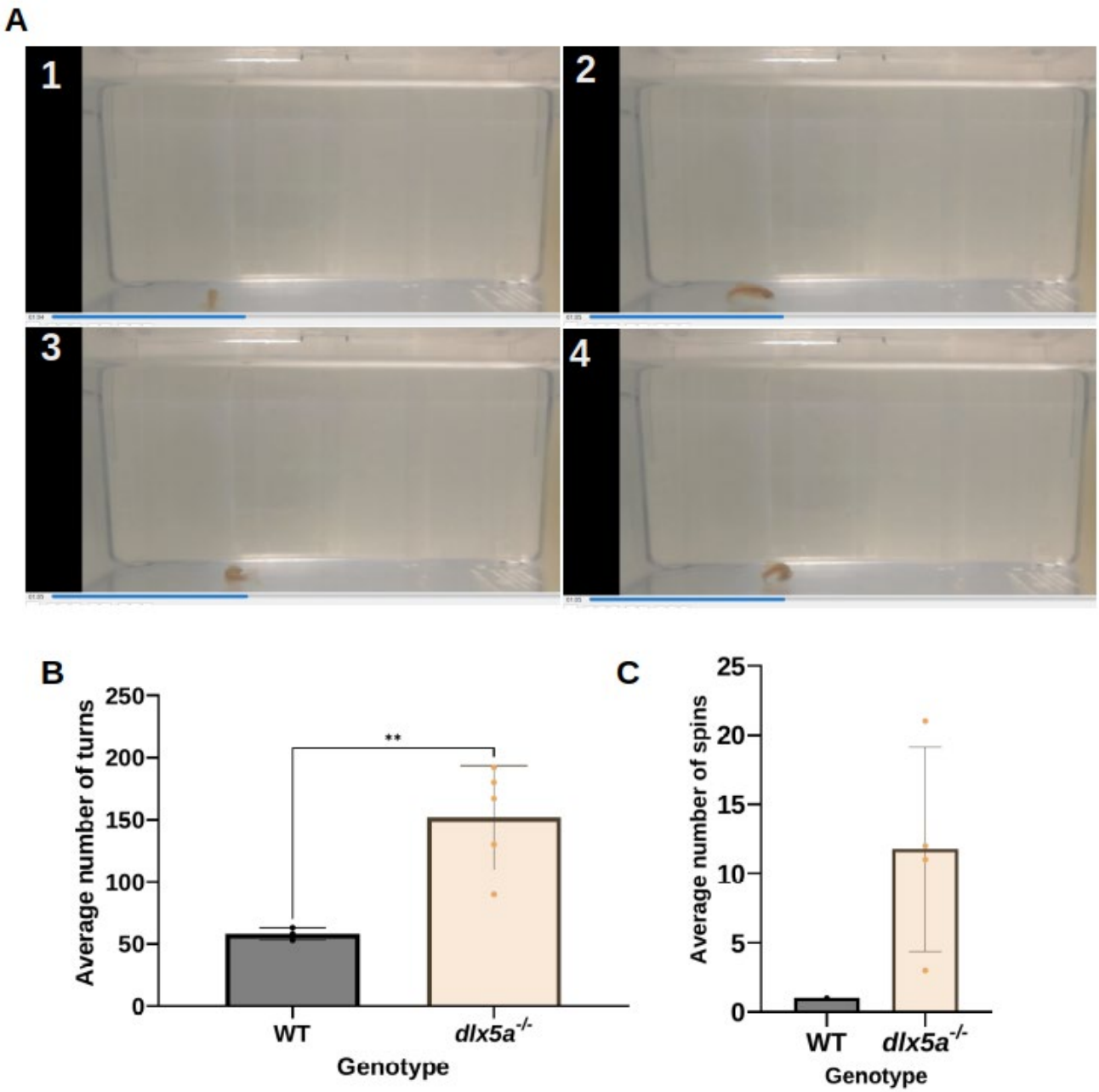

Figure 3.21. Swim behaviour of *dlx5a*$^{-/-}$ adults.

(A) Sequential screen captures of a *dlx5a*$^{-/-}$ fish spinning from recorded video made from the side of a tank. Spins can occur right after rest (depicted here) or during a swim bout and may also occur at any depth of the tank. **(B)** The total number of turns were counted for each fish recorded and averaged. **(C)** The number of spins performed by each fish was counted and averaged. A single WT performed one spin during the beginning of a recording session. Data presented as mean ± SD, from 3 WT fish and 5 *dlx5a*$^{-/-}$ fish.

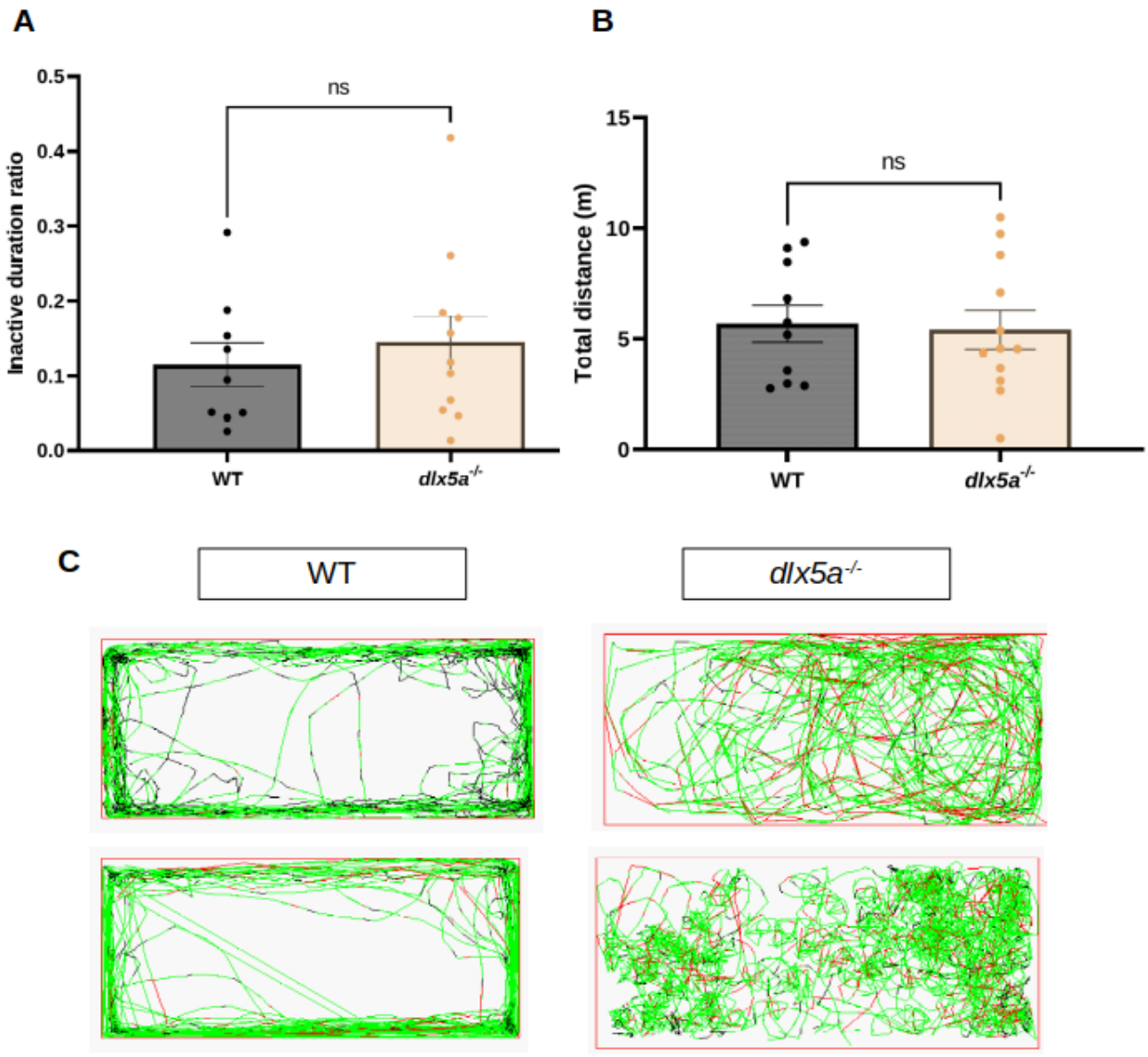

Figure 3.22. Locomotor activity recorded from open tank experiment using ZebraLab software.

(A) The inactive duration ratio of *dlx5a*$^{-/-}$ adults did not differ significantly to WT siblings. **(B)** The total distance also did not differ significantly between mutants and WT siblings. **(C)** Traces obtained through ZebraLab software during a recording session of 2 WT fish and 2 mutants revealed more activity in the center of the tank and more erratic swimming. Quantification for graphs A and B presented as mean ± SEM from 10 WT and 12 *dlx5a*$^{-/-}$ fish.

3.3.3 Lateral line organization is disrupted in *dlx5a*$^{-/-}$ fish with abnormal swim behaviour

One explanation for the abnormal swim behaviours described in 3.3.2 may be due to improper vestibular sensation. The vestibular system provides information about one's motion, head position and spatial orientation to coordinate movement and balance. In vertebrates, the main sensory tools are in the inner ear, comprising of the semicircular canals and otoliths which sense rotational and linear acceleration, respectively(Kingma & van de Berg, 2016). However, *dlx5a*$^{-/-}$ larvae do not display dysmorphology of semicircular canals or loss of otoliths in the otic placode at 4dpf (Fig. 3.23, c-f). Within the semicircular canals are hair cells that are able to sense rotational movement through fluid movement. Hair cells in the otic placode are present in 5dpf mutants and appear comparable to WT as well (Fig 3.24a, b).

Fish possess an additional system for vestibular and proprioception known as the lateral line which is composed of neuromasts. Neuromasts can be visualized by staining fish in a vital dye called DASPEI. To explore whether neuromasts are produced and if regular development of this system occurred, 3dpf larvae were stained with DASPEI, revealing that *dlx5a*$^{-/-}$ mutants do develop a lateral line system and placement of neuromasts are comparable to WT (Fig. 3.23, a-b). These neuromasts also possess hair cells at 5dpf (Fig. 3.24c, d). However, in adult mutants that display the abnormal swim behaviours, distribution of neuromasts was altered (Fig. 3.25a, b). In particular, the L branch was partially missing in most fish with a 70% decrease in average number. Overall, mutants had a 30% reduction in number of total neuromasts (Fig 3.25c).

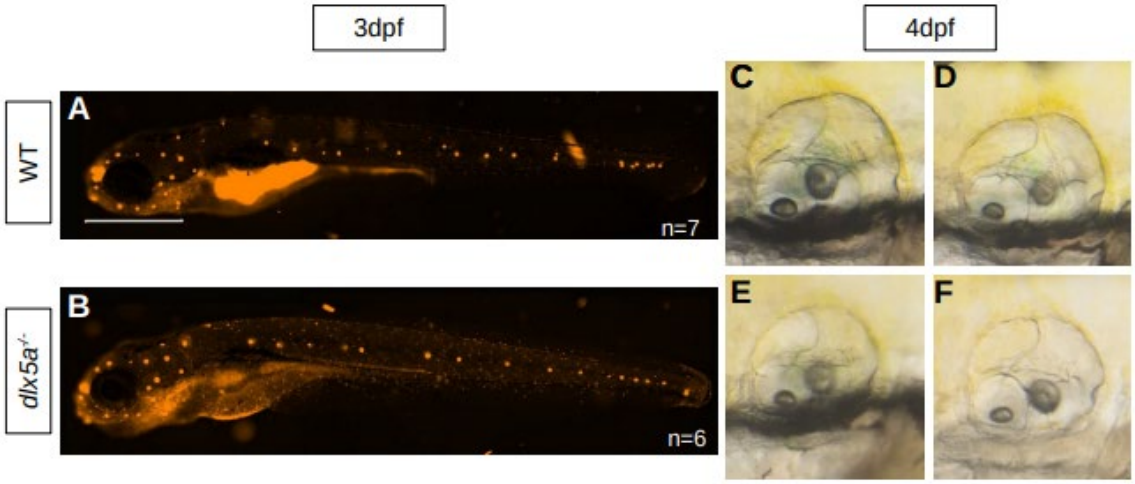

Figure 3.23. Mutant larvae do not possess morphological defects in posterior lateral line or semicircular canals.

(A, B) Larvae stained with DASPEI to show *dlx5a*$^{-/-}$ larvae develop rudimentary posterior lateral line at 3dpf that is comparable to WT. **(C-F)** Semicircular canals of WT **(C-D)** and *dlx5a*$^{-/-}$ larvae **(E-F)** at 4dpf demonstrating no morphological defects. DASPEI images from 6-7 animals, semicircular canal images are representative of 5 individuals per genotype. Scale = 500µm.

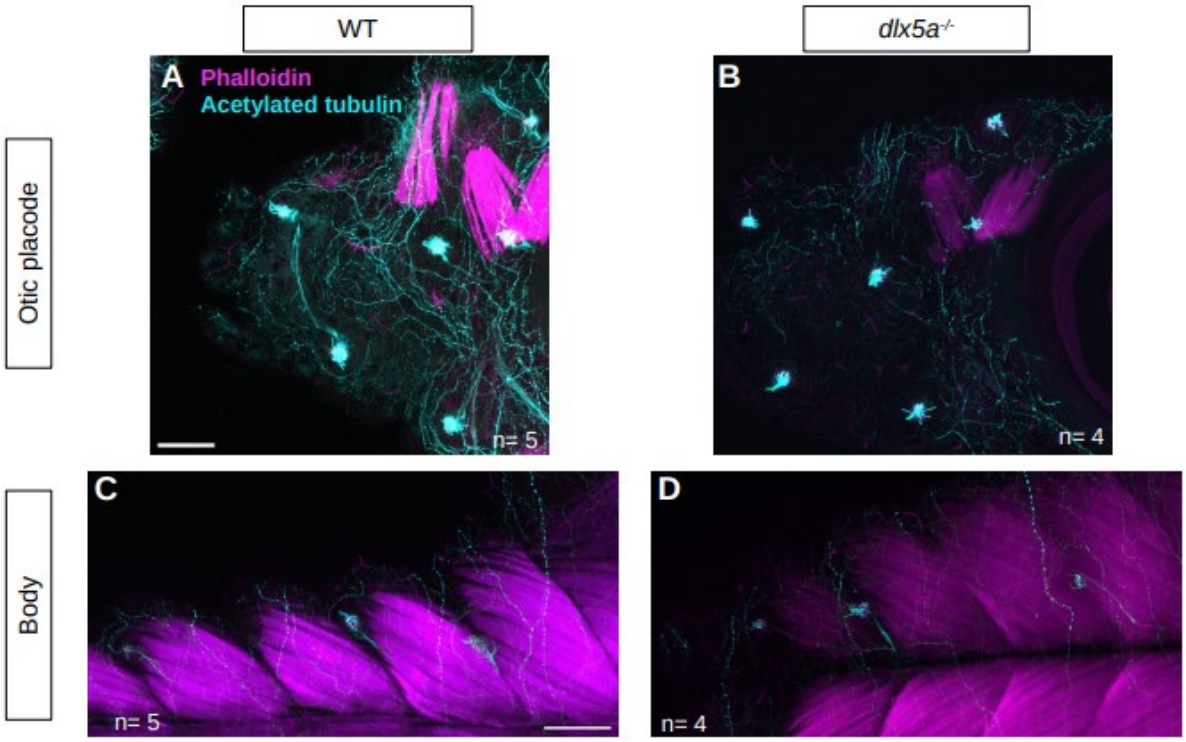

Figure 3.24. Hair cells are present in the otic placode and posterior lateral line neuromasts of 5dpf *dlx5a*$^{-/-}$ larvae.

(A-B) Phalloidin was used to label cell bodies and acetylated tubulin to label microtubule rich kinocillium of hair cells of the otic placode. **(C-D)** Neuromasts of the trunk also possess hair cells. Overstaining of acetylated tubulin antibody was also able to stain some nerves connecting neuromasts. Scale = 50μm.

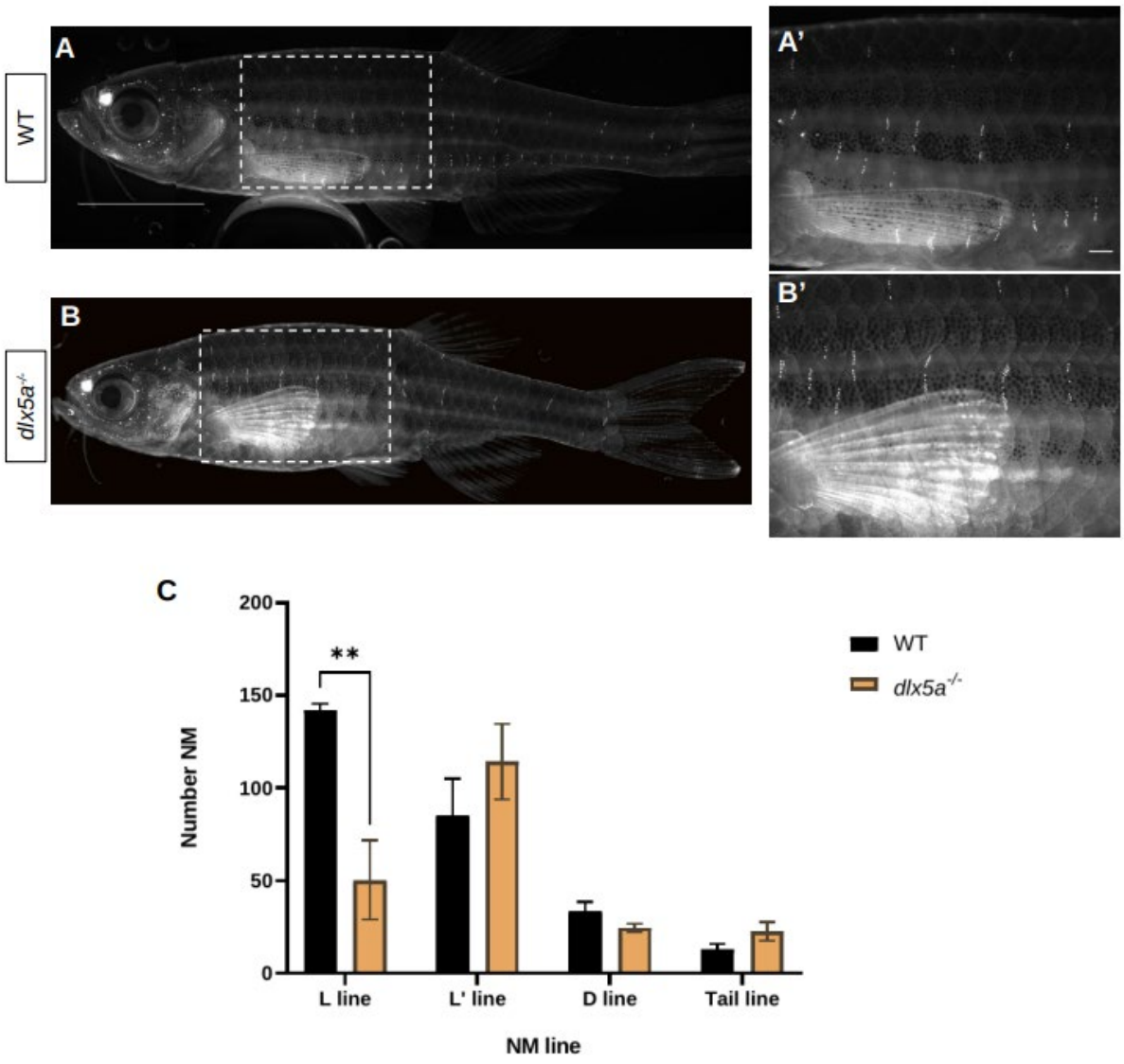

Figure 3.25. Neuromasts in adult *dlx5a*$^{-/-}$ have reduced number and altered distribution.

(A, B) Lateral images of DASPEI stained 8-month-old fish. Inset image of dashed box region showing *dlx5a*$^{-/-}$ fish possess longer L' line stitches and absent L line neuromasts. Images are representative of 4 individuals per genotype. Scale = 0.5cm; inset scale = 500µm. **(C)** Number of neuromasts per posterior line was counted revealing fewer neuromasts in the L branch. Neuromasts were counted from 3 individuals per genotype and data presented as mean ± SD. ** $p<0.01$.

3.3.4 Neuromast regeneration is altered in mutants following gentamycin exposure

As the fish body increases in size, the posterior lateral line becomes more elaborate through addition of intercalary neuromasts in "stitches"- vertical lines of neuromasts that develop from existing neuromasts. The altered distribution of and reduced number of neuromasts of the posterior lateral line in *dlx5a* adults suggest possible abnormalities in this process. To investigate this possibility, *dlx5a*$^{-/-}$ fish were challenged with antibiotic treatment to degenerate neuromasts and the ability of mutants to regenerate neuromasts was interrogated. Importantly, the process of regenerating neuromasts through latent precursors is thought to recapitulate formation of additional neuromasts in a stitch (Sánchez et al., 2016). Mutants and WT siblings that were 2.1-2.6cm in length and 2 months old were chosen for this experiment, finding that mutants had reduced capacity to regenerate neuromasts of all branches but the difference was especially striking in the L branch (Fig.3.26). Repeated exposure to the antibiotic did not exacerbate the difference in the L branch but did for the L' line.

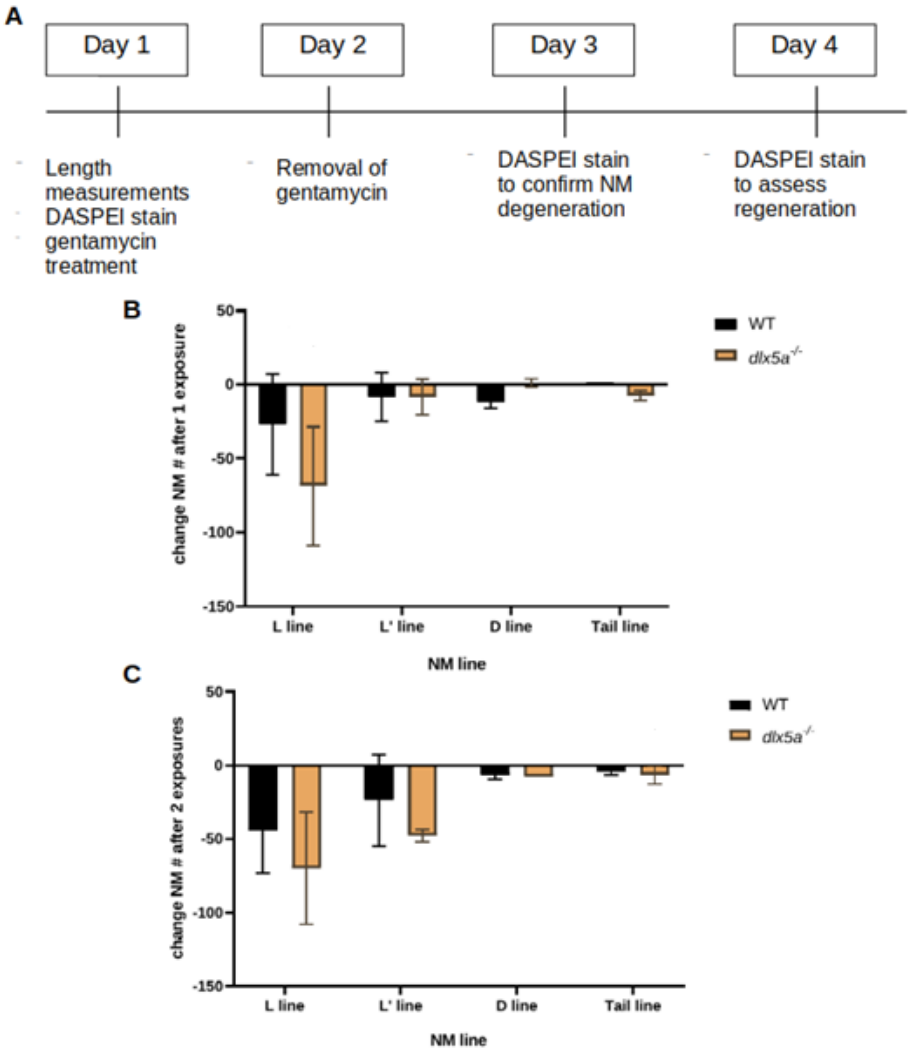

Figure 3.26. Neuromast regeneration of PLL following gentamycin treatment.

(A) Timeline of experiment. **(B)** Neuromasts were counted per line from 4 *dlx5a*$^{-/-}$ and 3WT size and age-matched fish before gentamycin exposure and after. The average change in neuromast number (post-treatment – pre-treatment) for each line was graphed and reported as mean ± SD. **(C)** A second trial was performed on 2 WT and 2 *dlx5a*$^{-/-}$ fish after a week of recovery, finding that similar reduction in regenerative capacity was observed in the L branch. The L' branch also regenerated less following the second trial.

Chapter 4

Discussion

4.1 Cross regulation of *dlx* expression

The expression of *dlx* paralogs in the absence of each *dlx* gene of interest was explored in 24hpf, 48hpf and 72hpf larvae. Evidence of cross-regulation between paralogs initially observed in mice was also seen here. Specifically, *dlx1a* expression is reduced in *dlx2a* mutants at 48hpf, a developmental timepoint comparable to E12.5-E13.5 in mouse brain development (Eisenstat et al., 1999; Mueller et al., 2006). However, some exceptions to previously observed cross-regulatory patterns were also observed.

4.1.1 Evidence suggests *dlx1a* and *dlx2a* are not completely compensatory

The expression of *dlx2a* was equal or slightly weaker in *dlx1a*$^{-/-}$ than WT at 24hpf and 48hpf, however, there may be increased expression of *dlx2a* in *dlx1a* mutants by 72hpf, suggesting the idea that a compensatory role for *dlx2a* may be time dependent. Importantly, a role for *dlx1a* compensating for *dlx2a* was not supported here. While it may be possible the amount of *Dlx1a* expressed in *dlx2a*$^{-/-}$ is sufficient to fulfill the function of both genes, it was unexpected that *dlx2a* expression decreased in *dlx1a* mutants.

4.1.2 Dlx2a is required for *dlx5a* maintenance and expression of these genes may be more interconnected than previously thought

At early time points, *dlx5a* is expressed in *dlx2a*$^{-/-}$ but transcript levels are reduced to near undetectable levels by 72hpf suggesting *dlx2a* may be important for the maintenance of *dlx5a* in zebrafish but not for its initial expression. It is possible that initial *dlx5a* expression seen in *dlx2a*$^{-/-}$ embryos is due to potential compensation by the unpaired *dlx* paralog *dlx2b*. However, current knowledge of compensation occurring after CRISPR-Cas9 mediated mutagenesis requires

nonsense-mediated decay of truncated RNA which is not likely in our mutants given the entire gene was deleted (El-Brolosy et al., 2019).

The increased expression of *dlx2a* in *dlx5a* mutants suggest a feedback loop exists in which *dlx5a* or a downstream gene regulated by *dlx5a* may in turn regulate the expression of *dlx2a*. Supporting this, binding sites for *dlx* genes exist on the CRE I12b between *Dlx1/Dlx2* and Dlx5a was shown to bind to this site in the CRE (Poitras et al., 2007). Potentially, this communication may exist to allow for differentiation of GABAergic interneurons and may even underlie differentiation into subtypes. For example, lineage tracing experiments demonstrated that cells that expressed *dlx1a*/*dlx2a* at 24hpf are associated with somatostatin and calretinin expressing neurons in juvenile fish while cells that expressed *dlx5a*/*dlx6a* at 24hpf are associated with parvalbumin neurons (Solek et al., 2017). Similarly, Dlx5/Dlx6 were to be important in regulating parvalbumin neuron development in the mouse, controlling differentiation and influencing neurite growth (Wang et al., 2010). How deletions of these paralogs influence GABAergic subtype differentiation remains to be determined.

4.1.3 Additional regulatory elements may regulate *dlx5a/dlx6a* expression in a redundant manner

Interestingly, *dlx5a*/*dlx6a* continues to be expressed in *inter56*$^{-/-}$ larvae wherein both CREs within the intergenic region are deleted. In the mouse, deletion of one of the CREs, i56ii, was found to reduce but not abolish *Dlx5/Dlx6* expression, with expression possible due to the remaining enhancer, I56i (Darbandi et al., 2016). However, since both enhancers are deleted here and *dlx5a*/*dlx6a* expression persists, it is likely other enhancers exist to regulate their expression (Cannavò et al., 2016). Indeed, other CREs that affect *Dlx5/Dlx6* expression have been identified in

the mouse and human with clinical and/or behavioural significance (Brown et al., 2010; Johnson et al., 2018). While it is unknown whether these other enhancers are active during brain development in mice or humans or even exist in zebrafish, the idea that alternative or compensatory CREs are present in the teleost *dlx* regulatory network warrants further investigation.

4.2 Effect of *dlx* loss on craniofacial development

During craniofacial development, *dlx* genes are important in providing neural crest cells positional identity for development of ventral craniofacial structures of the first two pharyngeal arches. However, little is known about the role of each of the six *dlx* genes expressed within the developing craniofacial tissues. Here, differential impact of *dlx* gene loss on ventral craniofacial structure size and shape was observed. Additionally, a role for *dlx5a* in in regulating morphogenesis of ventral facial cartilage, in particular the MC, through interaction with non-canonical Wnt signaling such as *wnt5b* was uncovered.

4.2.1 Phenotypes in *dlx* mutants generated by CRISPR-Cas9 are different from previously reported zebrafish and mouse mutants

Previous investigations in zebrafish have determined that *dlx5a* is involved in the intermediate region of the ventral pharyngeal skeleton, particularly where the MC contact the palatoquadrate (Coffin Talbot et al., 2010). Reduction in *dlx5a* expression in addition to reductions in *dlx3b* and *dlx4b* lead to reductions in the intermediate domain and fusion of the MC and palatoquadrate. While domain boundaries were not explored in this thesis directly, it is possible the intermediate domain described by Talbot and colleagues is reduced based on the reduced size of MC and PQ. However, work described here does not support the finding that reduced *dlx5a*

expression leads to fusion of MC and PQ since neither *dlx5a*$^{-/-}$, *dlx5i6*$^{-/-}$ nor *dlx2a*$^{-/-}$, which loses *dlx5a* expression by 3dpf display fusion. It is possible the fusion phenotype is absent in these mutants because *dlx3b* and *dlx4b* may be expressed at normal levels or is even able to compensate for some of the effects of *dlx5a* loss. This possibility will need to be further investigated, ideally through generation of a double or triple mutant.

Compound mutants for *Dlx5/Dlx6* in the mouse resulted in homeotic shift of the mandibles to a secondary maxilla (Beverdam et al., 2002; Depew et al., 2002; Merlo et al., 2002; Robledo et al., 2002). However, this was not observed in *dlx5i6* mutants, which were shown by WISH to have little to no expression of *dlx5a* and *dlx6a*. This discrepancy may be due to other *dlx* genes playing a larger role in craniofacial development in zebrafish than in mice, or that these paralogs (eg: *dlx3b, dlx4b*) are able to compensate for the loss of *dlx5a* and *dlx6a*. An additional or alternative explanation may be that the MC, which is a lower jaw structure that was most affected in *dlx5a*$^{-/-}$ and *dlx5i6*$^{-/-}$ larvae, is a permanent scaffold in zebrafish. However, in the mouse, the MC is a transient scaffold upon which further elaborate jaw structures are built, thus more severe consequences were observed in compound *Dlx* mutants in the mouse compared to zebrafish (Bhaskar et al., 1953; Svandova et al., 2020).

4.2.2 Loss of *dlx* paralogs alter size of MC, PQ and CH structures

Morphometric analysis revealed loss of *dlx* paralogs led to changes in the length of the MC, PQ and CH. At 5dpf, all three structures were significantly shorter in *dlx5a*$^{-/-}$ and *dlx5i6*$^{-/-}$ larvae. There was also a trend towards shorter structures in *dlx2a*$^{-/-}$ larvae. Conversely, there was a trend towards longer structures in *dlx1a, dlx6a* and *inter56* mutants. Interestingly, the mutants with shorter structures all share a lack of *dlx5a* expression by 3dpf whereas the group with longer structures have

either comparable levels of other *dlx* paralog expression or increased *dlx5a* expression (in the case of *dlx6a*$^{-/-}$ larvae). This suggests *dlx5a* is important in regulating cartilage size. Indeed, in the developing mouse limb, gain-of-function of *Dlx5* was found to promote chondrocyte hypertrophy (Chin et al., 2007). Additionally, smaller MC was also observed in mouse *Dlx5* null mutants, suggesting the role of *Dlx5/dlx5a* in regulating MC size is conserved (Beverdam et al., 2002; Depew et al., 2002; Merlo et al., 2002; Robledo et al., 2002).

The size and shape of craniofacial structures, in particular the MC, is likely autonomously regulated by NCC. This was demonstrated in chimeric analysis where quail NCC were transplanted unilaterally into a duck host resulting in quail cells in one side of the developing MC (Eames & Schneider, 2008). As the host developed, the quail side of the MC maintained a more quail-like structure in addition to accelerating certain stages of chondrogenic events such as *col2* upregulation and matrix deposition in the whole structure relative to age-matched hosts. The fact that loss of *dlx5a* expression leads to shorter structures, and size of cartilage structures is intrinsically regulated by NCC suggest *dlx5a* may regulate a network of genes involved in regulating cartilage size.

The size of MC, PQ and CH were also analyzed at 14dpf, finding that most of the differences observed at 5dpf have normalized. Particularly, while the MC is still significantly smaller in *dlx5a*$^{-/-}$ and *dlx5i6*$^{-/-}$ larvae, the sizes of the other two cartilages are no longer different. The only other exception is in *dlx1a*$^{-/-}$ which at this age also have shorter MC, PQ and CH. It is possible at this age that other mechanisms are involved in regulating cartilage size other than NCC expression profile. Importantly, the overall size of the head was also smaller in *dlx1a*$^{-/-}$ mutant larvae at this age, suggesting a possible growth defect in these mutants.

Osteogenesis was not investigated in this study however *dlx* genes are also involved in this process. Overexpression of *Dlx2* in NCC in the mouse or through *in vitro* experiments on bone

marrow stromal cells was found to increase expression of genes involved in ossification such as *osteocalcin* and *Alp* (Sun et al., 2022; Zhang et al., 2018). Additionally, osteogenic differentiation in human bone marrow stromal cells involves the activity of *Dlx2* on *Wnt1* activation (Zeng et al., 2020). Finally, Dlx3, Dlx5 and Dlx6 was found to recruit the key transcription factor of osteoblast differentiation, Sp7/Osterix to initiate osteoblast specification and may explain why *Dlx5/Dlx6* mouse mutants lack alizarin red staining (Depew et al., 2002; Hojo et al., 2016). Alizarin red staining in *dlx* zebrafish mutants at both time points did not yield meaningful differences between mutants and between WT but additional analysis such as calcein staining or probing expression differences in osteogenic genes will need to be performed. Since mutants develop relatively normal jaws as adults, it is possible that perichondral ossification, the type of ossification that occurs on the MC through aggregation of osteoblast occurs without defect, potentially rescuing abnormalities observed in the cartilaginous template of the MC.

4.2.3 Altered expression of chondrocyte markers in *dlx5a* mutants

To further explore the consequence of *dlx5a* loss in craniofacial development, the expression of NCC and chondrogenic markers was explored using WISH and RT-qPCR in developmentally relevant timepoints. Results from these experiments demonstrated expression of *sox9a* and *col11a2* was increased at 3dpf although *sox9a* qPCR results also showed increased expression at 2dpf. Increased expression of these markers suggested that despite having smaller structures, mutants experienced chondrogenesis and chondrocyte condensation.

Collagen is a protein that is secreted by chondrocytes and other cells such as notochord cells to produce a scaffold. It is remodeled in the ECM to modulate the flexibility of the environment to allow changes in cell morphology and cell migration through activity of proteins such as

metalloproteases (Szabó & Mayor, 2018). Reduced degradation or remodeling of collagen can result in stiffening of the ECM, affecting the ability of cells to attain the correct morphology. For example, larval zebrafish tail failed to uncurl and body axis did not extend in knock down of *Mmp2* (Zhang et al., 2003). Later work demonstrated that collagen degradation through Mmp2 activity is required at the time tail uncurling occurs (Wyatt & Crawford, 2021). Thus, it is possible that excess collagen produced in *dlx5a* mutants may be the reason MC chondrocytes fail to attain the correct cell morphology, outside of possible PCP effects. Future work to elucidate whether the balance in collagen secretion and remodeling is altered in *dlx5a* mutants will need to be performed, perhaps by using a collagen mimetic protein that can bind to degraded collagen (J. Hwang et al., 2017; Wyatt & Crawford, 2021). Interestingly, the overexpression of *Dlx2* was found to increase accumulation of type II collagen in mouse chondrocytes *in vitro*, by inhibiting MMP13 expression and activity (Zhang et al., 2018). Thus, if collagen remodeling defect is observed in *dlx5a* mutants, it is possible the effect is due to excess *dlx2a* activity.

4.2.4 Increased proliferation was observed in MC of *dlx5a* mutants

Proliferation and apoptosis were also investigated in *dlx5a* mutants since previous work from our laboratory have determined reduced *dlx1/2* expression leads to reduced survival of NCC and a downstream consequence of reduced *dlx2a* is reduced *dlx5a* expression. Additionally, it was possible that altered MC is a result of fewer NCC contributing to the structure. To observe amounts of apoptotic cells, larvae were stained with acridine orange which binds to DNA and acidic organelles to label cells undergoing apoptosis. This experiment revealed no differences in number of cells positive for the marker in the craniofacial region although more puncta were observed in

the brains of *dlx5a* mutants compared to WT. Proliferation was investigated through incubating larvae at 52hpf or 5dpf with BrdU and chasing for 4 hours, revealing *dlx5a* larvae at both time points have increased number of BrdU+ cells, suggesting proliferation occurred in the MC. These results are directly at odds with consequences of morpholino-mediated knockdown of *dlx1a/2a*. This may be explained by the known tendency of morpholinos to induce off-target effects such as p53 pathway activation leading to cell death. However, to confirm this, acridine orange should also be investigated in *dlx2a*$^{-/-}$ larvae.

Regulation of the cell cycle is an important component in development and influences events such as altering the time a cell can respond to differentiation cues and preserving multipotency in stem cells and progenitors (Langley et al., 2014; Soufi & Dalton, 2016). Previous work in cell lines have identified a role for *Dlx5* and *Dlx6* in cell cycle regulation, where expression of these genes resulted in antagonism of the G1/S transition (MacKenzie et al., 2019). Cells progressed through the cycle slower with fewer cells entering the S-phase. Importantly, these effects did not affect apoptosis. It is therefore possible that loss of *dlx5a/dlx6a* resulted in increased proliferation due to shorter cell cycle duration or there were simply more cells in S-phase without *dlx5a/dlx6a* expression leading to more cells being labeled by BrdU. To further confirm *dlx5a* mutants experience more cell proliferation, labeling with additional markers of proliferation such as PCNA or Ki67 will need to be performed.

NCC proliferation is tightly linked to migration and axial level. Trunk NCC are arrested in the G1 phase of the cell cycle, only entering S phase synchronously upon delamination (Burstyn-Cohen & Kalcheim, 2002). However, CNCC leave the neural tube in clusters and progression through the cell cycle is stochastic among this population (Théveneau et al., 2007). Further analysis of cell cycle progression of CNCC during migration in the chick revealed an increase of eightfold

to threefold in NCC of a migratory stream from leading to lagging cells (P. M. Kulesa et al., 2008). Once in the PA, NCC doubling time decreased (faster proliferation) suggesting permissive factors are present in the environment and/or CNCC are more responsive to pro-proliferative signals (Ridenour et al., 2014). Importantly, ablation of a subpopulation of CNCC before migration from the neural tube resulted in increased proliferation in migratory CNCC and suggest cell density within a migratory stream influences the rate of cell cycle progression. Based on these findings from the chick CNCC, it is possible that increased proliferation observed in *dlx5a* mutants may also arise from fewer cells migrating in a stream, leading to an increased rate of proliferation during migration and after invasion in the PA. While overall migration of NCC in *dlx5a* mutant larvae was investigated through extent of *foxd3* staining, a more detailed analysis of NCC migration was not performed. It will be important to elucidate whether the number of CNCC migrating from the neural tube is affected through confocal time-lapse imaging of live *sox10:GFP; dlx5a*$^{-/-}$ animals.

4.2.5 Interaction between *dlx* and the non-canonical Wnt signaling pathway during MC morphogenesis

One of the most interesting results in this section was the discovery that non-canonical Wnt signaling may be aberrant in *dlx5a* mutants, leading to abnormal morphogenesis of the MC. Morphometric analyses determined that the MC in fish without *dlx5a* have wider MC that did not protrude as far past the ethmoid plate as WT (ie: L/W ratio). This phenocopies mutants of non-canonical Wnt signaling such as *wnt5b, glypican* and *fzd7a* (Ling et al., 2017). Surprisingly, *dlx5a* mutants have reduced expression of *wnt5b* at 2dpf during onset of MC morphogenesis. However, by 3dpf, there is a drastic increase in *wnt5b* expression, suggesting that increased Wnt signaling may also lead to planar cell polarity defects. This is further supported by the observation that the

microtubule organizing center in chondrocytes of the midpoint of the MC are misoriented in *dlx5a* mutants and that chondrocytes fail to elongate, instead maintaining a spherical cell shape.

Planar cell polarity (PCP) describes a process in which a cell attains uniform orientation and structure within a tissue, mediated by non-canonical Wnt activity. Rather than activate β -catenin and gene expression, activity of non-canonical Wnts such as zebrafish *wnt5b, wnt9a* and *wnt11* lead to changes in microtubule dynamics and cytoskeletal rearrangements through mediators such as Rho-kinases or c-jun N-terminal kinase JNK (Perkins et al., 2022; Topczewski et al., 2011). Animals with PCP defects usually present with convergence and extension defects resulting in shorter, broader animals. The body axis of *dlx5a* mutants may be affected since *foxd3* WISH at early somitogenesis stages showed streaks of NCC that were further apart from the midline, suggesting a wider axis. However older larvae did not appear shorter or broader. Additional assays to determine if PCP is affected in the animal will need to be performed in the future, such as WISH for *krox20/myoD* to observe differences in the hindbrain and somite placement between *dlx5a* mutants and WT siblings.

Previous work in loss of function mutants of non-canonical Wnt signaling components such as *wnt5b*, *wnt9a*, *fzd7a* and *gpc4* determined the Meckel's cartilage were wider and shorter, potentially due to chondrocytes failing to elongate and stack properly (Ling et al., 2017; Sisson et al., 2015). Other defects included changes to osteogenesis and decreased proliferation. In the present work, an initial downregulation followed by upregulation of *wnt5b* was observed during the onset of Meckel's cartilage development, which contrasts with a complete loss of *wnt5b* expression at all timepoints. It is possible that much lower levels of non-canonical Wnt signaling *and* higher levels both lead to PCP defects (Jussila & Ciruna, 2017). For example, over-expression of Dishevelled, a downstream mediator following Wnt receptor activation, results in polarity and convergence and

extension defects in zebrafish and *Xenopus* (Tada & Smith, 2000; Wallingford et al., 2000). Ectopic expression of the co-receptor *ror2* also leads to convergence and extension defects in zebrafish similar to phenotypes in knock-down and introduction of dominant-negative constructs (Bai et al., 2014; Young et al., 2014). These examples and the present work suggest the proper dosage of non-canonical Wnt signaling components is essential for cell polarity and morphogenesis. To further support this idea, it will be important to investigate the expression of other non-canonical and canonical Wnts to determine if the morphological effects are only due to changes in *wnt5b* activity as well as other timepoints to determine if expression levels normalize.

Other signals may also be involved in morphogenesis of the MC, including FGFs. Interestingly, *wnt5b* mutant phenotypes such as shorter body axis, shorter and wider MC and CH can be rescued by ectopic *fgf3* mRNA (B. T. Wu et al., 2015b). It was also found that *fgf*3 expression was reduced along the AP axis in *wnt5b* mutants but not morphants for *wnt9a* or *wnt11* suggesting *fgf3* is downstream of *wnt5b* activity. Finally, loss of *wnt5b* or *wls* knock down resulted in reduced proliferation at 2dpf, potentially through regulating *fgf3* activity. Given that *dlx5a* mutants presented with proliferation and morphological abnormalities in the MC, and that these mutants mis-express *wnt5b* and *wls*, it is possible that *fgf3* expression is affected as well.

4.3 Consequence of *dlx* loss in the central and peripheral nervous system

4.3.1 No differences were observed in calretinin neuron number and distribution in the telencephalon and optic tectum of any *dlx* mutants

The distribution and number of CR neurons in adult *dlx* mutant telencephalon and optic tectum was explored in this thesis. In all mutants, no significant differences were identified in any of the brain regions chosen. However, *dlx5i6*$^{-/-}$ brains showed a trend towards fewer CR+ neurons in the entire optic tectum. This result is contrary to previous work in mice showing that loss of *Dlx1* resulted in fewer CR+ and somatostatin neurons without changing the number of other subtypes (Cobos et al., 2005). However, since large variation was observed in all mutants and brain regions, it is possible that trends observed in adult *dlx* mutant brains for CR+ neurons may reach significance with a larger sample size, in particular, for *dlx5i6*$^{-/-}$ brains. The discrepancies between the data described here and published work may also be due to difficulty in confirming true CR neurons since a counter label was not possible with the antibodies available. To address this issue, a transgenic line was created where mcherry fluorescent protein is under the regulation of *gad67* reporter to label cells that express GABA (plasmid construct from Song et al., 2017). These fish were crossed into all *dlx* mutants however I was unable to attain the F2 generation for homozygous adults. In the future, these fish may be used to ensure GABAergic neurons were counted. Additionally, a counter label may provide more information and landmarks to further differentiate specific clusters within the ventral and dorsal telencephalon.

The impact of *dlx* loss on the number and distribution of other types of GABAergic neurons will also need to be elucidated. Previous work in our laboratory suggested that different *dlx* genes are involved in development of different GABAergic subtypes. Enhancers for *dlx* genes drove

reporter expression in different GABAergic subtypes in the developing forebrain: URE2, I12b and I56i can all drive reporter expression in parvalbumin, CR+ and NPY neurons but URE2 reporter activity alone colocalized with nNOS neurons whereas I12b and I56i activity colocalized with VIP, CB and SOM neurons (Ghanem et al., 2007). Deletion of I56ii in the mouse also led to changes in the number of different GABAergic neuron subtypes: there was an increase of CR neurons and a decrease of PV neurons in the cortex at P17 (Darbandi et al., 2016). It is however also possible these results are characteristic of mouse and mammalian models since lineage tracing experiments in zebrafish demonstrated that majority of neurons that expressed *dlx1a/dlx2a* or *dlx5a/dlx6a* during early larval stages colocalize mostly with *gad65/67a* expression but not with many colocalized with markers of GABAergic subtypes, indicating these are neurons that have not fully differentiated yet (Solek et al., 2017). Nonetheless, this paper did find that cells that expressed *dlx1a/dlx2a* at 24hpf colocalize with CR+ and somatostatin subtypes but not parvalbumin, suggesting these *dlx* genes are more involved in the differentiation of CR+ and somatostatin neurons in zebrafish.

There was a trend towards fewer neurons in the PGZ of the optic tectum in *dlx5i6*$^{-/-}$ animals. The optic tectum is important for registering visual, auditory and other sensory information to form maps about the environment and position of stimuli in relation to the individual. This brain area and function is evolutionary conserved, although the region is called the superior colliculus in mammals. Interestingly, visual information from retinal ganglion cells is spatially mapped in the optic tectum, with cells reporting on the anterior visual field terminating in the caudal tectum while posterior visual field is registered in the caudal tectum (Isa et al., 2021). Dorsal and ventral information are registered in the lateral and medial tectum. With fewer inhibitory neurons in the PGZ, it may be possible visual information is not synthesized properly within these mutants. Furthermore, sensory information from the vestibular systems including the lateral line in aquatic animals are integrated

in the optic tectum to help trigger egocentric responses. Since *dlx5i6*$^{-/-}$ animals have fewer PGZ and tectal GABAergic neurons in this brain region, this may indicate vestibular responses are inappropriate and offer a biological basis to the abnormal swim behaviour observed in mutants.

4.3.2 Abnormal swimming behaviour was observed in *dlx5a* and *dlx5i6* adult homozygous mutants

In *dlx5a* and *dlx5i6* mutant adult zebrafish, an abnormal swimming behaviour was observed and characterized by frequent turning and spinning during a swim bout. Additionally, fish spent more time swimming in the middle of the tank than the edges. However, these differences do not affect overall distance travelled or frequency of inactivity. This characteristic behaviour of *dlx5a* and *dlx5i6* homozygous mutants does not appear until after the fish reaches 2.8-3cm in length (typically 2 months old). As larvae, these mutants do not have any differences swimming compared to WT and heterozygote siblings and they reacted appropriately in touch-evoked escape assays (E. Yu, unpublished observations).

There is a growing body of work correlating zebrafish swimming behaviours with neurodevelopmental and psychological conditions (Sakai et al., 2018; Tayanloo-Beik et al., 2022). For example, zebrafish mutants of genes associated with autism spectrum disorder (ASD) such as *shank3b* result in adult fish with abnormal swimming patterns such as frequent turning, “walling” (swimming against only one wall of the tank) or other repetitive behaviours (C. X Liu et al., 2018). There is also an indication that swimming along the edge of a tank (thigmotaxis) is associated with increased anxiety whereas greater time spent swimming in the center of an open tank is associated with lowered awareness of danger (Mathur & Guo, 2010). However, recent work also questioned

whether thigmotaxis is associated with anxiety or if it is simply a trait specific to zebrafish strains (Rajput et al., 2022).

Interestingly, ASD and a lowered sense of danger are both associated with *dlx* expression. Both bigene clusters investigated in this thesis are found in ASD susceptibility loci and various polymorphisms within enhancers of these clusters were identified in families of ASD patients (Hamilton et al., 2005; X. Liu et al., 2008; N. Nakashima et al., 2010). Furthermore, our laboratory demonstrated that one of these polymorphisms within the I56i enhancer resulted in reduced enhancer activity and prevented binding of *Dlx2* and *Dlx5* on the enhancer (Poitras et al., 2010). This same study identified another factor, Gtf2i that also interacts at this enhancer and may function synergistically with *Dlx2* or *Dlx5* to induce enhancer activity. Gtf2i is candidate gene for Williams-Beuren syndrome (WBS), which is characterized by distinct facial features, cognitive deficits, over-friendliness and increased trust in strangers (Francke, 1999). Importantly, almost half of WBS patients possess symptoms of ASD (Klein-Tasman et al., 2007; Lincoln et al., 2007). More recent work has also determined that loss of both I56i and I12b result in mice with increased sociability (Darbandi et al., 2021). Thus, it is possible that *dlx5a*$^{-/-}$ and *dlx5i6*$^{-/-}$ mutants may model some attributes of ASD and/or WBS through their swimming behaviour. In the case of *dlx5a*$^{-/-}$ mutants, a reduction in I56i activity may be occurring to explain the abnormal swim pattern. It is also curious that no reports of increased spinning are associated with ASD in zebrafish. Spinning during a swim bout may represent a different type of repetitive behaviour, or a consequence of potential vestibular deficits occurring concurrently with repetitive swimming behaviours associated with ASD. To further tease these behaviours apart, *inter56*$^{-/-}$ mutants should be recorded to determine if abnormal swimming occurs, since these mutants lack I56i but maintain expression of *dlx5a*.

4.3.3 Number and organization of neuromasts are disturbed in mutants with swim defect possibly due to decreased capacity to generate new neuromasts

To understand the biological basis of abnormal swimming behaviour, in particular the frequent spinning and turning during a swim bout, that was observed in *dlx5a*$^{-/-}$ and *dlx5i6*$^{-/-}$ adults, the vestibular and proprioceptive sensory system was examined. Larvae did not possess any phenotypes that would suggest a defect in the semicircular canals that contribute to vestibular sensation. Larvae also did not have defects in the lateral line neuromasts along the length of the body of mutant and WT animals were comparable at 3dpf. However, in adults 3cm or longer, which is when the swimming defect can be observed, fewer neuromasts were present in the posterior lateral line and in some animals, the L' branch was missing. We challenged, using antibiotic treatments, the ability of mutant neuromasts to regenerate but the difference we observed did not reach significance.

Stitch formation in the posterior lateral line is dependent on innervation. This was demonstrated by Wada et al. where the researchers ablated the PLL ganglion in larval zebrafish and found adult animals never developed stitches on the side without the ganglion (Wada et al., 2013). In addition, the size of primary neuromasts also decreased as the fish grew. Primary neuromasts completely degenerated when the fish reached 2.6cm on the side without PLL ganglion, demonstrating that innervation is also required for neuromast maintenance. Interestingly, this size of fish coincides with when abnormal swimming behaviour is observed in *dlx5a*$^{-/-}$ mutants along with loss of the L' stitch. This suggests neuromast innervation may have been affected in mutants and future work should utilize the *nbt:dsred* transgenic line and CLARITY protocols to investigate if neuromast innervation change as fish grow.

In *dlx5a* mutants, stitch formation occurred in the PLL for all lines, followed by reduction in numbers for the L' branch. Since degeneration of neuromasts and stitches is due to loss of innervation, loss of innervation may be occurring in *dlx5a* mutants. However, the question of how innervation was lost also requires investigation, particularly because the PLL nerve can regenerate. When larval zebrafish had a segment of the PLL nerve neuroectomized, Schwann cells at the injury site and distal from the site were observed to interact to form a scaffold allowing axon regrowth between the gap (Ceci et al., 2014). Schwann cells were found to be indispensable for the regeneration of the nerve axon since depletion of Schwann cells results in the inability of the axon to regenerate. Importantly, the ability for Schwann cells to aid in nerve regeneration may require loss of differentiation marker expression and attainment of an undifferentiated cell morphology. Schwann cells are also important for the regeneration of neuromasts themselves, as they interact with interneuromastic cells to form a new neuromast following degeneration (Sánchez et al., 2016). These dual roles of Schwann cells in neuromast and nerve regeneration suggest that the *dlx5a* mutant neuromast phenotypes may be due to abnormal Schwann cell function or to an alteration in the number of Schwann cells found along the lateral line ganglia. Importantly, Schwann cells are a NCC derivative. If cell morphology change is a required event for Schwann cell activation and function, a fascinating implication is that *dlx5a* loss may also affect PCP in Schwann cells similar to observations we made in Meckel's cartilage chondrocyte morphology.

4.4 General conclusions

In zebrafish, individuals homozygous for the deletion of *dlx1a*, *dlx2a*, *dlx5a*, *dlx6a*, of the enhancers of *dlx5a*/*dlx6a* (*inter56*), and with compound deletions of *dlx5a* and *dlx6a* (*dlx5i6*) are

all viable and fertile. The *dlx* genes in zebrafish also exhibit cross-regulation similar to what was observed in the mouse. However, some differences were observed such as continued expression of *dlx5a* in the absence of *dlx2a* until 3dpf. Additionally, expression of *dlx2a* may be increased in *dlx5a*$^{-/-}$ and *dlx5i6*$^{-/-}$ mutants. These expression relationships may influence some of the phenotypes observed with regards to craniofacial development and nervous system function. In *dlx5a*$^{-/-}$ and *dlx5i6*$^{-/-}$ mutant larvae, smaller Meckel's cartilage was formed that were also wider. This defect persisted up to 14dpf. NCC in these mutants also exhibited greater proliferation and more expression of chondrogenic markers. A novel interaction between loss of *dlx5a* and the non-canonical Wnt activity was identified that may underlie a mechanism behind Meckel's cartilage malformation, increased proliferation, and expression of chondrogenic genes. Within the nervous system, these same mutants also showed a trend towards fewer CR neurons in the optic tectum which is responsible for integrating visual, auditory, and vestibular information to generate an egocentric map of one's environment. This defect may underlie abnormal swimming behaviour observed in adult mutants that is reminiscent of ASD-like behaviours in zebrafish. Finally, a defect in neuromast survival and regeneration may implicate *dlx5a* function in maintenance of the lateral line ganglion and of an NCC derivative, Schwann cells, suggesting *dlx5a* may have a general role in neural crest cells differentiation or function.

Given the important roles already attributed to *dlx* function during development of craniofacial tissues and nervous system function, we believe the work presented in this study enriches the understanding of *dlx* genes during development and identifies many new avenues for further research.

Additional figures

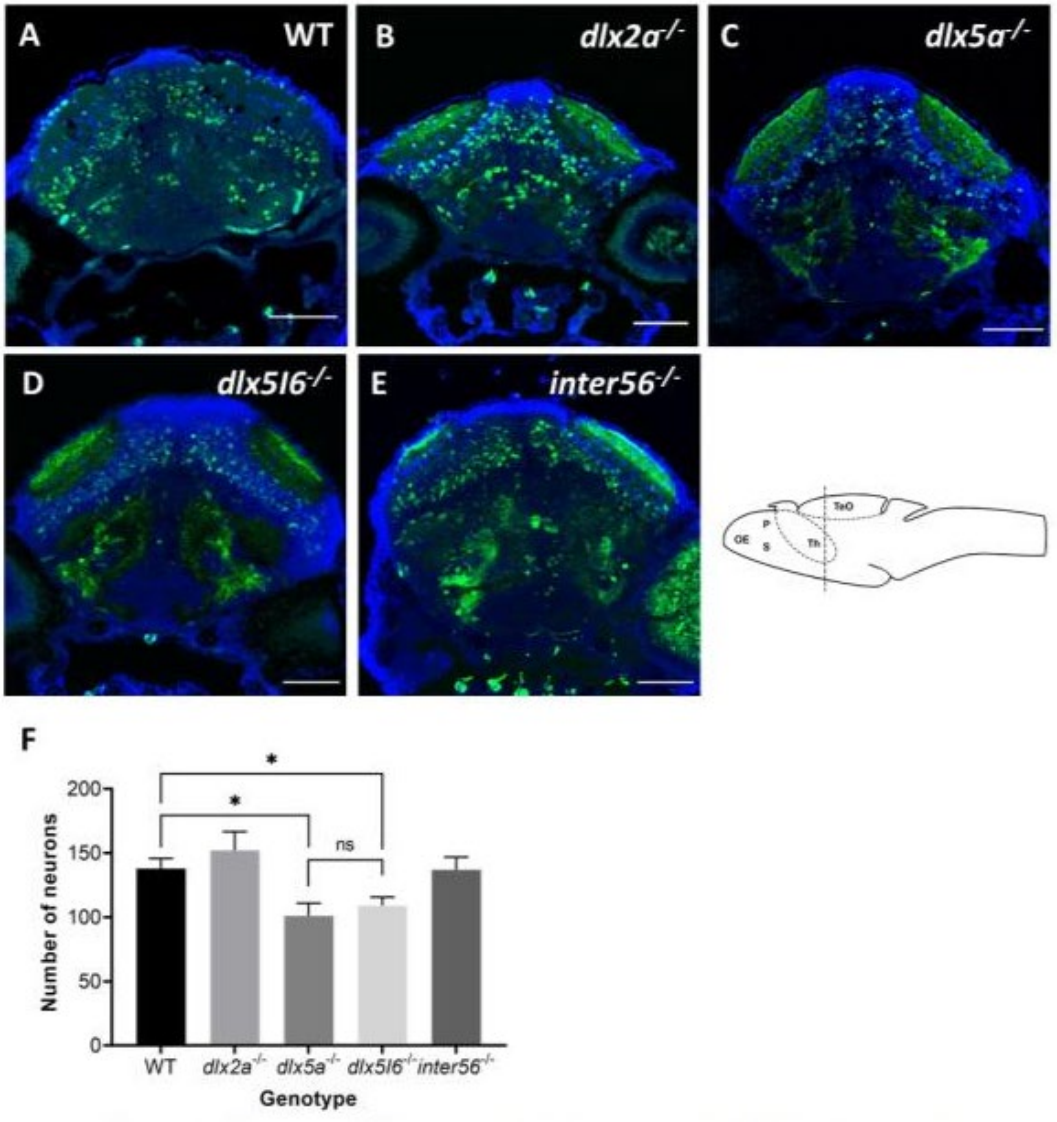

Figure A1. Labeling and quantification of CR+ neurons in the optic tectum of larval zebrafish heads.

(A-E) Transverse sections of 7dpf heads and immunohistochemistry was performed to label CR (green) and DAPI (blue). Schematic represents approximate location of sections. (F) The total number of CR+ neurons were counted and averaged for each genotype (WT: n=3; *dlx5a*$^{-/-}$: n=6; dlx5i6$^{-/-}$: n=6; *inter56*$^{-/-}$: n=4). Data is presented as mean ± SEM. Statistical significance was determined by two-tailed, unpaired t-test, *≤ 0.05. Scale = 75μm.

Bibliography

Acampora, D., Merlo, G. R., Paleari, L., Zerega, B., Postiglione, M. P., Mantero, S., Bober, E., Barbieri, O., Simeone, A., & Levi, G. (1999). Craniofacial, vestibular and bone defects in mice lacking the Distal-less-related gene Dlx5. *Development*, *126*(17), 3795–3809. https://doi.org/10.1242/DEV.126.17.3795

Akimenko, M. A., Ekker, M., Wegner, J., Lin, W., & Westerfield, M. (1994). Combinatorial expression of three zebrafish genes related to distal-less: Part of a homeobox gene code for the head. *Journal of Neuroscience*, *14*(6), 3475–3486. https://doi.org/10.1523/jneurosci.14-06-03475.1994

Aman, A., & Piotrowski, T. (2008). Wnt/beta-catenin and Fgf signaling control collective cell migration by restricting chemokine receptor expression. *Developmental Cell*, *15*(5), 749–761. https://doi.org/10.1016/J.DEVCEL.2008.10.002

Anderson, S. A., Qiu, M., Bulfone, A., Eisenstat, D. D., Meneses, J., Pedersen, R., & Rubenstein, J. L. R. (1997). Mutations of the homeobox genes Dlx-1 and Dlx-2 disrupt the striatal subventricular zone and differentiation of late born striatal neurons. *Neuron*, *19*(1), 27–37. https://doi.org/10.1016/S0896-6273(00)80345-1

Andzelm, M. M., Cherry, T. J., Harmin, D. A., Boeke, A. C., Lee, C., Hemberg, M., Pawlyk, B., Malik, A. N., Flavell, S. W., Sandberg, M. A., Raviola, E., & Greenberg, M. E. (2015). MEF2D drives photoreceptor development through a genome-wide competition for tissue-specific enhancers. *Neuron*, *86*(1), 247–263. https://doi.org/10.1016/J.NEURON.2015.02.038

Azim, E., Jabaudon, D., Fame, R. M., & MacKlis, J. D. (2009). SOX6 controls dorsal progenitor identity and interneuron diversity during neocortical development. *Nature Neuroscience 2009 12:10*, *12*(10), 1238–1247. https://doi.org/10.1038/nn.2387

Backman, M., Machon, O., Mygland, L., van den Bout, C. J., Zhong, W., Taketo, M. M., & Krauss, S. (2005). Effects of canonical Wnt signaling on dorso-ventral specification of the mouse telencephalon. *Developmental Biology*, *279*(1), 155–168. https://doi.org/10.1016/J.YDBIO.2004.12.010

Baggiolini, A., Varum, S., Mateos, J. M., Bettosini, D., John, N., Bonalli, M., Ziegler, U., Dimou, L., Clevers, H., Furrer, R., & Sommer, L. (2015). Premigratory and migratory neural crest cells are multipotent in vivo. *Cell Stem Cell*, *16*(3), 314–322. https://doi.org/10.1016/J.STEM.2015.02.017/ATTACHMENT/AD3F8E26-1992-4866-AF1C-D07F263F4CD2/MMC3.MP4

Bai, Y., Tan, X., Zhang, H., Liu, C., Zhao, B., Li, Y., Lu, L., Liu, Y., & Zhou, J. (2014). Ror2 receptor mediates wnt11 ligand signaling and affects convergence and extension movements in zebrafish. *Journal of Biological Chemistry*, *289*(30), 20664–20676. https://doi.org/10.1074/jbc.M114.586099

Bailey, A. P., Bhattacharyya, S., Bronner-Fraser, M., & Streit, A. (2006). Lens specification is the ground state of all sensory placodes, from which FGF promotes olfactory identity. *Developmental Cell*, *11*(4), 505–517. https://doi.org/10.1016/J.DEVCEL.2006.08.009

Baker, C. V. H., & Bronner-Fraser, M. (2001). Vertebrate cranial placodes I. Embryonic induction. *Developmental Biology*, *232*(1), 1–61. https://doi.org/10.1006/DBIO.2001.0156

Batlle, E., Sancho, E., Francí, C., Domínguez, D., Monfar, M., Baulida, J., & de Herreros, A. G. (2000). The transcription factor Snail is a repressor of E-cadherin gene expression in epithelial tumour cells. *Nature Cell Biology 2000 2:2*, *2*(2), 84–89. https://doi.org/10.1038/35000034

Beddington, R. S. P. (1994). Induction of a second neural axis by the mouse node. *Development*, *120*(3), 613–620. https://doi.org/10.1242/DEV.120.3.613

Begbie, J., Brunet, J. F., Rubenstein, J. L. R., & Graham, A. (1999). Induction of the epibranchial placodes. *Development*, *126*(5), 895–902. https://doi.org/10.1242/DEV.126.5.895

Begbie, J., & Graham, A. (2001). Integration Between the Epibranchial Placodes and the Hindbrain. *Science*, *294*(5542), 595–598. https://doi.org/10.1126/SCIENCE.1062028

Bell, D. M., Leung, K. K. H., Wheatley, S. C., Ling Jim Ng, Zhou, S., Kam Wing Ling, Mai Har Sham, Koopman, P., Tam, P. P. L., & Cheah, K. S. E. (1997). SOX9 directly regulates the type-ll collagen gene. *Nature Genetics 1997 16:2*, *16*(2), 174–178. https://doi.org/10.1038/ng0697-174

Berendsen, A. D., & Olsen, B. R. (2015). Bone development. *Bone*, *80*, 14–18. https://doi.org/10.1016/J.BONE.2015.04.035

Beverdam, A., Merlo, G. R., Paleari, L., Mantero, S., Genova, F., Barbieri, O., Janvier, P., & Levi, G. (2002). Jaw transformation with gain of symmetry after Dlx5/Dlx6 inactivation: Mirror of the past? *Genesis*, *34*(4), 221–227. https://doi.org/10.1002/GENE.10156

Bhaskar, S. N., Weinmann, J. P., & Schour, I. (1953). Role of Meckel's Cartilage in the Development and Growth of the Rat Mandible. *Journal of Dental Research*, *32*(3), 398–410. https://doi.org/10.1177/00220345530320031401/ASSET/00220345530320031401.FP.PNG_V03

Bi, W., Deng, J. M., Zhang, Z., Behringer, R. R., & de Crombrugghe, B. (1999). Sox9 is required for cartilage formation. *Nature Genetics 1999 22:1*, *22*(1), 85–89. https://doi.org/10.1038/8792

Borostyánkoi-Baldauf, Z., & Herczeg, L. (2002). Parcellation of the human pretectal complex: a chemoarchitectonic reappraisal. *Neuroscience*, *110*(3), 527–540. https://doi.org/10.1016/S0306-4522(01)00462-6

Bortone, D., & Polleux, F. (2009). KCC2 expression promotes the termination of cortical interneuron migration in a voltage-sensitive calcium-dependent manner. *Neuron*, *62*(1), 53–71. https://doi.org/10.1016/J.NEURON.2009.01.034

Brault, V., Moore, R., Kutsch, S., Ishibashi, M., Rowitch, D. H., McMahon, A. P., Sommer, L., Boussadia, O., & Kemler, R. (2001). Inactivation of the (β)-catenin gene by Wnt1-Cre-mediated deletion results in dramatic brain malformation and failure of craniofacial development. *Development*, *128*(8), 1253–1264. https://doi.org/10.1242/DEV.128.8.1253

Brown, K. K., Reiss, J. A., Crow, K., Ferguson, H. L., Kelly, C., Fritzsch, B., & Morton, C. C. (2010). Deletion of an enhancer near DLX5 and DLX6 in a family with hearing loss, craniofacial defects, and an inv(7)(q21.3q35). *Human Genetics*, *127*(1), 19–31. https://doi.org/10.1007/s00439-009-0736-4

Bulfone, A., Puelles, L., Porteus, M. H., Frohman, M. A., Martin, G. R., & Rubenstein, J. L. R. (1993). Spatially restricted expression of Dlx-1, Dlx-2 (Tes-1), Gbx-2, and Wnt- 3 in the embryonic day 12.5 mouse forebrain defines potential transverse and longitudinal segmental boundaries. *Journal of Neuroscience*, *13*(7), 3155–3172. https://doi.org/10.1523/JNEUROSCI.13-07-03155.1993

Bulfone, A., Wang, F., Hevner, R., Anderson, S., Cutforth, T., Chen, S., Meneses, J., Pedersen, R., Axel, R., & Rubenstein, J. L. R. (1998). An olfactory sensory map develops in the absence of normal projection neurons or GABAergic interneurons. *Neuron*, *21*(6), 1273–1282. https://doi.org/10.1016/S0896-6273(00)80647-9

Bürglin, T. R., & Affolter, M. (2015). Homeodomain proteins: an update. *Chromosoma 2015 125:3*, *125*(3), 497–521. https://doi.org/10.1007/S00412-015-0543-8

Burke, D., Wilkes, D., Blundell, T. L., & Malcolm, S. (1998). Fibroblast growth factor receptors: Lessons from the genes. *Trends in Biochemical Sciences*, *23*(2), 59–62. https://doi.org/10.1016/S0968-0004(97)01170-5

Burstein, D., Harrington, L. B., Strutt, S. C., Probst, A. J., Anantharaman, K., Thomas, B. C., Doudna, J. A., & Banfield, J. F. (2016). New CRISPR–Cas systems from uncultivated microbes. *Nature 2017 542:7640*, *542*(7640), 237–241. https://doi.org/10.1038/nature21059

Burstyn-Cohen, T., & Kalcheim, C. (2002). Association between the cell cycle and neural crest delamination through specific regulation of G1/S transition. *Developmental Cell*, *3*(3), 383–395. https://doi.org/10.1016/S1534-5807(02)00221-6

Butler, J. M., & Maruska, K. P. (2016). The Mechanosensory Lateral Line System Mediates Activation of Socially-Relevant Brain Regions during Territorial Interactions. *Frontiers in Behavioral Neuroscience*, *10*(MAY). https://doi.org/10.3389/FNBEH.2016.00093

Butt, S. J. B., Fuccillo, M., Nery, S., Noctor, S., Kriegstein, A., Corbin, J. G., & Fishell, G. (2005). The temporal and spatial origins of cortical interneurons predict their physiological subtype. *Neuron*, *48*(4), 591–604. https://doi.org/10.1016/J.NEURON.2005.09.034

Butt, S. J. B., Sousa, V. H., Fuccillo, M. v., Hjerling-Leffler, J., Miyoshi, G., Kimura, S., & Fishell, G. (2008). The requirement of Nkx2-1 in the temporal specification of cortical interneuron subtypes. *Neuron*, *59*(5), 722–732. https://doi.org/10.1016/J.NEURON.2008.07.031

Cannavò, E., Khoueiry, P., Garfield, D. A., Geeleher, P., Zichner, T., Gustafson, E. H., Ciglar, L., Korbel, J. O., & Furlong, E. E. M. (2016). Shadow Enhancers Are Pervasive Features of Developmental Regulatory Networks. *Current Biology*, *26*(1), 38–51. https://doi.org/10.1016/j.cub.2015.11.034

Casarosa, S., Fode, C., & Guillemot, F. (1999). Mash1 regulates neurogenesis in the ventral telencephalon. *Development*, *126*(3), 525–534. https://doi.org/10.1242/DEV.126.3.525

Catala, M., Teillet, M. A., & le Douarin, N. M. (1995). Organization and development of the tail bud analyzed with the quail-chick chimaera system. *Mechanisms of Development*, *51*(1), 51–65. https://doi.org/10.1016/0925-4773(95)00350-A

Cauli, B., Zhou, X., Tricoire, L., Toussay, X., & Staiger, J. F. (2014). Revisiting enigmatic cortical calretinin-expressing interneurons. *Frontiers in Neuroanatomy*, *8*(JUN), 1–18. https://doi.org/10.3389/fnana.2014.00052

Ceci, M. L. aura, Mardones-Krsulovic, C., Sánchez, M., Valdivia, L. E., & Allende, M. L. (2014). Axon-Schwann cell interactions during peripheral nerve regeneration in zebrafish larvae. *Neural Development*, *9*(1), 22. https://doi.org/10.1186/1749-8104-9-22

Chen, Y., Wang, Z., Chen, Y. P., & Zhang, Y. (2019). Conditional deletion of Bmp2 in cranial neural crest cells recapitulates Pierre Robin sequence in mice. *Cell and Tissue Research*, *376*(2), 199–210. https://doi.org/10.1007/S00441-018-2944-5/FIGURES/12

Chiang, E. F. L., Pai, C. I., Wyatt, M., Yan, Y. L., Postlethwait, J., & Chung, B. chu. (2001). Two Sox9 Genes on Duplicated Zebrafish Chromosomes: Expression of Similar Transcription Activators in Distinct Sites. *Developmental Biology*, *231*(1), 149–163. https://doi.org/10.1006/DBIO.2000.0129

Chin, H. J., Fisher, M. C., Li, Y., Ferrari, D., Wang, C. K. L., Lichtler, A. C., Dealy, C. N., & Kosher, R. A. (2007). Studies on the role of Dlx5 in regulation of chondrocyte differentiation during endochondral ossification in the developing mouse limb. *Development, Growth & Differentiation*, *49*(6), 515–521. https://doi.org/10.1111/J.1440-169X.2007.00940.X

Choe, S. K., Ladam, F., & Sagerström, C. G. (2014). TALE Factors Poise Promoters for Activation by Hox Proteins. *Developmental Cell*, *28*(2), 203–211. https://doi.org/10.1016/J.DEVCEL.2013.12.011

Clouthier, D. E., Garcia, E., & Schilling, T. F. (2010). Regulation of facial morphogenesis by endothelin signaling: Insights from mice and fish. *American Journal of Medical Genetics, Part A*, *152 A*(12), 2962–2973. https://doi.org/10.1002/AJMG.A.33568

Cobos, I., Borello, U., & Rubenstein, J. L. R. (2007). Dlx Transcription Factors Promote Migration through Repression of Axon and Dendrite Growth. *Neuron*, *54*(6), 873–888. https://doi.org/10.1016/j.neuron.2007.05.024

Cobos, I., Calcagnotto, M. E., Vilaythong, A. J., Thwin, M. T., Noebels, J. L., Baraban, S. C., & Rubenstein, J. L. R. (2005). Mice lacking Dlx1 show subtype-specific loss of interneurons, reduced inhibition and epilepsy. *Nature Neuroscience*, *8*(8), 1059–1068. https://doi.org/10.1038/nn1499

Coffin Talbot, J., Johnson, S. L., & Kimmel, C. B. (2010). hand2 and Dlx genes specify dorsal, intermediate and ventral domains within zebrafish pharyngeal arches. *Development*, *137*(15), 2507–2517. https://doi.org/10.1242/DEV.049700

Cohen, S. M., Bronner, G., Kuttner, F., Jurgens, G., & Jackie, H. (1989). *Distal-less encodes a homoeodomain protein required for limb development in Drosophila*.

Cohen, S. M., & Jurgens, G. (1989). Proximal-distal pattern formation in Drosophila: cell autonomous requirement for Distal-less gene activity in limb development. *The EMBO Journal*, *8*(7), 2045–2055. https://doi.org/10.1002/J.1460-2075.1989.TB03613.X

Collazo, A., Fraser, S. E., & Mabee, P. M. (1994). A Dual Embryonic Origin for Vertebrate Mechanoreceptors. *Science*, *264*(5157), 426–430. https://doi.org/10.1126/SCIENCE.8153631

Corbin, J. G., Rutlin, M., Gaiano, N., & Fishell, G. (2003). Combinatorial function of the homeodomain proteins Nkx2.1 and Gsh2 in ventral telencephalic patterning. *Development*, *130*(20), 4895–4906. https://doi.org/10.1242/DEV.00717

Couly, G. F., & le Douarin, N. M. (1987). Mapping of the early neural primordium in quail-chick chimeras: II. The prosencephalic neural plate and neural folds: Implications for the genesis of cephalic human congenital abnormalities. *Developmental Biology*, *120*(1), 198–214. https://doi.org/10.1016/0012-1606(87)90118-7

Couly, G., & le Douarin, N. M. (1990). Head morphogenesis in embryonic avian chimeras: evidence for a segmental pattern in the ectoderm corresponding to the neuromeres. *Development*, *108*(4), 543–558. https://doi.org/10.1242/DEV.108.4.543

Cox, W. G., & Hemmati-Brivanlou, A. (1995). Caudalization of neural fate by tissue recombination and bFGF. *Development*, *121*(12), 4349–4358. https://doi.org/10.1242/DEV.121.12.4349

Crump, J. G., Swartz, M. E., Eberhart, J. K., & Kimmel, C. B. (2006). Moz-dependent Hox expression controls segment-specific fate maps of skeletal precursors in the face. *Development*, *133*(14), 2661–2669. https://doi.org/10.1242/DEV.02435

Curtin, E., Hickey, G., Kamel, G., Davidson, A. J., & Liao, E. C. (2011). Zebrafish wnt9a is expressed in pharyngeal ectoderm and is required for palate and lower jaw development. *Mechanisms of Development*, *128*(1–2), 104–115. https://doi.org/10.1016/J.MOD.2010.11.003

Dambly-Chaudière, C., Cubedo, N., & Ghysen, A. (2007). Control of cell migration in the development of the posterior lateral line: antagonistic interactions between the chemokine receptors CXCR4 and CXCR7/RDC1. *BMC Developmental Biology*, *7*. https://doi.org/10.1186/1471-213X-7-23

Danesin, C., Peres, J. N., Johansson, M., Snowden, V., Cording, A., Papalopulu, N., & Houart, C. (2009). Integration of telencephalic Wnt and hedgehog signaling center activities by Foxg1. *Developmental Cell*, *16*(4), 576–587. https://doi.org/10.1016/J.DEVCEL.2009.03.007

Darbandi, S. F., Poitras, L., Monis, S., Lindtner, S., Yu, M., Hatch, G., Rubenstein, J. L., & Ekker, M. (2016). Functional consequences of I56ii Dlx enhancer deletion in the developing mouse forebrain. *Developmental Biology*, *420*(1), 32–42. https://doi.org/10.1016/j.ydbio.2016.10.015

David, N. B., Sapède, D., Saint-Etienne, L., Thisse, C., Thisse, B., Dambly-Chaudière, C., Rosa, F. M., & Ghysen, A. (2002). Molecular basis of cell migration in the fish lateral line: Role of the chemokine receptor CXCR4 and of its ligand, SDF1. *Proceedings of the National Academy of Sciences of the United States of America*, *99*(25), 16297–16302. https://doi.org/10.1073/PNAS.252339399/ASSET/30FA80F9-4F36-4E34-B313-34C9A290A800/ASSETS/GRAPHIC/PQ2523393003.JPEG

Day, T. F., Guo, X., Garrett-Beal, L., & Yang, Y. (2005). Wnt/beta-catenin signaling in mesenchymal progenitors controls osteoblast and chondrocyte differentiation during vertebrate skeletogenesis. *Developmental Cell*, *8*(5), 739–750. https://doi.org/10.1016/J.DEVCEL.2005.03.016

de Marco García, N. v., Karayannis, T., & Fishell, G. (2011). Neuronal activity is required for the development of specific cortical interneuron subtypes. *Nature 2011 472:7343*, *472*(7343), 351–355. https://doi.org/10.1038/nature09865

de Mendoza, A., Sebé-Pedrós, A., Šestak, M. S., Matejčić, M., Torruella, G., Domazet-Lošo, T., & Ruiz-Trillo, I. (2013). Transcription factor evolution in eukaryotes and the assembly of the regulatory toolkit in multicellular lineages. *Proceedings of the National Academy of Sciences of the United States of America*, *110*(50). https://doi.org/10.1073/PNAS.1311818110/-/DCSUPPLEMENTAL/PNAS.201311818SI.PDF

Deardorff, M. A., Tan, C., Saint-Jeannet, J. P., & Klein, P. S. (2001). A role for frizzled 3 in neural crest development. *Development*, *128*(19), 3655–3663. https://doi.org/10.1242/DEV.128.19.3655

Depew, M. J., Liu, J. K., Long, J. E., Presley, R., Meneses, J. J., Pedersen, R. A., & Rubenstein, J. L. R. (1999). Dlx5 regulates regional development of the branchial arches and sensory capsules. *Development*, *126*(17), 3831–3846.

Depew, M. J., Lufkin, T., & Rubenstein, J. L. R. (2002). Specification of jaw subdivisions by Dlx genes. *Science*, *298*(5592), 381–385. https://doi.org/10.1126/SCIENCE.1075703/SUPPL_FILE/DEPEWSOMTXT.PDF

di Gregorio, A., Spagnuolo, A., Ristoratore, F., Pischetola, M., Aniello, F., Branno, M., Cariello, L., & di Lauro, R. (1995). Cloning of ascidian homeobox genes provides evidence for a primordial chordate cluster. *Gene*, *156*(2), 253–257. https://doi.org/10.1016/0378-1119(95)00035-5

Dijkgraaf, S. (1963). THE FUNCTIONING and SIGNIFICANCE OF THE LATERAL-LINE ORGANS. *Biological Reviews*, *38*(1), 51–105. https://doi.org/10.1111/J.1469-185X.1963.TB00654.X

Dolzblasz, A., Nardmann, J., Clerici, E., Causier, B., van der Graaff, E., Chen, J., Davies, B., Werr, W., & Laux, T. (2016). Stem Cell Regulation by Arabidopsis WOX Genes. *Molecular Plant*, *9*(7), 1028–1039. https://doi.org/10.1016/j.molp.2016.04.007

Duggan, C. D., DeMaria, S., Baudhuin, A., Stafford, D., & Ngai, J. (2008). Foxg1 Is Required for Development of the Vertebrate Olfactory System. *The Journal of Neuroscience*, *28*(20), 5229. https://doi.org/10.1523/JNEUROSCI.1134-08.2008

Dupé, V., & Lumsden, A. (2001). Hindbrain patterning involves graded responses to retinoic acid signalling. *Development*, *128*(12), 2199–2208. https://doi.org/10.1242/DEV.128.12.2199

Dyachuk, V., Furlan, A., Shahidi, M. K., Giovenco, M., Kaukua, N., Konstantinidou, C., Pachnis, V., Memic, F., Marklund, U., Müller, T., Birchmeier, C., Fried, K., Ernfors, P., & Adameyko, I. (2014). Parasympathetic neurons originate from nerve-associated peripheral glial progenitors. *Science*, *345*(6192), 82–87. https://doi.org/10.1126/SCIENCE.1253281/SUPPL_FILE/DYACHUK.SM.PDF

Eames, B. F., & Schneider, R. A. (2008). The genesis of cartilage size and shape during development and evolution. *Development*, *135*(23), 3947–3958. https://doi.org/10.1242/DEV.023309

Echelard, Y., Epstein, D. J., St-Jacques, B., Shen, L., Mohler, J., McMahon, J. A., & McMahon, A. P. (1993). Sonic hedgehog, a member of a family of putative signaling molecules, is implicated in the regulation of CNS polarity. *Cell*, *75*(7), 1417–1430. https://doi.org/10.1016/0092-8674(93)90627-3

Eisenstat, D. D., Liu, J. K., Mione, M., Zhong, W., Yu, G., Anderson, S. A., Ghattas, I., Puelles, L., & Rubenstein, J. L. R. (1999). DLX-1, DLX-2, and DLX-5 expression define distinct stages of basal

forebrain differentiation. *Journal of Comparative Neurology*, *414*(2), 217–237. https://doi.org/10.1002/(SICI)1096-9861(19991115)414:2<217::AID-CNE6>3.0.CO;2-I

El-Brolosy, M. A., Kontarakis, Z., Rossi, A., Kuenne, C., Günther, S., Fukuda, N., Kikhi, K., Boezio, G. L. M., Takacs, C. M., Lai, S. L., Fukuda, R., Gerri, C., Giraldez, A. J., & Stainier, D. Y. R. (2019). Genetic compensation triggered by mutant mRNA degradation. *Nature*, *568*(7751), 193–197. https://doi.org/10.1038/s41586-019-1064-z

Ellies, D. L., Stock, D. W., Hatch, G., Giroux, G., Weiss, K. M., & Ekker, M. (1997). Relationship between the Genomic Organization and the Overlapping Embryonic Expression Patterns of the ZebrafishdlxGenes. *Genomics*, *45*(3), 580–590. https://doi.org/10.1006/GENO.1997.4978

Endo, Y., Osumi, N., & Wakamatsu, Y. (2002). Bimodal functions of Notch-mediated signaling are involved in neural crest formation during avian ectoderm development. *Development*, *129*(4), 863–873. https://doi.org/10.1242/DEV.129.4.863

Ericson, J., Morton, S., Kawakami, A., Roelink, H., & Jessell, T. M. (1996). Two critical periods of Sonic Hedgehog signaling required for the specification of motor neuron identity. *Cell*, *87*(4), 661–673. https://doi.org/10.1016/S0092-8674(00)81386-0

Espinosa-Medina, I., Outin, E., Picard, C. A., Chettouh, Z., Dymecki, S., Consalez, G. G., Coppola, E., & Brunet, J. F. (2014). Parasympathetic ganglia derive from Schwann cell precursors. *Science*, *345*(6192), 87–90. https://doi.org/10.1126/SCIENCE.1253286/SUPPL_FILE/ESPINOSA.SM.PDF

Fabik, J., Psutkova, V., & Machon, O. (2021). The Mandibular and Hyoid Arches-From Molecular Patterning to Shaping Bone and Cartilage. *International Journal of Molecular Sciences*, *22*(14). https://doi.org/10.3390/IJMS22147529

Fang, M., Adams, J. S., McMahan, B. L., Brown, R. J., & Oxford, J. T. (2010). The expression patterns of minor fibrillar collagens during development in zebrafish. *Gene Expression Patterns*, *10*(7–8), 315–322. https://doi.org/10.1016/J.GEP.2010.07.002

Fazel Darbandi, S., Esau, C., Lesage-Pelletier, C., Monis, S., Poitras, L., Yu, M., Perin, S., Hatch, G., & Ekker, M. (2021). Increased Sociability in Mice Lacking Intergenic Dlx Enhancers. *Frontiers in Neuroscience*, *15*, 1296. https://doi.org/10.3389/FNINS.2021.718948/BIBTEX

Feng, J., Bi, C., Clark, B. S., Mady, R., Shah, P., & Kohtz, J. D. (2006). The Evf-2 noncoding RNA is transcribed from the Dlx-5/6 ultraconserved region and functions as a Dlx-2 transcriptional coactivator. *Genes & Development*, *20*(11), 1470. https://doi.org/10.1101/GAD.1416106

Flames, N., Pla, R., Gelman, D. M., Rubenstein, J. L. R., Puelles, L., & Marín, O. (2007). Delineation of multiple subpallial progenitor domains by the combinatorial expression of transcriptional codes. *The*

Journal of Neuroscience : The Official Journal of the Society for Neuroscience, *27*(36), 9682–9695. https://doi.org/10.1523/JNEUROSCI.2750-07.2007

Fogarty, M., Grist, M., Gelman, D., Marín, O., Pachnis, V., & Kessaris, N. (2007). Spatial Genetic Patterning of the Embryonic Neuroepithelium Generates GABAergic Interneuron Diversity in the Adult Cortex. *Journal of Neuroscience*, *27*(41), 10935–10946. https://doi.org/10.1523/JNEUROSCI.1629-07.2007

Francke, U. (1999). Williams-Beuren Syndrome: Genes and Mechanisms. *Human Molecular Genetics*, *8*(10), 1947–1954. https://doi.org/10.1093/HMG/8.10.1947

Freter, S., Muta, Y., Mak, S. S., Rinkwitz, S., & Ladher, R. K. (2008). Progressive restriction of otic fate: the role of FGF and Wnt in resolving inner ear potential. *Development*, *135*(20), 3415–3424. https://doi.org/10.1242/DEV.026674

Gagnon, J. A., Valen, E., Thyme, S. B., Huang, P., Ahkmetova, L., Pauli, A., Montague, T. G., Zimmerman, S., Richter, C., & Schier, A. F. (2014). Efficient mutagenesis by Cas9 protein-mediated oligonucleotide insertion and large-scale assessment of single-guide RNAs. *PloS One*, *9*(5). https://doi.org/10.1371/JOURNAL.PONE.0098186

Gans, C., & Northcutt, R. G. (1983). Neural Crest and the Origin of Vertebrates: A New Head. *Science*, *220*(4594), 268–274. https://doi.org/10.1126/SCIENCE.220.4594.268

Garcia-Lopez, R., Vieira, C., Echevarria, D., & Martinez, S. (2004). Fate map of the diencephalon and the zona limitans at the 10-somites stage in chick embryos. *Developmental Biology*, *268*(2), 514–530. https://doi.org/10.1016/j.ydbio.2003.12.038

Ghanem, N., Andrusiak, M. G., Svoboda, D., al Lafi, S. M., Julian, L. M., McClellan, K. A., de Repentigny, Y., Kothary, R., Ekker, M., Blais, A., Park, D. S., & Slack, R. S. (2012). The Rb/E2F pathway modulates neurogenesis through direct regulation of the Dlx1/Dlx2 bigene cluster. *Journal of Neuroscience*, *32*(24), 8219–8230. https://doi.org/10.1523/JNEUROSCI.1344-12.2012

Ghanem, N., Jarinova, O., Amores, A., Long, Q., Hatch, G., Park, B. K., Rubenstein, J. L. R., & Ekker, M. (2003). Regulatory roles of conserved intergenic domains in vertebrate Dlx bigene clusters. *Genome Research*, *13*(4), 533–543. https://doi.org/10.1101/GR.716103

Ghanem, N., Yu, M., Long, J., Hatch, G., Rubenstein, J. L. R., & Ekker, M. (2007). Distinct cis-regulatory elements from the Dlx1/Dlx2 locus mark different progenitor cell populations in the ganglionic eminences and different subtypes of adult cortical interneurons. *Journal of Neuroscience*, *27*(19), 5012–5022. https://doi.org/10.1523/JNEUROSCI.4725-06.2007

Ghanem, N., Yu, M., Poitras, L., Rubenstein, J. L. R., & Ekker, M. (2008). Characterization of a distinct subpopulation of striatal projection neurons expressing the Dlx genes in the basal ganglia through the

activity of the I56ii enhancer. *Developmental Biology*, *322*(2), 415–424. https://doi.org/10.1016/j.ydbio.2008.07.029

Ghysen, A., & Dambly-Chaudière, C. (2007). The lateral line microcosmos. *Genes & Development*, *21*(17), 2118–2130. https://doi.org/10.1101/GAD.1568407

Gilmour, D., Knaut, H., Maischein, H. M., & Nüsslein-Volhard, C. (2004). Towing of sensory axons by their migrating target cells in vivo. *Nature Neuroscience 2004 7:5*, *7*(5), 491–492. https://doi.org/10.1038/nn1235

Gilmour, D. T., Maischein, H. M., & Nüsslein-Volhard, C. (2002). Migration and function of a glial subtype in the vertebrate peripheral nervous system. *Neuron*, *34*(4), 577–588. https://doi.org/10.1016/S0896-6273(02)00683-9

Golding, J. P., Sobieszczuk, D., Dixon, M., Coles, E., Christiansen, J., Wilkinson, D., & Gassmann, M. (2004). Roles of erbB4, rhombomere-specific, and rhombomere-independent cues in maintaining neural crest-free zones in the embryonic head. *Developmental Biology*, *266*(2), 361–372. https://doi.org/10.1016/j.ydbio.2003.11.003

Gonchar, Y., & Burkhalter, A. (1997). Three distinct families of GABAergic neurons in rat visual cortex. *Cerebral Cortex (New York, N.Y. : 1991)*, *7*(4), 347–358. https://doi.org/10.1093/CERCOR/7.4.347

Goodnough, L. H., DiNuoscio, G. J., Ferguson, J. W., Williams, T., Lang, R. A., & Atit, R. P. (2014). Distinct Requirements for Cranial Ectoderm and Mesenchyme-Derived Wnts in Specification and Differentiation of Osteoblast and Dermal Progenitors. *PLOS Genetics*, *10*(2), e1004152. https://doi.org/10.1371/JOURNAL.PGEN.1004152

Graham, A. (2008). Deconstructing the pharyngeal metamere. *Journal of Experimental Zoology Part B: Molecular and Developmental Evolution*, *310B*(4), 336–344. https://doi.org/10.1002/JEZ.B.21182

Grant, K. A., Raible, D. W., & Piotrowski, T. (2005). Regulation of latent sensory hair cell precursors by glia in the zebrafish lateral line. *Neuron*, *45*(1), 69–80. https://doi.org/10.1016/j.neuron.2004.12.020

Grigoriou, M., Tucker, A. S., Sharpe, P. T., & Pachnis, V. (1998). Expression and regulation of Lhx6 and Lhx7, a novel subfamily of LIM homeodomain encoding genes, suggests a role in mammalian head development. *Development*, *125*(11), 2063–2074. https://doi.org/10.1242/DEV.125.11.2063

Grocott, T., Tambalo, M., & Streit, A. (2012). The peripheral sensory nervous system in the vertebrate head: a gene regulatory perspective. *Developmental Biology*, *370*(1), 3–23. https://doi.org/10.1016/J.YDBIO.2012.06.028

Gunhaga, L., Marklund, M., Sjödal, M., Hsieh, J. C., Jessell, T. M., & Edlund, T. (2003). Specification of dorsal telencephalic character by sequential Wnt and FGF signaling. *Nature Neuroscience 2003 6:7*, *6*(7), 701–707. https://doi.org/10.1038/nn1068

Gutin, G., Fernandes, M., Palazzolo, L., Paek, H. K., Yu, K., Ornitz, D. M., McConnell, S. K., & Hébert, J. M. (2006). FGF signalling generates ventral telencephalic cells independently of SHH. *Development (Cambridge, England)*, *133*(15), 2937–2946. https://doi.org/10.1242/DEV.02465

Hall, B. K. (2015). Bones and Cartilage: Developmental and Evolutionary Skeletal Biology. In *Bones and Cartilage: Developmental and Evolutionary Skeletal Biology*. Elsevier. https://doi.org/10.1016/B978-0-12-416678-3.00048-3

Hamilton, S. P., Woo, J. M., Carlson, E. J., Ghanem, N., Ekker, M., & Rubenstein, J. L. R. (2005). Analysis of four DLX homeobox genes in autistic probands. *BMC Genetics*, *6*(1), 1–11. https://doi.org/10.1186/1471-2156-6-52/FIGURES/1

Harrington, M. J., Hong, E., Brewster, R., & Harrington, M. (2009). *Comparative Analysis of Neurulation: First Impressions Do Not Count*. https://doi.org/10.1002/mrd.21085

Hatten, M. E. (2003). CENTRAL NERVOUS SYSTEM NEURONAL MIGRATION. *Https://Doi.Org/10.1146/Annurev.Neuro.22.1.511*, *22*, 511–539. https://doi.org/10.1146/ANNUREV.NEURO.22.1.511

Hava, D., Forster, U., Matsuda, M., Cui, S., Link, B. A., Eichhorst, J., Wiesner, B., Chitnis, A., & Abdelilhah-Seyfried, S. (2009). Apical membrane maturation and cellular rosette formation during morphogenesis of the zebrafish lateral line. *Journal of Cell Science*, *122*(Pt 5), 687–695. https://doi.org/10.1242/JCS.032102

Hikosaka, O. (2010). The habenula: from stress evasion to value-based decision-making. *Nature Reviews Neuroscience 2010 11:7*, *11*(7), 503–513. https://doi.org/10.1038/nrn2866

Hojo, H., Ohba, S., He, X., Lai, L. P., & McMahon, A. P. (2016). Sp7/Osterix Is Restricted to Bone-Forming Vertebrates where It Acts as a Dlx Co-factor in Osteoblast Specification. *Developmental Cell*, *37*(3), 238–253. https://doi.org/10.1016/j.devcel.2016.04.002

Holland, P. W. H. (2013). Evolution of homeobox genes. *Wiley Interdisciplinary Reviews: Developmental Biology*, *2*(1), 31–45. https://doi.org/10.1002/wdev.78

Holzschuh, J., Wada, N., Wada, C., Schaffer, A., Javidan, Y., Tallafuß, A., Bally-Cuif, L., & Schiling, T. F. (2005). Requirements for endoderm and BMP signaling in sensory neurogenesis in zebrafish. *Development (Cambridge, England)*, *132*(16), 3731–3742. https://doi.org/10.1242/DEV.01936

Hwang, J., Huang, Y., Burwell, T. J., Peterson, N. C., Connor, J., Weiss, S. J., Yu, S. M., & Li, Y. (2017). In Situ Imaging of Tissue Remodeling with Collagen Hybridizing Peptides. *ACS Nano*, *11*(10), 9825–9835. https://doi.org/10.1021/ACSNANO.7B03150/SUPPL_FILE/NN7B03150_SI_001.PDF

Hwang, W. Y., Fu, Y., Reyon, D., Maeder, M. L., Tsai, S. Q., Sander, J. D., Peterson, R. T., Yeh, J. R. J., & Joung, J. K. (2013). Efficient genome editing in zebrafish using a CRISPR-Cas system. *Nature Biotechnology 2013 31:3*, *31*(3), 227–229. https://doi.org/10.1038/nbt.2501

Ikenouchi, J., Matsuda, M., Furuse, M., & Tsukita, S. (2003). Regulation of tight junctions during the epithelium-mesenchyme transition:direct repression of the gene expression of claudins/occludin by Snail. *Journal of Cell Science*, *116*(10), 1959–1967. https://doi.org/10.1242/JCS.00389

Isa, T., Marquez-Legorreta, E., Grillner, S., & Scott, E. K. (2021). The tectum/superior colliculus as the vertebrate solution for spatial sensory integration and action. *Current Biology*, *31*(11), R741–R762. https://doi.org/10.1016/J.CUB.2021.04.001

Ishino, Y., Krupovic, M., & Forterre, P. (2018). History of CRISPR-Cas from encounter with a mysterious repeated sequence to genome editing technology. *Journal of Bacteriology*, *200*(7). https://doi.org/10.1128/JB.00580-17/ASSET/DE8FEBC5-B202-4B94-A69A-7B1049774EFA/ASSETS/GRAPHIC/ZJB9990946770007.JPEG

Ishino, Y., Shinagawa, H., Makino, K., Amemura, M., & Nakatura, A. (1987). Nucleotide sequence of the iap gene, responsible for alkaline phosphatase isozyme conversion in Escherichia coli, and identification of the gene product. *Journal of Bacteriology*, *169*(12), 5429–5433. https://doi.org/10.1128/JB.169.12.5429-5433.1987

Iwata, J. I., Hosokawa, R., Sanchez-Lara, P. A., Urata, M., Slavkin, H., & Chai, Y. (2010). Transforming growth factor-beta regulates basal transcriptional regulatory machinery to control cell proliferation and differentiation in cranial neural crest-derived osteoprogenitor cells. *The Journal of Biological Chemistry*, *285*(7), 4975–4982. https://doi.org/10.1074/JBC.M109.035105

Jansen, R., van Embden, J. D. A., Gaastra, W., & Schouls, L. M. (2002). Identification of genes that are associated with DNA repeats in prokaryotes. *Molecular Microbiology*, *43*(6), 1565–1575. https://doi.org/10.1046/J.1365-2958.2002.02839.X

Jao, L. E., Wente, S. R., & Chen, W. (2013). Efficient multiplex biallelic zebrafish genome editing using a CRISPR nuclease system. *Proceedings of the National Academy of Sciences of the United States of America*, *110*(34), 13904–13909. https://doi.org/10.1073/PNAS.1308335110

Jinek, M., Chylinski, K., Fonfara, I., Hauer, M., Doudna, J. A., & Charpentier, E. (2012). A programmable dual-RNA-guided DNA endonuclease in adaptive bacterial immunity. *Science*, *337*(6096), 816–821. https://doi.org/10.1126/SCIENCE.1225829/SUPPL_FILE/JINEK.SM.PDF

John, N., Cinelli, P., Wegner, M., & Sommer, L. (2011). Transforming Growth Factor β-Mediated Sox10 Suppression Controls Mesenchymal Progenitor Generation in Neural Crest Stem Cells. *Stem Cells*, *29*(4), 689–699. https://doi.org/10.1002/STEM.607

Johnson, K. R., Gagnon, L. H., Tian, C., Longo-Guess, C. M., Low, B. E., Wiles, M. v., & Kiernan, A. E. (2018). Deletion of a long-range Dlx5 enhancer disrupts inner ear development in mice. *Genetics*, *208*(3), 1165–1179. https://doi.org/10.1534/genetics.117.300447

Jones, D. L., Howard, M. A., Stanco, A., Rubenstein, J. L. R., & Baraban, S. C. (2011). Deletion of Dlx1 results in reduced glutamatergic input to hippocampal interneurons. *Journal of Neurophysiology*, *105*(5), 1984–1991. https://doi.org/10.1152/jn.00056.2011

Jussila, M., & Ciruna, B. (2017). Zebrafish models of non-canonical Wnt/planar cell polarity signalling: fishing for valuable insight into vertebrate polarized cell behavior. *Wiley Interdisciplinary Reviews: Developmental Biology*, *6*(3), e267. https://doi.org/10.1002/WDEV.267

Kalyn, M., & Ekker, M. (2021). Cerebroventricular Microinjections of MPTP on Adult Zebrafish Induces Dopaminergic Neuronal Death, Mitochondrial Fragmentation, and Sensorimotor Impairments. *Frontiers in Neuroscience*, *15*. https://doi.org/10.3389/FNINS.2021.718244

Kamel, G., Hoyos, T., Rochard, L., Dougherty, M., Kong, Y., Tse, W., Shubinets, V., Grimaldi, M., & Liao, E. C. (2013). Requirement for frzb and fzd7a in cranial neural crest convergence and extension mechanisms during zebrafish palate and jaw morphogenesis. *Developmental Biology*, *381*(2), 423–433. https://doi.org/10.1016/J.YDBIO.2013.06.012

Kanatani, S., Yozu, M., Tabata, H., & Nakajima, K. (2008). COUP-TFII is preferentially expressed in the caudal ganglionic eminence and is involved in the caudal migratory stream. *The Journal of Neuroscience : The Official Journal of the Society for Neuroscience*, *28*(50), 13582–13591. https://doi.org/10.1523/JNEUROSCI.2132-08.2008

Karagiannis, A., Gallopin, T., Dávid, C., Battaglia, D., Geoffroy, H., Rossier, J., Hillman, E. M. C., Staiger, J. F., & Cauli, B. (2009). Classification of NPY-expressing neocortical interneurons. *The Journal of Neuroscience : The Official Journal of the Society for Neuroscience*, *29*(11), 3642–3659. https://doi.org/10.1523/JNEUROSCI.0058-09.2009

Kimmel, C. B., Miller, C. T., & Moens, C. B. (2001). Specification and morphogenesis of the zebrafish larval head skeleton. *Developmental Biology*, *233*(2), 239–257. https://doi.org/10.1006/DBIO.2001.0201

Kindberg, A. A., & Bush, J. O. (2019). Cellular organization and boundary formation in craniofacial development. *Genesis*, *57*(1), e23271. https://doi.org/10.1002/DVG.23271

Kingma, H., & van de Berg, R. (2016). Anatomy, physiology, and physics of the peripheral vestibular system. *Handbook of Clinical Neurology*, *137*, 1–16. https://doi.org/10.1016/B978-0-444-63437-5.00001-7

Kissinger, C. R., Liu, B., Martin-Blanco, E., Kornberg, T. B., & Pabo, C. O. (1990). Crystal structure of an engrailed homeodomain-DNA complex at 2.8 Å resolution: A framework for understanding homeodomain-DNA interactions. *Cell*, *63*(3), 579–590. https://doi.org/10.1016/0092-8674(90)90453-L

Klein-Tasman, B. P., Mervis, C. B., Lord, C., & Phillips, K. D. (2007). Socio-Communicative Deficits in Young Children with Williams Syndrome: Performance on the Autism Diagnostic Observation Schedule. *Http://Dx.Doi.Org/10.1080/09297040601033680*, *13*(5), 444–467. https://doi.org/10.1080/09297040601033680

Knoepfler, P. S., Bergstrom, D. A., Uetsuki, T., Dac-Korytko, L., Sun, Y. H., Wright, W. E., Tapscott, S. J., & Kamps, M. P. (1999). A conserved motif N-terminal to the DNA-binding domains of myogenic bHLH transcription factors mediates cooperative DNA binding with pbx-Meis1/Prep1. *Nucleic Acids Research*, *27*(18), 3752–3761. https://doi.org/10.1093/NAR/27.18.3752

Komori, T., Yagi, H., Nomura, S., Yamaguchi, A., Sasaki, K., Deguchi, K., Shimizu, Y., Bronson, R. T., Gao, Y. H., Inada, M., Sato, M., Okamoto, R., Kitamura, Y., Yoshiki, S., & Kishimoto, T. (1997). Targeted disruption of Cbfa1 results in a complete lack of bone formation owing to maturational arrest of osteoblasts. *Cell*, *89*(5), 755–764. https://doi.org/10.1016/S0092-8674(00)80258-5

Kubota, Y., Hattori, R., & Yui, Y. (1994). Three distinct subpopulations of GABAergic neurons in rat frontal agranular cortex. *Brain Research*, *649*(1–2), 159–173. https://doi.org/10.1016/0006-8993(94)91060-X

Kulesa, P., Ellies, D. L., & Trainor, P. A. (2004). Comparative analysis of neural crest cell death, migration, and function during vertebrate embryogenesis. *Developmental Dynamics : An Official Publication of the American Association of Anatomists*, *229*(1), 14–29. https://doi.org/10.1002/DVDY.10485

Kulesa, P. M., Teddy, J. M., Stark, D. A., Smith, S. E., & McLennan, R. (2008). Neural crest invasion is a spatially-ordered progression into the head with higher cell proliferation at the migratory front as revealed by the photoactivatable protein, KikGR. *Developmental Biology*, *316*(2), 275–287. https://doi.org/10.1016/J.YDBIO.2008.01.029

Laclef, C., & Métin, C. (2018). Conserved rules in embryonic development of cortical interneurons. *Seminars in Cell & Developmental Biology*, *76*, 86–100. https://doi.org/10.1016/J.SEMCDB.2017.09.017

Ladher, R. K., O'Neill, P., & Begbie, J. (2010). From shared lineage to distinct functions: the development of the inner ear and epibranchial placodes. *Development*, *137*(11), 1777–1785. https://doi.org/10.1242/DEV.040055

Langley, A. R., Smith, J. C., Stemple, D. L., & Harvey, S. A. (2014). New insights into the maternal to zygotic transition. *Development*, *141*(20), 3834–3841. https://doi.org/10.1242/DEV.102368

Laughon, A., & Scott, M. P. (1984). Sequence of a Drosophila segmentation gene: protein structure homology with DNA-binding proteins. *Nature 1984 310:5972*, *310*(5972), 25–31. https://doi.org/10.1038/310025a0

Lavdas, A. A., Grigoriou, M., Pachnis, V., & Parnavelas, J. G. (1999). The medial ganglionic eminence gives rise to a population of early neurons in the developing cerebral cortex. *The Journal of Neuroscience : The Official Journal of the Society for Neuroscience*, *19*(18), 7881–7888. https://doi.org/10.1523/JNEUROSCI.19-18-07881.1999

Le, T. N., Du, G., Fonseca, M., Zhou, Q. P., Wigle, J. T., & Eisenstat, D. D. (2007). Dlx homeobox genes promote cortical interneuron migration from the basal forebrain by direct repression of the semaphorin receptor neuropilin-2. *Journal of Biological Chemistry*, *282*(26), 19071–19081. https://doi.org/10.1074/jbc.M607486200

Lecaudey, V., Cakan-Akdogan, G., Norton, W. H. J., & Gilmour, D. (2008). Dynamic Fgf signaling couples morphogenesis and migration in the zebrafish lateral line primordium. *Development (Cambridge, England)*, *135*(16), 2695–2705. https://doi.org/10.1242/DEV.025981

Ledent, V. (2002). Postembryonic development of the posterior lateral line in zebrafish. *Development*, *129*(3), 597–604. https://doi.org/10.1242/DEV.129.3.597

Lefebvre, V., Huang, W., Harley, V. R., Goodfellow, P. N., & de Crombrugghe, B. (1997). SOX9 is a potent activator of the chondrocyte-specific enhancer of the pro alpha1(II) collagen gene. *Molecular and Cellular Biology*, *17*(4), 2336–2346. https://doi.org/10.1128/MCB.17.4.2336

Levi, G., Puche, A. C., Mantero, S., Barbieri, O., Trombino, S., Paleari, L., Egeo, A., & Merlo, G. R. (2003). *The Dlx5 homeodomain gene is essential for olfactory development and connectivity in the mouse*. https://doi.org/10.1016/S1044-7431(02)00041-6

Lewis, J. L., Bonner, J., Modrell, M., Ragland, J. W., Moon, R. T., Dorsky, R. I., & Raible, D. W. (2004). Reiterated Wnt signaling during zebrafish neural crest development. *Development*, *131*(6), 1299–1308. https://doi.org/10.1242/DEV.01007

Lim, L., Mi, D., Llorca, A., & Marín, O. (2018). Development and Functional Diversification of Cortical Interneurons. *Neuron*, *100*(2), 294–313. https://doi.org/10.1016/j.neuron.2018.10.009

Lincoln, A. J., Searcy, Y. M., Jones, W., & Lord, C. (2007). Social Interaction Behaviors Discriminate Young Children With Autism and Williams Syndrome. *Journal of the American Academy of Child & Adolescent Psychiatry*, *46*(3), 323–331. https://doi.org/10.1097/CHI.0B013E31802B9522

Ling, I. T., Rochard, L., & Liao, E. C. (2017). Distinct requirements of wls, wnt9a, wnt5b and gpc4 in regulating chondrocyte maturation and timing of endochondral ossification. *Developmental Biology*, *421*(2), 219–232. https://doi.org/10.1016/j.ydbio.2016.11.016

Liu, C. X., Li, C. Y., Hu, C. C., Wang, Y., Lin, J., Jiang, Y. H., Li, Q., & Xu, X. (2018). CRISPR/Cas9-induced shank3b mutant zebrafish display autism-like behaviors. *Molecular Autism*, *9*(1), 1–13. https://doi.org/10.1186/S13229-018-0204-X/FIGURES/7

Liu, J. K., Ghattas, I., Liu, S., Chen, S., & Rubenstein, J. L. R. (1997). Dlx Genes Encode DNA-Binding Proteins That Are Expressed in an Overlapping And Sequential Pattern During Basal Ganglia Differentiation. *Dev. Dyn*, *210*, 498–512. https://doi.org/10.1002/(SICI)1097-0177(199712)210:4

Liu, X., Novosedlik, N., Wang, A., Hudson, M. L., Cohen, I. L., Chudley, A. E., Forster-Gibson, C. J., Lewis, S. M. E., & Holden, J. J. A. (2008). The DLX1and DLX2 genes and susceptibility to autism spectrum disorders. *European Journal of Human Genetics 2009 17:2*, *17*(2), 228–235. https://doi.org/10.1038/ejhg.2008.148

Long, J. E., Garel, S., Depew, M. J., Tobet, S., & Rubenstein, J. L. R. (2003). DLX5 regulates development of peripheral and central components of the olfactory system. *The Journal of Neuroscience : The Official Journal of the Society for Neuroscience*, *23*(2), 568–578. https://doi.org/10.1523/JNEUROSCI.23-02-00568.2003

Long, J. E., Swan, C., Liang, W. S., Cobos, I., Potter, G. B., & Rubenstein, J. L. R. (2009). Dlx1&2 and Mash1 transcription factors control striatal patterning and differentiation through parallel and overlapping pathways. *Journal of Comparative Neurology*, *512*(4), 556–572. https://doi.org/10.1002/cne.21854

López-Bendito, G., & Martini, F. J. (2020). Patterning of thalamus. *Patterning and Cell Type Specification in the Developing CNS and PNS*, 69–86. https://doi.org/10.1016/B978-0-12-814405-3.00004-7

López-Schier, H., & Hudspeth, A. J. (2005). Supernumerary neuromasts in the posterior lateral line of zebrafish lacking peripheral glia. *Proceedings of the National Academy of Sciences of the United States of America*, *102*(5), 1496–1501. https://doi.org/10.1073/PNAS.0409361102/SUPPL_FILE/09361MOVIE1.MOV

Lowery, L. A., & Sive, H. (2004). Strategies of vertebrate neurulation and a re-evaluation of teleost neural tube formation. *Mechanisms of Development*, *121*(10), 1189–1197. https://doi.org/10.1016/J.MOD.2004.04.022

Lumsden, A., & Krumlauf, R. (1996). Patterning the Vertebrate Neuraxis. *Science*, *274*(5290), 1109–1115. https://doi.org/10.1126/SCIENCE.274.5290.1109

Lush, M. E., & Piotrowski, T. (2014). ErbB expressing Schwann cells control lateral line progenitor cells via non-cell-autonomous regulation of Wnt/β-catenin. *ELife*, *3*(3). https://doi.org/10.7554/ELIFE.01832

Ma, E. Y., & Raible, D. W. (2009). Signaling pathways regulating zebrafish lateral line development. *Current Biology : CB*, *19*(9). https://doi.org/10.1016/J.CUB.2009.03.057

MacDonald, R. B., Debiais-Thibaud, M., Talbot, J. C., & Ekker, M. (2010). The relationship between dlx and gad1 expression indicates highly conserved genetic pathways in the zebrafish forebrain. *Developmental Dynamics*, *239*(8), 2298–2306. https://doi.org/10.1002/dvdy.22365

MacDonald, R. B., Pollack, J. N., Debiais-Thibaud, M., Heude, E., Coffin Talbot, J., & Ekker, M. (2013). The ascl1a and dlx genes have a regulatory role in the development of GABAergic interneurons in the zebrafish diencephalon. *Developmental Biology*, *381*(1), 276–285. https://doi.org/10.1016/j.ydbio.2013.05.025

MacKenzie, R. K., Sankar, P. R., & Bendall, A. J. (2019). Dlx5 and Dlx6 can antagonize cell division at the G1/S checkpoint. *BMC Molecular and Cell Biology*, *20*(1), 1–12. https://doi.org/10.1186/S12860-019-0191-6/TABLES/1

Maj, E., Künneke, L., Loresch, E., Grund, A., Melchert, J., Pieler, T., Aspelmeier, T., & Borchers, A. (2016). Controlled levels of canonical Wnt signaling are required for neural crest migration. *Developmental Biology*, *417*(1), 77–90. https://doi.org/10.1016/J.YDBIO.2016.06.022

Makarova, K. S., Aravind, L., Grishin, N. v., Rogozin, I. B., & Koonin, E. v. (2002). A DNA repair system specific for thermophilic Archaea and bacteria predicted by genomic context analysis. *Nucleic Acids Research*, *30*(2), 482–496. https://doi.org/10.1093/NAR/30.2.482

Makarova, K. S., Grishin, N. v., Shabalina, S. A., Wolf, Y. I., & Koonin, E. v. (2006). A putative RNA-interference-based immune system in prokaryotes: computational analysis of the predicted enzymatic machinery, functional analogies with eukaryotic RNAi, and hypothetical mechanisms of action. *Biology Direct*, *1*. https://doi.org/10.1186/1745-6150-1-7

Mann, R. S., Lelli, K. M., & Joshi, R. (2009). Chapter 3 Hox Specificity: Unique Roles for Cofactors and Collaborators. *Current Topics in Developmental Biology*, *88*, 63–101. https://doi.org/10.1016/S0070-2153(09)88003-4

Mao, R., Page, D. T., Merzlyak, I., Kim, C., Tecott, L. H., Janak, P. H., Rubenstein, J. L. R., & Sur, M. (2009). Reduced conditioned fear response in mice that lack Dlx1 and show subtype-specific loss of interneurons. *Journal of Neurodevelopmental Disorders*, *1*(3), 224–236. https://doi.org/10.1007/s11689-009-9025-8

Marchant, L., Linker, C., Ruiz, P., Guerrero, N., & Mayor, R. (1998). The inductive properties of mesoderm suggest that the neural crest cells are specified by a BMP gradient. *Developmental Biology*, *198*(2), 319–329. https://doi.org/10.1016/S0012-1606(98)80008-0

Marín, O., & Rubenstein, J. L. R. (2001). A long, remarkable journey: Tangential migration in the telencephalon. *Nature Reviews Neuroscience 2001 2:11*, *2*(11), 780–790. https://doi.org/10.1038/35097509

Marín, O., Yaron, A., Bagri, A., Tessier-Lavigne, M., & Rubenstein, J. L. R. (2001). Sorting of striatal and cortical interneurons regulated by semaphorin-neuropilin interactions. *Science*, *293*(5531), 872–875. https://doi.org/10.1126/SCIENCE.1061891/SUPPL_FILE/1061891S3_THUMB.GIF

Martynoga, B., Morrison, H., Price, D. J., & Mason, J. O. (2005). Foxg1 is required for specification of ventral telencephalon and region-specific regulation of dorsal telencephalic precursor proliferation and apoptosis. *Developmental Biology*, *283*(1), 113–127. https://doi.org/10.1016/J.YDBIO.2005.04.005

Masuda, Y., Sasak, A., Shibuya, H., Ueno, N., Ikeda, K., & Watanabe, K. (2001). Dlxin-1, a novel protein that binds Dlx5 and regulates its transcriptional function. *The Journal of Biological Chemistry*, *276*(7), 5331–5338. https://doi.org/10.1074/JBC.M008590200

Mathur, P., & Guo, S. (2010). Use of zebrafish as a model to understand mechanisms of addiction and complex neurobehavioral phenotypes. *Neurobiology of Disease*, *40*(1), 66–72. https://doi.org/10.1016/J.NBD.2010.05.016

Matsunaga, E., Araki, I., & Nakamura, H. (2000). Pax6 defines the di-mesencephalic boundary by repressing En1 and Pax2. *Development*, *127*(11), 2357–2365. https://doi.org/10.1242/DEV.127.11.2357

Matsunaga, E., Araki, I., & Nakamura, H. (2001). Role of Pax3/7 in the tectum regionalization. *Development*, *128*(20), 4069–4077. https://doi.org/10.1242/DEV.128.20.4069

Maves, L., Jackman, W., & Kimmel, C. B. (2002). FGF3 and FGF8 mediate a rhombomere 4 signaling activity in the zebrafish hindbrain. *Development*, *129*(16), 3825–3837. https://doi.org/10.1242/DEV.129.16.3825

McCurley, A. T., & Callard, G. v. (2008). Characterization of housekeeping genes in zebrafish: Male-female differences and effects of tissue type, developmental stage and chemical treatment. *BMC Molecular Biology*, *9*(1), 1–12. https://doi.org/10.1186/1471-2199-9-102/FIGURES/3

McGinnis, W., Garber, R. L., Wirz, J., Kuroiwa, A., & Gehring, W. J. (1984). A homologous protein-coding sequence in drosophila homeotic genes and its conservation in other metazoans. *Cell*, *37*(2), 403–408. https://doi.org/10.1016/0092-8674(84)90370-2

McKinney, M. C., McLennan, R., Giniunaite, R., Baker, R. E., Maini, P. K., Othmer, H. G., & Kulesa, P. M. (2020). Visualizing mesoderm and neural crest cell dynamics during chick head morphogenesis. *Developmental Biology*, *461*(2), 184–196. https://doi.org/10.1016/J.YDBIO.2020.02.010

McLarren, K. W., Litsiou, A., & Streit, A. (2003). DLX5 positions the neural crest and preplacode region at the border of the neural plate. *Developmental Biology*, *259*(1), 34–47. https://doi.org/10.1016/S0012-1606(03)00177-5

Medina, L., Legaz, I., González, G., de Castro, F., Rubenstein, J. L. R., & Puelles, L. (2004). Expression of Dbx1, Neurogenin 2, Semaphorin 5A, Cadherin 8, and Emx1 distinguish ventral and lateral pallial histogenetic divisions in the developing mouse claustroamygdaloid complex. *Journal of Comparative Neurology*, *474*(4), 504–523. https://doi.org/10.1002/CNE.20141

Mendes, H. W., Taktek, M., Duret, T., & Ekker, M. (2020). Expression of dlx genes in the normal and regenerating brain of adult zebrafish. *PLoS ONE*, *15*(6). https://doi.org/10.1371/journal.pone.0229549

Merlo, G. R., Paleari, L., Mantero, S., Genova, F., Beverdam, A., Palmisano, G. L., Barbieri, O., & Levi, G. (2002). Mouse model of split hand/foot malformation type I. *Genesis*, *33*(2), 97–101. https://doi.org/10.1002/GENE.10098

Mermod, N., O'Neill, E. A., Kelly, T. J., & Tjian, R. (1989). The proline-rich transcriptional activator of CTF/NF-I is distinct from the replication and DNA binding domain. *Cell*, *58*(4), 741–753. https://doi.org/10.1016/0092-8674(89)90108-6

Metcalfe, W. K., Kimmel, C. B., & Schabtach, E. (1985). Anatomy of the posterior lateral line system in young larvae of the zebrafish. *Journal of Comparative Neurology*, *233*(3), 377–389. https://doi.org/10.1002/CNE.902330307

Miller, C. T., Maves, L., & Kimmel, C. B. (2004). moz regulates Hox expression and pharyngeal segmental identity in zebrafish. *Development (Cambridge, England)*, *131*(10), 2443–2461. https://doi.org/10.1242/DEV.01134

Miller, C. T., Swartz, M. E., Khuu, P. A., Walker, M. B., Eberhart, J. K., & Kimmel, C. B. (2007). mef2ca is required in cranial neural crest to effect Endothelin1 signaling in zebrafish. *Developmental Biology*, *308*(1), 144–157. https://doi.org/10.1016/J.YDBIO.2007.05.018

Minoux, M., & Rijli, F. M. (2010). Molecular mechanisms of cranial neural crest cell migration and patterning in craniofacial development. *Development (Cambridge, England)*, *137*(16), 2605–2621. https://doi.org/10.1242/DEV.040048

Miyoshi, G., Young, A., Petros, T., Karayannis, T., Chang, M. M. K., Lavado, A., Iwano, T., Nakajima, M., Taniguchi, H., Josh Huang, Z., Heintz, N., Oliver, G., Matsuzaki, F., Machold, R. P., & Fishell, G. (2015). Prox1 Regulates the Subtype-Specific Development of Caudal Ganglionic Eminence-

Derived GABAergic Cortical Interneurons. *The Journal of Neuroscience : The Official Journal of the Society for Neuroscience*, *35*(37), 12869–12889. https://doi.org/10.1523/JNEUROSCI.1164-15.2015

Mojica, F. J. M., Díez-Villaseñor, C., García-Martínez, J., & Soria, E. (2005). Intervening Sequences of Regularly Spaced Prokaryotic Repeats Derive from Foreign Genetic Elements. *Journal of Molecular Evolution 2005 60:2*, *60*(2), 174–182. https://doi.org/10.1007/S00239-004-0046-3

Mojica, F. J. M., Juez, G., & Rodriguez-Valera, F. (1993). Transcription at different salinities of Haloferax mediterranei sequences adjacent to partially modified PstI sites. *Molecular Microbiology*, *9*(3), 613–621. https://doi.org/10.1111/J.1365-2958.1993.TB01721.X

Montague, T. G., Cruz, J. M., Gagnon, J. A., Church, G. M., & Valen, E. (2014). CHOPCHOP: a CRISPR/Cas9 and TALEN web tool for genome editing. *Nucleic Acids Research*, *42*(Web Server issue). https://doi.org/10.1093/NAR/GKU410

Montgomery, J., Carton, G., Voigt, R., Baker, C., & Diebel, C. (2000). Sensory processing of water currents by fishes. *Philosophical Transactions of the Royal Society of London. Series B: Biological Sciences*, *355*(1401), 1325–1327. https://doi.org/10.1098/RSTB.2000.0693

Mori-Akiyama, Y., Akiyama, H., Rowitch, D. H., & de Crombrugghe, B. (2003). Sox9 is required for determination of the chondrogenic cell lineage in the cranial neural crest. *Proceedings of the National Academy of Sciences of the United States of America*, *100*(16), 9360–9365. https://doi.org/10.1073/PNAS.1631288100/ASSET/BC4D4242-E4C5-4DCB-AD41-DF77B891AAF5/ASSETS/GRAPHIC/PQ1631288005.JPEG

Mueller, T., Vernier, P., & Wullimann, M. F. (2006). A phylotypic stage in vertebrate brain development: GABA cell patterns in zebrafish compared with mouse. *Journal of Comparative Neurology*, *494*(4), 620–634. https://doi.org/10.1002/cne.20824

Mueller, T., & Wullimann, M. F. (2009). An Evolutionary Interpretation of Teleostean Forebrain Anatomy. *Brain, Behavior and Evolution*, *74*(1), 30–42. https://doi.org/10.1159/000229011

Mukherjee, D., Wagh, G., Mokalled, M. H., Kontarakis, Z., Dickson, A. L., Rayrikar, A., Günther, S., Poss, K. D., Stainier, D. Y. R., & Patra, C. (2021). Ccn2a is an injury-induced matricellular factor that promotes cardiac regeneration in zebrafish. *Development (Cambridge)*, *148*(2). https://doi.org/10.1242/DEV.193219/267024/AM/CCN2A-CTGFA-IS-AN-INJURY-INDUCED-MATRICELLULAR

Nakashima, K., Zhou, X., Kunkel, G., Zhang, Z., Deng, J. M., Behringer, R. R., & de Crombrugghe, B. (2002). The novel zinc finger-containing transcription factor Osterix is required for osteoblast differentiation and bone formation. *Cell*, *108*(1), 17–29. https://doi.org/10.1016/S0092-8674(01)00622-5

Nakashima, N., Yamagata, T., Mori, M., Kuwajima, M., Suwa, K., & Momoi, M. Y. (2010). Expression analysis and mutation detection of DLX5 and DLX6 in autism. *Brain and Development*, *32*(2), 98–104. https://doi.org/10.1016/j.braindev.2008.12.021

Nechiporuk, A., & Raible, D. W. (2008). FGF-dependent mechanosensory organ patterning in zebrafish. *Science*, *320*(5884), 1774–1777. https://doi.org/10.1126/SCIENCE.1156547/SUPPL_FILE/NECHIPORUK.SOM.PDF

Neuteboom, S. T. C., Peltenburg, L. T. C., van Dijk, M. A., & Murre, C. (1995). The hexapeptide LFPWMR in Hoxb-8 is required for cooperative DNA binding with Pbx1 and Pbx2 proteins. *Proceedings of the National Academy of Sciences of the United States of America*, *92*(20), 9166–9170. https://doi.org/10.1073/PNAS.92.20.9166

Niehrs, C. (1999). Head in the WNT the molecular nature of Speamanns' head organizer. *Trends in Genetics*, *15*(8), 314–319. https://doi.org/10.1016/S0168-9525(99)01767-9

Nieuwenhuys, R., & Meek, J. (1990). *The Telencephalon of Actinopterygian Fishes*. 31–73. https://doi.org/10.1007/978-1-4757-9622-3_2

Nomura, T., & Fujisawa, H. (2000). Alteration of the retinotectal projection map by the graft of mesencephalic floor plate or sonic hedgehog. *Development*, *127*(9), 1899–1910. https://doi.org/10.1242/DEV.127.9.1899

Nordström, U., Jessell, T. M., & Edlund, T. (2002). Progressive induction of caudal neural character by graded Wnt signaling. *Nature Neuroscience 2002 5:6*, *5*(6), 525–532. https://doi.org/10.1038/nn0602-854

Northcutt, R. G., & Braford, M. R. (1980). New Observations on the Organization and Evolution of the Telencephalon of Actinopterygian Fishes. *Comparative Neurology of the Telencephalon*, 41–98. https://doi.org/10.1007/978-1-4613-2988-6_3

Ohyama, T., Mohamed, O. A., Taketo, M. M., Dufort, D., & Groves, A. K. (2006). Wnt signals mediate a fate decision between otic placode and epidermis. *Development*, *133*(5), 865–875. https://doi.org/10.1242/DEV.02271

Oka, K., Oka, S., Hosokawa, R., Bringas, P., Brockhoff, H. C., Nonaka, K., & Chai, Y. (2008). TGF-β mediated Dlx5 signaling plays a crucial role in osteo-chondroprogenitor cell lineage determination during mandible development. *Developmental Biology*, *321*(2), 303–309. https://doi.org/10.1016/J.YDBIO.2008.03.046

Olesnicky Killian, E. C., Birkholz, D. A., & Artinger, K. B. (2009). A role for chemokine signaling in neural crest cell migration and craniofacial development. *Developmental Biology*, *333*(1), 161–172. https://doi.org/10.1016/J.YDBIO.2009.06.031

Oppenheimer, J. M. (1953). The Development of Transplanted Fragments of Fundulus Gastrulae. *Proceedings of the National Academy of Sciences*, *39*(11), 1149–1152. https://doi.org/10.1073/PNAS.39.11.1149

Osborne, N. J., Begbie, J., Chilton, J. K., Schmidt, H., & Eickholt, B. J. (2005). Semaphorin/neuropilin signaling influences the positioning of migratory neural crest cells within the hindbrain region of the chick. *Developmental Dynamics : An Official Publication of the American Association of Anatomists*, *232*(4), 939–949. https://doi.org/10.1002/DVDY.20258

Ota, S., Hisano, Y., Ikawa, Y., & Kawahara, A. (2014). Multiple genome modifications by the CRISPR/Cas9 system in zebrafish. *Genes to Cells : Devoted to Molecular & Cellular Mechanisms*, *19*(7), 555–564. https://doi.org/10.1111/GTC.12154

Otto, F., Thornell, A. P., Crompton, T., Denzel, A., Gilmour, K. C., Rosewell, I. R., Stamp, G. W. H., Beddington, R. S. P., Mundlos, S., Olsen, B. R., Selby, P. B., & Owen, M. J. (1997). Cbfa1, a candidate gene for cleidocranial dysplasia syndrome, is essential for osteoblast differentiation and bone development. *Cell*, *89*(5), 765–771. https://doi.org/10.1016/S0092-8674(00)80259-7

Ozair, M. Z., Kintner, C., & Brivanlou, A. H. (2013). Neural induction and early patterning in vertebrates. *Wiley Interdisciplinary Reviews: Developmental Biology*, *2*(4), 479–498. https://doi.org/10.1002/WDEV.90

Paek, H., Gutin, G., & Hébert, J. M. (2009). FGF signaling is strictly required to maintain early telencephalic precursor cell survival. *Development*, *136*(14), 2457–2465. https://doi.org/10.1242/DEV.032656

Paina, S., Garzotto, D., DeMarchis, S., Marino, M., Moiana, A., Conti, L., Cattaneo, E., Perera, M., Corte, G., Calautti, E., & Merlo, G. R. (2011). Wnt5a is a transcriptional target of Dlx homeogenes and promotes differentiation of interneuron progenitors in vitro and in vivo. *Journal of Neuroscience*, *31*(7), 2675–2687. https://doi.org/10.1523/JNEUROSCI.3110-10.2011

Panganiban, G., & Rubenstein, J. L. R. (2002). Developmental functions of the Distal-less/Dlx homeobox genes. *Development*, *129*(19), 4371–4386.

Park, B. K., Sperber, S. M., Choudhury, A., Ghanem, N., Hatch, G. T., Sharpe, P. T., Thomas, B. L., & Ekker, M. (2004). Intergenic enhancers with distinct activities regulate Dlx gene expression in the mesenchyme of the branchial arches. *Developmental Biology*, *268*(2), 532–545. https://doi.org/10.1016/j.ydbio.2004.01.010

Passner, J. M., Ryoo, H. D., Shen, L., Mann, R. S., & Aggarwal, A. K. (1999). Structure of a DNA-bound Ultrabithorax–Extradenticle homeodomain complex. *Nature 1999 397:6721*, *397*(6721), 714–719. https://doi.org/10.1038/17833

Pellegrini, E., Mouriec, K., Anglade, I., Menuet, A., le Page, Y., Gueguen, M. M., Marmignon, M. H., Brion, F., Pakdel, F., & Kah, O. (2007). Identification of aromatase-positive radial glial cells as progenitor cells in the ventricular layer of the forebrain in zebrafish. *Journal of Comparative Neurology*, *501*(1), 150–167. https://doi.org/10.1002/CNE.21222

Perera, M., Merlo, G. R., Verardo, S., Paleari, L., Corte, G., & Levi, G. (2004). Defective neuronogenesis in the absence of Dlx5. *Molecular and Cellular Neuroscience*, *25*(1), 153–161. https://doi.org/10.1016/j.mcn.2003.10.004

Perkins, R. S., Suthon, S., Miranda-Carboni, G. A., & Krum, S. A. (2022). WNT5B in cellular signaling pathways. *Seminars in Cell & Developmental Biology*, *125*, 11–16. https://doi.org/10.1016/J.SEMCDB.2021.09.019

Petryniak, M. A., Potter, G. B., Rowitch, D. H., & Rubenstein, J. L. R. (2007). Dlx1 and Dlx2 control neuronal versus oligodendroglial cell fate acquisition in the developing forebrain. *Neuron*, *55*(3), 417–433. https://doi.org/10.1016/J.NEURON.2007.06.036

Piacentino, M. L., Hutchins, E. J., & Bronner, M. E. (2021). Essential function and targets of BMP signaling during midbrain neural crest delamination. *Developmental Biology*, *477*, 251–261. https://doi.org/10.1016/J.YDBIO.2021.06.003

Pick, L., & Heffer, A. (2012). Hox gene evolution: multiple mechanisms contributing to evolutionary novelties. *Annals of the New York Academy of Sciences*, *1256*(1), 15–32. https://doi.org/10.1111/J.1749-6632.2011.06385.X

Pinal, C. S., & Tobin, A. J. (1998). Uniqueness and redundancy in GABA production. *Article in Perspectives on Developmental Neurobiology*. https://www.researchgate.net/publication/13507869

Piotrowski, T., Schilling, T. F., Brand, M., Jiang, Y. J., Heisenberg, C. P., Beuchle, D., Grandel, H., van Eeden, F. J. M., Furutani-Seiki, M., Granato, M., Haffter, P., Hammerschmidt, M., Kane, D. A., Kelsh, R. N., Mullins, M. C., Odenthal, J., Warga, R. M., & Nüsslein-Volhard, C. (1996). Jaw and branchial arch mutants in zebrafish II: anterior arches and cartilage differentiation. *Development*, *123*(1), 345–356. https://doi.org/10.1242/DEV.123.1.345

Poitras, L., Ghanem, N., Hatch, G., & Ekker, M. (2007). The proneural determinant MASH1 regulates forebrain Dlx1/2 expression through the l12b intergenic enhancer. *Development*, *134*(9), 1755–1765. https://doi.org/10.1242/dev.02845

Poitras, L., Yu, M., Lesage-Pelletier, C., MacDonald, R. B., Gagné, J. P., Hatch, G., Kelly, I., Hamilton, S. P., Rubenstein, J. L. R., Poirier, G. G., & Ekker, M. (2010). An SNP in an ultraconserved regulatory element affects Dlx5/Dlx6 regulation in the forebrain. *Development*, *137*(18), 3089–3097. https://doi.org/10.1242/dev.051052

Potter, G. B., Petryniak, M. A., Shevchenko, E., McKinsey, G. L., Ekker, M., & Rubenstein, J. L. R. (2009). Generation of Cre-transgenic mice using Dlx1/Dlx2 enhancers and their characterization in GABAergic interneurons. *Molecular and Cellular Neuroscience*, *40*(2), 167–186. https://doi.org/10.1016/J.MCN.2008.10.003

Puelles, L., Kuwana, E., Puelles, E., Bulfone, A., Shimamura, K., Keleher, J., Smiga, S., & Rubenstein, J. L. R. (2000). *Pallial and subpallial derivatives in the embryonic chick and mouse telencephalon, traced by the expression of the genes Dlx-2, Emx-1, Nkx-2.1, Pax-6, and Tbr-1*. J. Comp Neurol. https://onlinelibrary-wiley-com.proxy.bib.uottawa.ca/doi/epdf/10.1002/1096-9861%2820000828%29424%3A3%3C409%3A%3AAID-CNE3%3E3.0.CO%3B2-7

Purves, D., Augustine, G. J., Fitzpatrick, D., Katz, L. C., LaMantia, A.-S., McNamara, J. O., & Williams, S. M. (2001). *Neuroscience*. 1–2. https://www.ncbi.nlm.nih.gov/books/NBK10799/

Qiu, M., Bulfone, A., Ghattas, I., Meneses, J. J., Christensen, L., Sharpe, P. T., Presley, R., Pedersen, R. A., & Rubenstein, J. L. R. (1997). Role of the Dlx homeobox genes in proximodistal patterning of the branchial arches: Mutations of Dlx-1, Dlx-2, and Dlx-1 and -2 alter morphogenesis of proximal skeletal and soft tissue structures derived from the first and second arches. *Developmental Biology*, *185*(2), 165–184. https://doi.org/10.1006/dbio.1997.8556

Qiu, M., Bulfone, A., Martinez, S., Meneses, J. J., Shimamura, K., Pedersen, R. A., & Rubenstein, J. L. R. (1995). Null mutation of Dlx-2 results in abnormal morphogenesis of proximal first and second branchial arch derivatives and abnormal differentiation in the forebrain. *Genes and Development*, *9*(20), 2523–2538. https://doi.org/10.1101/gad.9.20.2523

Rajput, N., Parikh, K., & Kenney, J. W. (2022). Beyond bold versus shy: Zebrafish exploratory behavior falls into several behavioral clusters and is influenced by strain and sex. *Biology Open*, *11*(8). https://doi.org/10.1242/BIO.059443/276471

Ridenour, D. A., Mclennan, R., Teddy, J. M., Semerad, C. L., Haug, J. S., & Kulesa, P. M. (2014). The neural crest cell cycle is related to phases of migration in the head. *Development (Cambridge)*, *141*(5), 1095–1103. https://doi.org/10.1242/DEV.098855/VIDEO-2

Robinson-Rechavi, M., Marchand, O., Escriva, H., Bardet, P. L., Zelus, D., Hughes, S., & Laudet, V. (2001). Euteleost fish genomes are characterized by expansion of gene families. *Genome Research*, *11*(5), 781–788. https://doi.org/10.1101/GR.165601

Robledo, R. F., Rajan, L., Li, X., & Lufkin, T. (2002). The Dlx5 and Dlx6 homeobox genes are essential for craniofacial, axial, and appendicular skeletal development. *Genes & Development*, *16*(9), 1089–1101. https://doi.org/10.1101/GAD.988402

Rodríguez-Vázquez, J. F., Mérida-Velasco, J. R., Verdugo-López, S., Sánchez-Montesinos, I., & Mérida-Velasco, J. A. (2006). Morphogenesis of the second pharyngeal arch cartilage (Reichert's cartilage) in human embryos. *Journal of Anatomy*, *208*(2), 179–189. https://doi.org/10.1111/J.1469-7580.2006.00524.X

Rodríguez-Vázquez, J. F., Yamamoto, M., Abe, S., Katori, Y., & Murakami, G. (2018). Development of the Human Incus With Special Reference to the Detachment From the Chondrocranium to be Transferred into the Middle Ear. *The Anatomical Record*, *301*(8), 1405–1415. https://doi.org/10.1002/AR.23832

Rohs, R., West, S. M., Sosinsky, A., Liu, P., Mann, R. S., & Honig, B. (2009). The role of DNA shape in protein–DNA recognition. *Nature 2009 461:7268*, *461*(7268), 1248–1253. https://doi.org/10.1038/nature08473

Sakai, C., Ijaz, S., & Hoffman, E. J. (2018). Zebrafish Models of Neurodevelopmental Disorders: Past, Present, and Future. *Frontiers in Molecular Neuroscience*, *11*. https://doi.org/10.3389/FNMOL.2018.00294

Sánchez, M., Ceci, M. L., Gutiérrez, D., Anguita-Salinas, C., & Allende, M. L. (2016). Mechanosensory organ regeneration in zebrafish depends on a population of multipotent progenitor cells kept latent by Schwann cells. *BMC Biology*, *14*(1), 1–20. https://doi.org/10.1186/S12915-016-0249-2/FIGURES/8

Santagati, F., & Rijli, F. M. (2003). Cranial neural crest and the building of the vertebrate head. *Nature Reviews Neuroscience 2003 4:10*, *4*(10), 806–818. https://doi.org/10.1038/nrn1221

Sarkar, S., Petiot, A., Copp, A., Ferretti, P., & Thorogood, P. (2001). FGF2 promotes skeletogenic differentiation of cranial neural crest cells. *Development*, *128*(11), 2143–2152. https://doi.org/10.1242/DEV.128.11.2143

Sauka-Spengler, T., & Bronner-Fraser, M. (2008). A gene regulatory network orchestrates neural crest formation. *Nature Reviews Molecular Cell Biology 2008 9:7*, *9*(7), 557–568. https://doi.org/10.1038/nrm2428

Schilling, T. F., & Kimmel, C. B. (1994). Segment and cell type lineage restrictions during pharyngeal arch development in the zebrafish embryo. *Development*, *120*(3), 483–494. https://doi.org/10.1242/DEV.120.3.483

Schilling, T. F., & le Pabic, P. (2014). Neural Crest Cells in Craniofacial Skeletal Development. *Neural Crest Cells: Evolution, Development and Disease*, 127–151. https://doi.org/10.1016/B978-0-12-401730-6.00008-9

Schimmang, T. (2007). Expression and functions of FGF ligands during early otic development. *The International Journal of Developmental Biology*, *51*(6–7), 473–481. https://doi.org/10.1387/IJDB.072334TS

Schlosser, G. (2010). Making Senses: Development of Vertebrate Cranial Placodes. *International Review of Cell and Molecular Biology*, *283*(C), 129–234. https://doi.org/10.1016/S1937-6448(10)83004-7

Schlosser, G. (2014). Early embryonic specification of vertebrate cranial placodes. *Wiley Interdisciplinary Reviews: Developmental Biology*, *3*(5), 349–363. https://doi.org/10.1002/WDEV.142

Schlosser, G., & Ahrens, K. (2004). Molecular anatomy of placode development in Xenopus laevis. *Developmental Biology*, *271*(2), 439–466. https://doi.org/10.1016/j.ydbio.2004.04.013

Schwaller, B. (2014). Calretinin: from a "simple" Ca(2+) buffer to a multifunctional protein implicated in many biological processes. *Frontiers in Neuroanatomy*, *8*(FEB). https://doi.org/10.3389/FNANA.2014.00003

Schwarz, Q., Vieira, J. M., Howard, B., Eickholt, B. J., & Ruhrberg, C. (2008). Neuropilin 1 and 2 control cranial gangliogenesis and axon guidance through neural crest cells. *Development*, *135*(9), 1605–1613. https://doi.org/10.1242/DEV.015412

Scott, M. P., & Weiner, A. J. (1984). Structural relationships among genes that control development: sequence homology between the Antennapedia, Ultrabithorax, and fushi tarazu loci of Drosophila. *Proceedings of the National Academy of Sciences*, *81*(13), 4115–4119. https://doi.org/10.1073/PNAS.81.13.4115

Shamim, H., & Mason, I. (1998). Expression of Gbx-2 during early development of the chick embryo. *Mechanisms of Development*, *76*(1–2), 157–159. https://doi.org/10.1016/S0925-4773(98)00102-6

Shanmugalingam, S., Houart, C., Picker, A., Reifers, F., Macdonald, R., Barth, A., Griffin, K., Brand, M., & Wilson, S. W. (2000). Ace/Fgf8 is required for forebrain commissure formation and patterning of the telencephalon. *Development*, *127*(12), 2549–2561. https://doi.org/10.1242/DEV.127.12.2549

Shiau, C. E., Lwigale, P. Y., Das, R. M., Wilson, S. A., & Bronner-Fraser, M. (2008). Robo2-Slit1 dependent cell-cell interactions mediate assembly of the trigeminal ganglion. *Nature Neuroscience 2008 11:3*, *11*(3), 269–276. https://doi.org/10.1038/nn2051

Shimo, T., Kanyama, M., Wu, C., Sugito, H., Billings, P. C., Abrams, W. R., Rosenbloom, J., Iwamoto, M., Pacifici, M., & Koyama, E. (2004). Expression and roles of connective tissue growth factor in Meckel's cartilage development. *Developmental Dynamics : An Official Publication of the American Association of Anatomists*, *231*(1), 136–147. https://doi.org/10.1002/DVDY.20109

Shinya, M., Koshida, S., Sawada, A., Kuroiwa, A., & Takeda, H. (2001). Fgf signalling through MAPK cascade is required for development of the subpallial telencephalon in zebrafish embryos. *Development*, *128*(21), 4153–4164. https://doi.org/10.1242/DEV.128.21.4153

Shirai, Y., Kawabe, K., Tosa, I., Tsukamoto, S., Yamada, D., & Takarada, T. (2019). Runx2 function in cells of neural crest origin during intramembranous ossification. *Biochemical and Biophysical Research Communications*, *509*(4), 1028–1033. https://doi.org/10.1016/J.BBRC.2019.01.059

Shmakov, S., Smargon, A., Scott, D., Cox, D., Pyzocha, N., Yan, W., Abudayyeh, O. O., Gootenberg, J. S., Makarova, K. S., Wolf, Y. I., Severinov, K., Zhang, F., & Koonin, E. v. (2017). Diversity and evolution of class 2 CRISPR–Cas systems. *Nature Reviews Microbiology 2017 15:3*, *15*(3), 169–182. https://doi.org/10.1038/nrmicro.2016.184

Si Dong, P. D., Chu, J., & Panganiban, G. (2000). Coexpression of the homeobox genes Distal-less and homothorax determines Drosophila antennal identity. *Development*, *127*(2), 209–216. https://doi.org/10.1242/DEV.127.2.209

Simeone, A., Acampora, D., Gulisano, M., Stornaiuolo, A., & Boncinelli, E. (1992). Nested expression domains of four homeobox genes in developing rostral brain. *Nature 1992 358:6388*, *358*(6388), 687–690. https://doi.org/10.1038/358687a0

Simeone, A., Acampora, D., PANNESEt, M., Stornaiuolo, A., GULISANOtt, M., MALLAMACIt, A., Kastury, K., Druck, T., Huebner, K., & BONCINELLIt, E. (1994). Cloning and characterization of two members of the vertebrate Dlx gene. *Developmental Biology* (Vol. 91). https://www.pnas.org

Sisson, B. E., Dale, R. M., Mui, S. R., Topczewska, J. M., & Topczewski, J. (2015). A role of glypican4 and wnt5b in chondrocyte stacking underlying craniofacial cartilage morphogenesis. *Mechanisms of Development*, *138*, 279–290. https://doi.org/10.1016/J.MOD.2015.10.001

Solek, C. M., Feng, S., Perin, S., Weinschutz Mendes, H., & Ekker, M. (2017). Lineage tracing of dlx1a/2a and dlx5a/6a expressing cells in the developing zebrafish brain. *Developmental Biology*, *427*(1), 131–147. https://doi.org/10.1016/j.ydbio.2017.04.019

Song, Y., Tao, B., Chen, J., Jia, S., Zhu, Z., Trudeau, V. L., & Hu, W. (2017). GABAergic Neurons and Their Modulatory Effects on GnRH3 in Zebrafish. *Endocrinology*, *158*(4), 874–886. https://doi.org/10.1210/EN.2016-1776

Soufi, A., & Dalton, S. (2016). Cycling through developmental decisions: how cell cycle dynamics control pluripotency, differentiation and reprogramming. *Development*, *143*(23), 4301–4311. https://doi.org/10.1242/DEV.142075

Spemann, H., & Mangold, H. (2003). Induction of embryonic primordia by implantation of organizers from a different species. 1923. *International Journal of Developmental Biology*, *45*(1), 13–38. https://doi.org/10.1387/IJDB.11291841

Sperber, S. M., Saxena, V., Hatch, G., & Ekker, M. (2008). Zebrafish dlx2a contributes to hindbrain neural crest survival, is necessary for differentiation of sensory ganglia and functions with dlx1a in maturation of the arch cartilage elements. *Developmental Biology*, *314*(1), 59–70. https://doi.org/10.1016/j.ydbio.2007.11.005

Stock, D. W., Ellies, D. L., Zhao, Z., Ekker, M., Ruddle, F. H., & Weiss, K. M. (1996). The evolution of the vertebrate Dlx gene family. *Proceedings of the National Academy of Sciences of the United States of America*, *93*(20), 10858–10863. https://doi.org/10.1073/pnas.93.20.10858

Stühmer, T., Anderson, S. A., Ekker, M., & Rubenstein, J. L. R. (2002). Ectopic expression of the Dlx genes induces glutamic acid decarboxylase and Dlx expression. *Development*, *129*(1), 245–252.

Sugii, H., Grimaldi, A., Li, J., Parada, C., Vu-Ho, T., Feng, J., Jing, J., Yuan, Y., Guo, Y., Maeda, H., & Chai, Y. (2017). The DLx5-FGF10 signaling cascade controls cranial neural crest and myoblast interaction during oropharyngeal patterning and development. *Development (Cambridge)*, *144*(21), 4037–4045. https://doi.org/10.1242/dev.155176

Sun, J., Ha, N. Y., Liu, Z., Bian, Q., & Wang, X. (2022). A Neural Crest-specific Overexpression Mouse Model Reveals the Transcriptional Regulatory Effects of Dlx2 During Maxillary Process Development. *Frontiers in Physiology*, *13*, 589. https://doi.org/10.3389/FPHYS.2022.855959/BIBTEX

Sunkel, C. E., & Whittle, J. R. S. (1987). Brista: a gene involved in the specification and differentiation of distal cephalic and thoracic structures in Drosophila melanogaster. *Roux's Archives of Developmental Biology : The Official Organ of the EDBO*, *196*(2), 124–132. https://doi.org/10.1007/BF00402034

Svandova, E., Anthwal, N., Tucker, A. S., & Matalova, E. (2020). Diverse Fate of an Enigmatic Structure: 200 Years of Meckel's Cartilage. *Frontiers in Cell and Developmental Biology*, *8*, 821. https://doi.org/10.3389/FCELL.2020.00821/BIBTEX

Swartz, M. E., Nguyen, V., McCarthy, N. Q., & Eberhart, J. K. (2012). Hh signaling regulates patterning and morphogenesis of the pharyngeal arch-derived skeleton. *Developmental Biology*, *369*(1), 65–75. https://doi.org/10.1016/J.YDBIO.2012.05.032

Szabó, A., & Mayor, R. (2018). Mechanisms of Neural Crest Migration. *Https://Doi.Org/10.1146/Annurev-Genet-120417-031559*, *52*, 43–63. https://doi.org/10.1146/ANNUREV-GENET-120417-031559

Tada, M., & Smith, J. C. (2000). Xwnt11 is a target of Xenopus Brachyury: regulation of gastrulation movements via Dishevelled, but not through the canonical Wnt pathway. *Development*, *127*(10), 2227–2238. https://doi.org/10.1242/DEV.127.10.2227

Tamamaki, N., Fujimori, K., Nojyo, Y., Kaneko, T., & Takauji, R. (2003). Evidence that Sema3A and Sema3F regulate the migration of GABAergic neurons in the developing neocortex. *The Journal of Comparative Neurology*, *455*(2), 238–248. https://doi.org/10.1002/CNE.10476

Taneyhill, L. A., & Padmanabhan, R. (2014). The Cell Biology of Neural Crest Cell Delamination and EMT. *Neural Crest Cells: Evolution, Development and Disease*, 51–72. https://doi.org/10.1016/B978-0-12-401730-6.00003-X

Tao, G., Kahr, P. C., Morikawa, Y., Zhang, M., Rahmani, M., Heallen, T. R., Li, L., Sun, Z., Olson, E. N., Amendt, B. A., & Martin, J. F. (2016). Pitx2 promotes heart repair by activating the antioxidant response after cardiac injury. *Nature 2016 534:7605*, *534*(7605), 119–123. https://doi.org/10.1038/nature17959

Tayanloo-Beik, A., Hamidpour, S. K., Abedi, M., Shojaei, H., Tavirani, M. R., Namazi, N., Larijani, B., & Arjmand, B. (2022). Zebrafish Modeling of Autism Spectrum Disorders, Current Status and Future Prospective. *Frontiers in Psychiatry*, *13*, 1514. https://doi.org/10.3389/FPSYT.2022.911770/BIBTEX

Théveneau, E., Duband, J. L., & Altabef, M. (2007). Ets-1 Confers Cranial Features on Neural Crest Delamination. *PLOS ONE*, *2*(11), e1142. https://doi.org/10.1371/JOURNAL.PONE.0001142

Theveneau, E., Steventon, B., Scarpa, E., Garcia, S., Trepat, X., Streit, A., & Mayor, R. (2013). Chase-and-run between adjacent cell populations promotes directional collective migration. *Nature Cell Biology 2013 15:7*, *15*(7), 763–772. https://doi.org/10.1038/ncb2772

Thiery, J. P., Duband, J. L., & Delouvée, A. (1982). Pathways and mechanisms of avian trunk neural crest cell migration and localization. *Developmental Biology*, *93*(2), 324–343. https://doi.org/10.1016/0012-1606(82)90121-X

Thiery, J. P., & Sleeman, J. P. (2006). Complex networks orchestrate epithelial–mesenchymal transitions. *Nature Reviews Molecular Cell Biology 2006 7:2*, *7*(2), 131–142. https://doi.org/10.1038/nrm1835

Thisse, C., & Thisse, B. (2008). High-resolution in situ hybridization to whole-mount zebrafish embryos. *Nature Protocols*, *3*(1), 59–69. https://doi.org/10.1038/nprot.2007.514

Thomas, B. L., Liu, J. K., Rubenstein, J. L. R., & Sharpe, P. T. (2000). Independent regulation of Dlx2 expression in the epithelium and mesenchyme of the first branchial arch. *Development*, *127*(2), 217–224. https://doi.org/10.1242/DEV.127.2.217

Thomas, E. D., Cruz, I. A., Hailey, D. W., & Raible, D. W. (2015). There and back again: development and regeneration of the zebrafish lateral line system. *Wiley Interdisciplinary Reviews: Developmental Biology*, *4*(1), 1–16. https://doi.org/10.1002/WDEV.160

Topczewski, J., Dale, R. M., & Sisson, B. E. (2011). Planar cell polarity signaling in craniofacial development. *Organogenesis*, *7*(4), 255–259. https://doi.org/10.4161/ORG.7.4.18797

Tricoire, L., Pelkey, K. A., Daw, M. I., Sousa, V. H., Miyoshi, G., Jeffries, B., Cauli, B., Fishell, G., & McBain, C. J. (2010). Common Origins of Hippocampal Ivy and Nitric Oxide Synthase Expressing Neurogliaform Cells. *Journal of Neuroscience*, *30*(6), 2165–2176. https://doi.org/10.1523/JNEUROSCI.5123-09.2010

Tucker, A. S., Matthews, K. L., & Sharpe, P. T. (1998). Transformation of Tooth Type Induced by Inhibition of BMP Signaling. *Science*, *282*(5391), 1136–1138. https://doi.org/10.1126/SCIENCE.282.5391.1136

Tucker, A. S., Yamada, G., Grigoriou, M., Pachnis, V., & Sharpe, P. T. (1999). Fgf-8 determines rostral-caudal polarity in the first branchial arch. *Development*, *126*(1), 51–61. https://doi.org/10.1242/DEV.126.1.51

Ulloa, F., & Briscoe, J. (2007). Morphogens and the control of cell proliferation and patterning in the spinal cord. *Cell Cycle (Georgetown, Tex.)*, *6*(21), 2640–2649. https://doi.org/10.4161/CC.6.21.4822

van Trump, W. J., Coombs, S., Duncan, K., & McHenry, M. J. (2010). Gentamicin is ototoxic to all hair cells in the fish lateral line system. *Hearing Research*, *261*(1–2), 42–50. https://doi.org/10.1016/J.HEARES.2010.01.001

Vanyai, H. K., Garnham, A., May, R. E., McRae, H. M., Collin, C., Wilcox, S., Smyth, G. K., Thomas, T., & Voss, A. K. (2019). MOZ directs the distal-less homeobox gene expression program during craniofacial development. *Development (Cambridge)*, *146*(14), 1–13. https://doi.org/10.1242/dev.175042

Varshney, G. K., Pei, W., Lafave, M. C., Idol, J., Xu, L., Gallardo, V., Carrington, B., Bishop, K., Jones, M., Li, M., Harper, U., Huang, S. C., Prakash, A., Chen, W., Sood, R., Ledin, J., & Burgess, S. M. (2015). High-throughput gene targeting and phenotyping in zebrafish using CRISPR/Cas9. *Genome Research*, *25*(7), 1030–1042. https://doi.org/10.1101/GR.186379.114

Veitch, E., Begbie, J., Schilling, T. F., Smith, M. M., & Graham, A. (1999). Pharyngeal arch patterning in the absence of neural crest. *Current Biology : CB*, *9*(24), 1481–1484. https://doi.org/10.1016/S0960-9822(00)80118-9

Verduzco, D., & Amatruda, J. F. (2011). Analysis of Cell Proliferation, Senescence, and Cell Death in Zebrafish Embryos. *Methods in Cell Biology*, *101*, 19–38. https://doi.org/10.1016/B978-0-12-387036-0.00002-5

Verzi, M. P., Agarwal, P., Brown, C., McCulley, D. J., Schwarz, J. J., & Black, B. L. (2007). The transcription factor MEF2C is required for craniofacial development. *Developmental Cell*, *12*(4), 645–652. https://doi.org/10.1016/J.DEVCEL.2007.03.007

Vieux-Rochas, M., Mantero, S., Heude, E., Barbieri, O., Astigiano, S., Couly, G., Kurihara, H., Levi, G., & Merlo, G. R. (2010). Spatio-temporal dynamics of gene expression of the Edn1-Dlx5/6 pathway during development of the lower jaw. *Genesis*, *48*(6), 262–373. https://doi.org/10.1002/dvg.20625

Wada, H., Dambly-Chaudière, C., Kawakami, K., & Ghysen, A. (2013). Innervation is required for sense organ development in the lateral line system of adult zebrafish. *Proceedings of the National Academy of Sciences of the United States of America*, *110*(14), 5659–5664. https://doi.org/10.1073/PNAS.1214004110

Walker, M. B., & Kimmel, C. B. (2009). A two-color acid-free cartilage and bone stain for zebrafish larvae. *Http://Dx.Doi.Org/10.1080/10520290701333558*, *82*(1), 23–28. https://doi.org/10.1080/10520290701333558

Wallingford, J. B., Rowning, B. A., Vogell, K. M., Rothbächer, U., Fraser, S. E., & Harland, R. M. (2000). Dishevelled controls cell polarity during Xenopus gastrulation. *Nature 2000 405:6782*, *405*(6782), 81–85. https://doi.org/10.1038/35011077

Walshe, J., & Mason, I. (2000). Expression of FGFR1, FGFR2 and FGFR3 during early neural development in the chick embryo. *Mechanisms of Development*, *90*(1), 103–110. https://doi.org/10.1016/S0925-4773(99)00225-7

Walther, C., & Gruss, P. (1991). Pax-6, a murine paired box gene, is expressed in the developing CNS. *Development*, *113*(4), 1435–1449. https://doi.org/10.1242/DEV.113.4.1435

Wang, Y., Dye, C. A., Sohal, V., Long, J. E., Estrada, R. C., Roztocil, T., Lufkin, T., Deisseroth, K., Baraban, S. C., & Rubenstein, J. L. R. (2010). Dlx5 and Dlx6 regulate the development of parvalbumin-expressing cortical interneurons. *Journal of Neuroscience*, *30*(15), 5334–5345. https://doi.org/10.1523/JNEUROSCI.5963-09.2010

Wang, Y., Gupta, A., Toledo-Rodriguez, M., Wu, C. Z., & Markram, H. (2002). Anatomical, Physiological, Molecular and Circuit Properties of Nest Basket Cells in the Developing Somatosensory Cortex. *Cerebral Cortex*, *12*(4), 395–410. https://doi.org/10.1093/CERCOR/12.4.395

Wang, Y., Toledo-Rodriguez, M., Gupta, A., Wu, C., Silberberg, G., Luo, J., & Markram, H. (2004). Anatomical, physiological and molecular properties of Martinotti cells in the somatosensory cortex of

the juvenile rat. *The Journal of Physiology*, *561*(1), 65–90. https://doi.org/10.1113/JPHYSIOL.2004.073353

Weigele, J., & Franz-Odendaal, T. A. (2016). Functional bone histology of zebrafish reveals two types of endochondral ossification, different types of osteoblast clusters and a new bone type. *Journal of Anatomy*, *229*(1), 92–103. https://doi.org/10.1111/JOA.12480

Werner, J. M., Negesse, M. Y., Brooks, D. L., Caldwell, A. R., Johnson, J. M., & Brewster, R. M. (2021). Hallmarks of primary neurulation are conserved in the zebrafish forebrain. *Communications Biology*, *4*(1). https://doi.org/10.1038/S42003-021-01655-8

Wichterle, H., Garcia-Verdugo, J. M., Herrera, D. G., & Alvarez-Buylla, A. (1999). Young neurons from medial ganglionic eminence disperse in adult and embryonic brain. *Nature Neuroscience 1999 2:5*, *2*(5), 461–466. https://doi.org/10.1038/8131

Wilkie, A. O. M. (1997). Craniosynostosis: Genes and Mechanisms. *Human Molecular Genetics*, *6*(10), 1647–1656. https://doi.org/10.1093/HMG/6.10.1647

Witten, P. E., & Huysseune, A. (2009). A comparative view on mechanisms and functions of skeletal remodelling in teleost fish, with special emphasis on osteoclasts and their function. *Biological Reviews of the Cambridge Philosophical Society*, *84*(2), 315–346. https://doi.org/10.1111/J.1469-185X.2009.00077.X

Woronowicz, K. C., & Schneider, R. A. (2019). Molecular and cellular mechanisms underlying the evolution of form and function in the amniote jaw. *EvoDevo*, *10*(1). https://doi.org/10.1186/S13227-019-0131-8

Wu, B. T., Wen, S. H., Hwang, S. P. L., Huang, C. J., & Kuan, Y. S. (2015a). Control of Wnt5b secretion by Wntless modulates chondrogenic cell proliferation through fine-tuning fgf3 expression. *Journal of Cell Science*, *128*(12), 2328–2339. https://doi.org/10.1242/jcs.167403

Wu, B. T., Wen, S. H., Hwang, S. P. L., Huang, C. J., & Kuan, Y. S. (2015b). Control of Wnt5b secretion by Wntless modulates chondrogenic cell proliferation through fine-tuning fgf3 expression. *Journal of Cell Science*, *128*(12), 2328–2339. https://doi.org/10.1242/JCS.167403/260396/AM/CONTROL-OF-WNT5B-SECRETION-BY-WNTLESS-MODULATES

Wu, J., & Cohen, S. M. (1999). Proximodistal axis formation in the Drosophila leg: subdivision into proximal and distal domains by Homothorax and Distal-less. *Development*, *126*(1), 109–117. https://doi.org/10.1242/DEV.126.1.109

Wu, T., Pi, E. X., Tsai, S. N., Lam, H. M., Sun, S. M., Kwan, Y. W., & Ngai, S. M. (2011). GmPHD5 acts as an important regulator for crosstalk between histone H3K4 di-methylation and H3K14 acetylation

in response to salinity stress in soybean. *BMC Plant Biology*, *11*. https://doi.org/10.1186/1471-2229-11-178

Wullimann, M. F. (2009). Secondary neurogenesis and telencephalic organization in zebrafish and mice: a brief review. *Integrative Zoology*, *4*(1), 123–133. https://doi.org/10.1111/J.1749-4877.2008.00140.X

Wullimann, M. F., & Mueller, T. (2004). Teleostean and mammalian forebrains contrasted: Evidence from genes to behavior. *Journal of Comparative Neurology*, *475*(2), 143–162. https://doi.org/10.1002/CNE.20183

Wurdak, H., Ittner, L. M., Lang, K. S., Leveen, P., Suter, U., Fischer, J. A., Karlsson, S., Born, W., & Sommer, L. (2005). Inactivation of TGFbeta signaling in neural crest stem cells leads to multiple defects reminiscent of DiGeorge syndrome. *Genes & Development*, *19*(5), 530–535. https://doi.org/10.1101/GAD.317405

Wyatt, R. A., & Crawford, B. D. (2021). Post-translational activation of Mmp2 correlates with patterns of active collagen degradation during the development of the zebrafish tail. *Developmental Biology*, *477*, 155–163. https://doi.org/10.1016/J.YDBIO.2021.05.016

Xiao, S., McCarthy, J. G., Aster, J. C., & Fletcher, J. A. (2000). ZNF198–FGFR1 transforming activity depends on a novel proline-rich ZNF198 oligomerization domain. *Blood*, *96*(2), 699–704. https://doi.org/10.1182/BLOOD.V96.2.699

Xu, Q., Cobos, I., de La Cruz, E. D., Rubenstein, J. L., & Anderson, S. A. (2004). Origins of cortical interneuron subtypes. *The Journal of Neuroscience : The Official Journal of the Society for Neuroscience*, *24*(11), 2612–2622. https://doi.org/10.1523/JNEUROSCI.5667-03.2004

Xu, Q., Tam, M., & Anderson, S. A. (2008). Fate mapping Nkx2.1-lineage cells in the mouse telencephalon. *Journal of Comparative Neurology*, *506*(1), 16–29. https://doi.org/10.1002/CNE.21529

Xuan, S., Saptista, C. A., Balas, G., Tao, W., Soares, V. C., & Lai, E. (1995). *Winged Helix Transcription Factor BF-1 Is Essential for the Development of the Cerebral Hemispheres*. *14*, 1141–1152.

Yan, Y. L., Miller, C. T., Nissen, R., Singer, A., Liu, D., Kirn, A., Draper, B., Willoughby, J., Morcos, P. A., Amsterdam, A., Chung, B. C., Westerfield, M., Haffter, P., Hopkins, N., Kimmel, C., & Postlethwait, J. H. (2002). A zebrafish sox9 gene required for cartilage morphogenesis. *Development*, *129*(21), 5065–5079. https://doi.org/10.1242/dev.129.21.5065

Yang, L., Zhang, H., Hu, G., Wang, H., Abate-Shen, G., & Shen, M. M. (1998). An early phase of embryonic Dlx5 expression defines the rostral boundary of the neural plate. *Journal of Neuroscience*, *18*(20), 8322–8330. https://doi.org/10.1523/jneurosci.18-20-08322.1998

Yelick, P. C., & Schilling, T. F. (2002). *Molecular dissection of craniofacial development using zebrafish*. https://doi.org/10.1177/154411130201300402

Young, T., Poobalan, Y., Tan, E. K., Tao, S., Ong, S., Wehner, P., Schwenty-Lara, J., Lim, C. Y., Sadasivam, A., Lovatt, M., Wang, S. T., Ali, Y., Borchers, A., Sampath, K., & Dunn, N. R. (2014). The PDZ domain protein Mcc is a novel effector of non-canonical Wnt signaling during convergence and extension in zebrafish. *Development*, *141*(18), 3505–3516. https://doi.org/10.1242/DEV.114033

Yu, E. P. Y., Perin, S., Saxena, V., & Ekker, M. (2021). Novel cross-regulation interactions between dlx genes in larval zebrafish. *Gene*, *801*(July), 145848. https://doi.org/10.1016/j.gene.2021.145848

Yu, M., Xi, Y., Pollack, J., Debiais-Thibaud, M., MacDonald, R. B., & Ekker, M. (2011). Activity of dlx5a/dlx6a regulatory elements during zebrafish GABAergic neuron development. *International Journal of Developmental Neuroscience*, *29*(7), 681–691. https://doi.org/10.1016/j.ijdevneu.2011.06.005

Yun, K., Fischman, S., Johnson, J., Hrabe de Angelis, M., Weinsmaster, G., & Rubenstein, J. L. R. (2002). Modulation of the notch signaling by Mash1 and Dlx1/2regulates sequential specification and differentiation of progenitor cell types in the subcortical telencephalon. *Development*, *129*(21), 5029–5040. https://doi.org/10.1242/DEV.129.21.5029

Zeng, X., Wang, Y., Dong, Q., Ma, M. X., & Liu, X. de. (2020). DLX2 activates Wnt1 transcription and mediates Wnt/β-catenin signal to promote osteogenic differentiation of hBMSCs. *Gene*, *744*, 144564. https://doi.org/10.1016/J.GENE.2020.144564

Zerucha, T., & Ekker, M. (2000). Distal-less-related homeobox genes of vertebrates: Evolution, function, and regulation. *Biochemistry and Cell Biology*, *78*(5), 593–601.

Zerucha, T., Stühmer, T., Hatch, G., Park, B. K., Long, Q., Yu, G., Gambarotta, A., Schultz, J. R., Rubenstein, J. L. R., & Ekker, M. (2000). A highly conserved enhancer in the Dlx5/Dlx6 intergenic region is the site of cross-regulatory interactions between Dlx genes in the embryonic forebrain. *Journal of Neuroscience*, *20*(2), 709–721. https://doi.org/10.1523/jneurosci.20-02-00709.2000

Zerucha, T., Stühmer, T., Hatch, G., Park, B. K., Long, Q., Yu, G., Gambarotta, A., Schultz, J. R., Rubenstein, J. L. R., Ekker, M., Anderson, S. A., Ekker, M., Rubenstein, J. L. R., Puelles, L., Ekker, M., Rubenstein, J. L. R., de Melo, J., Qiu, X., Du, G., … Ekker, M. (2009). A highly conserved enhancer in the Dlx5/Dlx6 intergenic region is the site of cross-regulatory interactions between Dlx genes in the embryonic forebrain. *Journal of Neuroscience*, *29*(2), 5012–5022. https://doi.org/10.1242/dev.01560

Zhang, J., Bai, S., Zhang, X., Nagase, H., & Sarras, M. P. (2003). The expression of gelatinase A (MMP-2) is required for normal development of zebrafish embryos. *Development Genes and Evolution 2003 213:9*, *213*(9), 456–463. https://doi.org/10.1007/S00427-003-0346-4

Zhang, J., Zhang, W., Shi, J., Dai, J., & Shen, S. G. (2018). Dlx2 overexpression enhanced accumulation of type II collagen and aggrecan by inhibiting MMP13 expression in mice chondrocytes. *Biochemical and Biophysical Research Communications*, *503*(2), 528–535. https://doi.org/10.1016/J.BBRC.2018.05.066

Zupanc, G. K. H., Hinsch, K., & Gage, F. H. (2005). Proliferation, migration, neuronal differentiation, and long-term survival of new cells in the adult zebrafish brain. *Journal of Comparative Neurology*, *488*(3), 290–319. https://doi.org/10.1002/CNE.20571